# The Impact of Convection-Permitting ~~-~~Model Rainfall on the Dryland Water Balance

George Blake[1], Katerina Michaelides[1], Elizabth Kendon[1,2], Mark Cuthbert[3], Michael Bliss Singer[3,4]

[1] School of Geographical Sciences, University of Bristol, Bristol, BS8 BSS, United Kingdom
[2]Met Office Hadley Centre, Fitzroy Road, Exeter, EX1 3PB, United Kingdom
[3]School of Earth and Environmental Sciences, Cardiff University, Cardiff, CF10 3AT, United Kingdom
[4] Earth Research Institute, University of California Santa Barbara, CA 93106, USA

*Correspondence to*: George Blake (george.blake@bristol.ac.uk)

**Abstract.** In drylands, rainfall is typically delivered during short-lived, ~~and~~ localised convective storms, whose characteristics strongly influence how ~~the characteristics of which determine how~~ water is partitioned into different terrestrial stores. However, the ~~-~~rainfall data~~sets~~ often used in ~~hydrological~~ modelling future projections of ~~and assessments of~~ water resources is~~are~~ typically derived from climate models that are too coarse to represent convective processes ~~that are~~ occurring at scales smaller than the model grid. In this paper we quantify the impact of climate model representation of convection on the simulated water balance at four locations in the Horn of Africa: a humid site in the Ethiopian Highlands, a semi-arid site in southern Kenya, an arid site in eastern Ethiopia, and a hyper-arid site in northern Somalia. We benchmark a ~~the~~ novel pan-Africa convection permitting climate model (CP4A) and its parameterised counterpart (P25) against high-resolution satellite-derived gridded datasets of rainfall (IMERG) and PET (hPET). The comparison shows that explicitly resolving convection improves the representation of dryland rainfall characteristics: such as ~~characterisation of~~ rainfall frequency, intensity, and the relative contribution of low vs high-intensity rainfall to annual totals. We also demonstrate that ~~the representation of convection~~convective representation can impact model PET, but differences ~~although differences in PET between CP4A and P25~~ are more muted relative to rainfall, and both CP4A/P25 can capture seasonal and diurnal PET dynamics. To establish how the impact of ~~climate model representation of convection can~~connective representation on rainfall characteristics can control ~~impact~~ hydrology, we used Hydrus 1-D to run ~~then ran a series of one-dimensional~~1D vadose zone hydrological simulations at our four study sites, where ~~model experiments along an aridity gradient across the Horn of Africa using Hydrus 1-D, where at each of our four sties~~ Hydrus is~~was~~ driven by rainfall and PET from CP4A and P25 (and hPET). We find that the 'drizzle' bias in P25 means when rainfall is propagated through Hydrus, wetting fronts ~~are more restricted~~are confined to upper soil layers, resulting in higher evaporative losses, lower soil moisture, and bottom drainage in drylands. The improved representation of dryland rainfall characteristics in CP4A means that cumulative (in mm) surface runoff is up to ten times higher (over the ten-year simulation), bottom drainage (indicative of potential recharge) is up to 25 times higher, and soil moisture remains above the wilting point for longer compared to P25 Hydrus runs (despite simulating lower total rainfall and infiltration). Whereas at our humid site, water partitioning is less sensitive to rainfall characteristics and hydrological fluxes more closely follow annual rainfall totals. ~~While at our humid site in the Ethiopian Highlands there are minimal differences in hydrological outcomes, in drylands the more intense and intermittent rainfall in CP4A means surface runoff is up to ten times higher and bottom~~

**Commented [KM1]:** Because otherwise it doesn't make sense (there is no such thing as "convection-permitting rainfall" in of itself

**Commented [GB2R1]:** Yeah good point - I am guessing it doesn't matter if we change the title now…

~~drainage up to 25 times higher. We~~Our results demonstrate dryland vadose zone hydrology is highly sensitive to the impact of convective representation on rainfall characteristics, ~~conclude that dryland hydrology is highly sensitive to climate model representation of convection,~~ and that studies focused on modelling future water resources using ~~forcing hydrological model projections with convectional~~ climate models that parameterise the average effects of convection risk~~s~~ misrepresenting societally relevant fluxes such as~~underestimating~~ soil moisture~~future crop health~~, groundwater availability, and~~or~~ surface runoff~~flood risk~~.

## 1 Introduction

Drylands ~~regions~~ (regions ~~which for this study refers to any area with an aridity index <= 0.5 rather than 0.65) are~~ are characterised by limited and highly variable rainfall (both in space and time), where high temperatures, minimal humidity, and high solar radiation means the atmospheric water demand exceeds the available moisture supply (J Reynolds et al., 2007). When rainfall does occur in drylands, it typically falls during intense, localised, short duration rainstorms that are convective in nature (Nicholson, 2011; Singer and Michaelides, 2017; Singer et al., 2018; Hill et al., 2023). These storms are a critical source of moisture and represent a key control on dryland sub-surface water availability (Singer et al., 2018; Quichimbo et al., 2021, 2023). Therefore, the representation of convection and convective storms in climate models is critical for capturing dryland rainfall characteristics and subsequent water partitioning when rainfall is propagated through hydrological models. However, the grid resolution of general (global) or regional climate models (GCM/RCMs), which can range from 10 – 250 km, means they are unable to explicitly represent convective processes, which are occurring at the sub-grid scale (Prein et al., 2015; Clark et al., 2016).

The inability of GCM/RCMs to explicitly resolve convection means they may fail to adequately represent dryland rainfall characteristics, which is a ~~potential~~ major limitation in understanding future global climate resilience, as drylands cover ~45% of the Earth's land surface, are home to around 3 billion people, and represent the largest biome on Earth (Schimel, 2010; Mirzabaev et al., 2019). This is particularly important for people ~~For humans~~ living in drylands, where ~~their~~ livelihoods are often ~~intrinsically~~ tightly linked to the regional expression of climatic variability, especially ~~particularly~~ where populations primarily rely on intermittent surface water resources and rainfed pasture and crops (Stringer et al., 2009; Davenport et al., 2017, 2018; Hoffman et al., 2022).

One such region is the Horn of Africa (HOA), where inconsistent seasonal rainfall during the~~ir~~ two rainy seasons of Mar – May and Oct – Dec, and increasingly severe and frequent drought (Lyon and DeWitt, 2012; Lyon, 2014; Funk et al; 2019;~~,~~ Wainwright et al; 2019) are~~is~~ increasing the risk of regional food and water insecurity (Cheechi and Robinson, 2013; Nicholson, 2014; Funk et al., 2019). With research suggesting climate change will exacerbate water stress, desertification, and land degradation (Cook et al., 2020; Hoffman et al., 2022; Kimutai et al., 2023), there is a pressing need to understand how future rainfall will ~~translate into~~impact surface and subsurface water availability in the HOA.

**Commented [GB3]:** Define drylands later on in the methods - update response to reviewer

**Commented [KM4]:** I don't agree with this addition. It's moisture supply in rivers, lakes, soil etc. Not just soil

**Commented [GB5R4]:** Okay, I will update our response to this revision saying we will reject it

However, hydrological processes are particularly complex in drylands as the partitioning between infiltration, runoff, evaporation, transpiration, and recharge is highly dependent on the spatial and temporal characteristics of rainfall, rather than annual or seasonal totals (R Taylor et al., 2013; Arpuv et al., 2017; Singer and Michaelides, 2017; Cuthbert et al., 2019; Adloff et al., 2022; Kipkemoi et al., 2021; Quichimbo et al., 2021, 2023). ~~In addition to rainfall characteristics, t~~The dryland water balance is also sensitive to atmospheric evaporative demand (PET or potential evapotranspiration), both in how high PET impacts antecedent soil moisture conditions (soils quickly dry out between rainfall events) (Zhang and Shilling, 2006; Nazarieh et al., 2018; Cuthbert et al., 2019; Schoener and Stone, 2019; Schoener, 2021; Boas and Mallants, 2022) and its direct impact on agricultural yields and drought severity (Porporato et al., 2002; Lobell et al., 2011; Vicente-Serrano et al., 2018; Tugwell-Wootton et al., 2020; Kimutai et al., 2023).~~In addition to rainfall characteristics, the dryland water balance is also sensitive how synchronicity between rainfall and evaporative demand impacts antecedent soil moisture conditions (Zhang and Shilling, 2006; Nazarieh et al., 2018; Cuthbert et al., 2019; Schoener and Stone, 2019; Schoener, 2021; Boas and Mallants, 2022), with temporal offsets between potential evapotranspiration (PET) and rainfall capable of directly influencing impacting soil moisture, agricultural yields, and drought severity (Porporato et al., 2002; Lobell et al., 2011; Vicente-Serrano et al., 2018; Tugwell-Wootton et al., 2020; Kimutai et al., 2023).~~

I~~The high evaporative demand i~~n drylands ~~means it is typically only~~ high-intensity, short-lived, and localised convective rainfall events (or longer duration rainfall events of sufficient intensity) are a vital source of moisture, as they can produce ~~that can yield~~ sufficient rainfall to overcome the high evaporative demand, ~~for moisture to overcome this PET burden,~~ resulting in high infiltration rates, enhanced soil moisture, and groundwater recharge (R Taylor et al., 2013; Batalha et al., 2018; Kipkemoi et al., 2021; Adloff et al., 2022; Boas and Mallants, 2022). These intense convective events can also yield additional focused recharge when rainfall is heavy enough to generate surface runoff, where a certain proportion of runoff can enter dry ephemeral river channels and generate ~~locally~~ substantial flows that can lead to localised transmission losses ~~runoff is significant enough to generate flow in dry channels, leading to localised transmission losses~~ (Osborn 1983; Scanlon et al., 2006; Cuthbert et al., 2016, 2019, Singer and Michaelides, 2017; Seddon et al., 2021; Zarate et al 2022; Quichimbo et al., 2021, 2023). ~~Whereas~~On the contrary, if rainfall is low-intensity and long-duration, evaporative losses will be higher and rainfall will be quickly returned to the atmosphere (Batalha et al., 2018, Kipkemoi et al., 2021). Furthermore, precipitation dry spell length can impact evaporative losses and influence the antecedent soil moisture conditions that can govern hydrological responses to rainfall (Zhang and Shilling, 2006; Nazarieh et al., 2018; Schoener and Stone, 2019; Schoener, 2021; Boas and Mallants, 2022).

**Commented [KM6]:** Also long duration rainfall of sufficient intensity

The non-linear relationship between rainfall and hydrology in drylands makes it challenging to understand how anthropogenically-driven changes in rainfall and PET will impact dryland water security in the HOA, particularly as t~~T~~he GCMs and RCMs often used to make future assessments of dryland water resources (Crosbie et al., 2010; Mckenna and Sala, 2017; Razack et al., 2019; Cook et al., 2022) poorly represent convective processes. C~~convection~~

~~due to their spatial and temporal scale~~ limate models with horizontal grid spacings larger than 10 km must rely on parameterisation schemes to estimate the average effects of convection (Prein et al., 2015, Kendon et al., 2017)~~. As climate models with horizontal grid spacings larger than 10 km rely on parameterisation schemes to estimate the average effects of convection occurring at scales smaller than the model scale (Prein et al., 2015). This is a well-known source of model error (Prein et al., 2015; Kendon et al., 2017),~~, which results in 'parameterised' climate models systematically overestimating the frequency of low intensity rainfall events, simulating rainfall too early in the day, and underestimating the magnitude of extreme rainfall (Stephens et al., 2010; Stratton and Stirling, 2012; Prein et al., 2013; Ban et al., 2014; Kendon et al., 2019; Finney et al., 2019). As water partitioning in drylands is highly sensitive to rainfall characteristics, such biases could have significant impacts on future water resource projections.

One approach to improving the representation of dryland rainfall characteristics is through the use of convection-permitting models (CPMs)~~However, ,~~ ~~computational advances have led to an increase in the availability of convection-permitting model (CPM) simulations,~~ which are run at sufficiently high resolution (< 5 km) to explicitly resolve deep convection and represent a step-change in climate modelling capabilities (Clark et al., 2016). ~~This offers the possibility of assessing~~ Here, we assess whether CPMs can better capture dryland rainfall characteristics relative to traditional parameterised climate models, if there are differences in PET dynamics between CPMs and parameterised climate models, and critically if~~s~~ dryland water partitioning is sensitive to climate model representation of convection (via its impact on rainfall and PET).

W~~In this study w~~e compare two climate models that share the same underlying model physics and driving GCM, ~~use broadly the same model~~ but o~~physics but go about representing convection in fundamentally opposing ways. O~~ne is ~~,~~ a high-resolution (~4.5 km) convection-permitting model explicitly represents convection (CP4A), while the other is ~~,~~ a regional climate model (~25 km) that parameterises the average effects of convection (P25). While both models simulate comparable annual and seasonal rainfall totals (Kendon et al., 2019; Wainwright et al., 2019), the impact of convective representation on rainfall characteristics could ~~ir respective representation of convection is likely to control how rainfall is typically delivered, which could~~ have implications for how moisture propagates through a dryland hydrological system. Furthermore, to our knowledge no studies to date have assessed ~~how~~ how model representation of convection affects~~can impact the atmospheric variables that control~~ PET when it is externally calculated from model atmospheric variables (using the~~.~~ Penman-Monteith equation for reference crop evapotranspiration - see section 2.2 and Eq. (1)). ~~Hence, utilising these~~Accordingly, we ~~two models we~~ consider three key questions:

(1) Does explicitly resolving convection in climate models improve the representation of dryland rainfall characteristics and ~~hydrologically-relevant~~hydrologically relevant rainfall metrics in the Horn of Africa?

(2) Does ~~explicitly resolving convection in climate models affect the~~ convective representation affect simulated~~of~~ PET dynamics in the Horn of Africa?

(3) Does the impact of convective representation on rainfall characteristics and PET ~~explicitly resolving convection on rainfall and PET~~ influence how water is partitioned between different stores in drylands?

To do this we compare our ~~a~~ CPM (CP4A) and a conventional RCM (P25) to high-resolution hourly gridded satellite derived datasets of rainfall (IMERG) ~~-~~and PET (hPET), focusing on the ability of each model to capture key hydrologically relevant dryland rainfall and PET metrics. Then to assess hydrological sensitivity to rainfall characteristics and PET, ~~Subsequently, we~~ we force ~~establish how differences in model representation of convection impacts water partitioning when rainfall and PET is propagated through~~ a 1-D vadose zone hydrological model (Hydrus 1-D) with climate model rainfall and PET at four locations ~~, by running a series of point-based, one-dimensional simulations~~ along an aridity gradient across the HOA.

## 2 Methods

### 2.1 Climate Model Description

This study utilises data from two pan-African climate models ru~~a~~n under the Future Climate for Africa (FCFA) Improving Model Processes for African cLimAte (IMPALA) project (Stratton et al 2018.; Kendon et al., 2019). Both the Convection-Permitting Model for Africa (CP4A) and the 25-km regional model (P25) are configurations of the Met Office Unified Model (Walters et al., 2017). Two ten-year time-slices of hourly data run at a horizontal resolution of 4.5 km x 4.5 km in CP4A and 26 x 39 km in P25 are available for a historical (1997-2007) and a future period (2095-2105 RCP8.5). Both CP4A and P25 utilise the same domain, aerosol and land surface forcing, and are forced by the 25 km Unified Model GCM at their lateral boundaries and Reynolds sea-surface temperature observations (R Reynolds et al., 2007; Walters et al., 2017; Stratton et al., 2018). While CP4A and P25 use different cloud and blended boundary layer schemes, and CP4A also considers moisture conservation, the biggest difference is that the deep convection parameterisation scheme has been ‘switched off’ in CP4A (Stratton et al., 2018).

While CP4A is clearly a potential step forward, it remains subject to certain limitations, such as the use of a uniform ~~soil map (assumes all soils to be sandy)~~sandy soil across the entire domain. For water limited regions such as the HOA, soil moisture (partly a function of soil properties) directly regulates evapotranspiration and can contribute to precipitation via moisture recycling (Seneviratne et al, 2010), so a uniform soil map risks poor representation of the soil moisture – precipitation feedbacks critical to inducing convective rainfall and a realistic spatial pattern of rainfall (Taylor et al., 2011, 2012; Hsu et al., 2017; Zhou et al., 2021). ~~However, it is important to note that CP4A uses a uniform soil map that assumes all soils to be sandy, which risks poor representation of soil moisture – precipitation feedbacks that are critical to inducing convective rainfall and a realistic spatial pattern of rainfall in drylands (Taylor et al., 2011, 2012; Hsu et al., 2017; Zhou et al., 2021).~~ There are also clearly limitations with results based upon the use of a single climate model, ~~(as opposed to typical practice of employing an ensemble of models),~~ although consistent agreement between CP4A and other CPMs in terms of reproducing~~capturing~~ rainfall characteristics ~~compared to~~seen in observations increases confidence in CP4A (Kouadio et al., 2018; Luu et al., 2022).

### 2.2 Climate Data

To establish whether CP4A can better capture dryland rainfall characteristics and PET dynamics (relative to P25), we compared both climate models (historical run) to the gridded Integrated Multi-satellitE Retrievals for GPM (IMERG, Huffman et al., 2012) rainfall product and an hourly potential evapotranspiration dataset (hPET, Singer et al., 2021). ~~Understanding historical dynamics of dryland hydrology using CPM rainfall is a prerequisite for exploring the impact of future rainfall projections on water resources which can be done using the future time slice of CP4A (2095 – 2105). This study es To establish whether CP4A can better capture dryland rainfall characteristics (relative to P25) .w~~We ~~compared both models to the gridded Integrated Multi-satellitE Retrievals for GPM (IMERG, Huffman et al., 2012) rainfall product and an hourly potential evapotranspiration dataset (hPET, Singer et al 2021).~~

IMERG provides rainfall estimates at 0.1° (spatial) and 30 mins (temporal) resolution using ~~utilises~~ space-based radar, passive microwave, infrared, and rain gauge data from the Global Monthly Precipitation Climatology Centre (Huffman et al., 2012). A~~,~~lthough in the HOA there are persistent gaps in any available rain gauge data, and it is typically only available at daily resolution (Cocking et al., 2024). The ~~its~~ high spatial ~~(30 mins)~~ and temporal resolution of IMERG ~~(half-hourly)~~ means it is the most appropriate for evaluating dryland rainfall metrics at a regional scale (Ageet et al., 2022), ~~.~~however, it is only available from June 2000, so we can only compare CP4A/P25 to 6.5 years of rainfall data.~~there are are However, IMERG is only available from June 2000, so we can only compare CP4A/P25 to 6.5 years of rainfall data.~~

The hPET global hourly PET dataset (Singer et al., 2021) is derived from ERA5-Land variables (Muñoz Sabater, 2024) using the~~ved from the~~ Food and Agriculture Organisations' (FAO) Penman-Monteith equation (Eq. (1)) for reference crop evapotranspiration (Allen et al., 1998). ~~using the ERA5-Land climate variables (Muñoz Sabater, 2024)~~hPET~~, it~~ is available at a high spatial (0.1 degrees) and temporal ~~resolution~~ (hourly) resolution and can capture both diurnal and seasonal variability in atmospheric evaporative demand (Singer et al., 2021). We computed PET from CP4A and P25 outputs using the same FAO equation (Eq. (1)). Note while most variables could be directly outputted from the model, this did require converting 10-m wind speeds to 2-m (Eq. (2)) and estimating relative humidity from specific humidity, surface pressure, and air temperature. Full details of the PET calculation (Eq. (5) – Eq. (14)) and rationale behind this approach is provided in Appendix 6.1.

Climate model ~~To compare against hPET, we~~ ~~computed~~ PET using output variables from CP4A and P25 within ~~computed CP4A and P25 PET with the FAO Penman-Monteith equation~~ to compute CP4A and P25 PET at an hourly resolution ($t$) at each pixel ($x$) in our domain~~using the same seven atmospheric variables that are output from these models~~ was calculated using Eq. (1). ~~:~~

$$hPET_{x,t} = \frac{0.408\Delta(R_n - G + \gamma(\frac{37}{T_a + 273})u_2(e_s - e_a)}{\Delta + \gamma(1 + 0.34u_2)} \quad (1)$$

**Commented [KM7]:** I'm not sure this adds anything. It starts the paragraph backwards and may confuse the reader (that is not the reviewer!)

**Commented [KM8]:** I'm not sure this adds anything. It starts the paragraph backwards and may confuse the reader (that is not the reviewer!)

Where $R_n$ is hourly net radiation (MJ m$^{-2}$), $G$ is the soil heat flux (MJ m$^{-2}$), $\gamma$ is the psychometric constant (kPA °C$^{-1}$), $\Delta$ is the slope of saturation vapour pressure (kPA °C$^{-1}$), $T_a$ is hourly air temperature (°C), $e_s$ is saturation vapour pressure (kPa), $e_a$ is the actual vapour pressure, and $u_2$ is wind speed (m s$^{-1}$) at 2 m above the land surface.

Surface net solar radiation (J m-2), surface net thermal radiation (J m-2), atmospheric surface pressure (Pa), and 2 m air temperature (K) can all be directly outputted from CP4A/P25. Wind speed is also directly outputted from CP4A/P25 but is only available at 10 m above the surface, so zonal and meridional wind speed was converted to the required 2 metre value using the logarithmic velocity profile above a short grass surface (Eq. (2)):

$$u_2 = u_z \left(\frac{4.87}{\ln(67.8z - 5.42)}\right) \tag{2}$$

Where $u_z$ is the wind speed at height $z$ above the land surface (10 meters in this case) computed as (Eq. (3)):

$$u_z = \sqrt{u^2 + v^2} \tag{3}$$

Since the 2 m dew point temperature is not directly outputted from CP4A/P25, it was calculated using the 2 m air temperature and relative humidity (also not directly outputted by CP4A/P25), with relative humidity calculated using 2 m air temperature, surface pressure, and specific humidity (see Appendix A Eq. (5) – Eq. (8)). For a breakdown of how the saturation vapour pressure ($e_s$), actual vapour pressure ($e_a$), slope of saturation vapour pressure ($\Delta$), net radiation ($R_n$), and the soil heat flux ($G$) used in Eq 1 were calculated please refer to Eq. (9) – Eq. (14) given in Appendix 6.1.

~~Since t~~

~~used~~

1. ~~10 m zonal (u) wind speed (m s-1)~~
2. ~~10 m meridional (v) wind speed~~
3. ~~2 m dew point temperature (K)~~
4. ~~2 m air temperature (K)~~
5. ~~Surface net solar radiation (J m-2)~~
6. ~~Surface net thermal radiation (J m-2)~~
7. ~~Atmospheric surface pressure (Pa)~~

### 2.3 Dryland Rainfall Metrics

~~While other~~Several studies have demonstrated that CP4A better captures rainfall frequency, extremes, the diurnal cycle, and the spatial structure of rainfall events (Ban et al., 2014; Prein et al., 2015; Kendon et al., 2017, 2019; Finney et al., 2019, 2020). But h~~H~~ere we benchmark CP4A and P25 against a series of metrics that are explicitly indicative of the key dryland rainfall characteristics that are important in ~~control~~ hydrological partitioning:

1. Rainfall mode – Percentage of annual rainfall from high intensity (>95$^{th}$ percentile IMERG rainfall) versus low-intensity drizzle (<= 1 mm/hr).~~delivered via heavy rainfall vs drizzle~~
2. Maximum dry spell length – average longest run of dry days in any given year.
3. Extreme rainfall ~~-~~magnitude – ~~(~~99$^{th}$ percentile of wet hour rainfall in the dominant rainy season. ~~rainy season wet hours)~~

~~We used the above metrics because as dryland hydrology can be more sensitive to the mode of rainfall delivery (light vs intense rainfall) than seasonal/annual totals (R Taylor et al., 2013; Arpuv et al., 2017; Singer and Michaelides, 2017; Cuthbert et al., 2019; Kipkemoi et al., 2021; Quichimbo et al., 2023), particularly when it comes to extreme rainfall events (R Taylor et al., 2013; Batalha et al., 2018; Adloff et al., 2022; Boas and Mallants, 2022). Furthermore, dry spell length can impact evaporative losses and influence the antecedent soil moisture conditions that can govern the hydrological responses to rainfall (Zhang and Shilling, 2006; Nazarieh et al., 2018; Schoener and Stone, 2019; Schoener, 2021; Boas and Mallants, 2022), with soils typically drying out between convective storms (C Taylor et al., 2011, 2012; Hsu et al., 2017; Zhou et al., 2021).~~

For the above metrics we define a wet hour as ~~:~~ ~~low-intensity rainfall ('drizzle') as any wet hour where rainfall is <= 1 mm/hr;~~, ~~high-intensity ('heavy') rainfall~~ as a rainfall ~~as any wet hour above the 95$^{th}$ percentile (using IMERG) of wet season precipitation,~~; ~~while 'extreme' rainfall is defined as the 99$^{th}$ percentile of wet season precipitation. These percentile-based metrics only consider wet hours (~~any hour with~~hour~~ >= 0.1 mm of rainfall, and defined the~~) during the~~ wettest season at each grid cell based on the percentage of annual rainfall delivered in each of the following seasons: ~~(either~~ Jan-Feb, Mar-May, Jun-Sep, and Oct-Dec~~)~~. ~~for each grid cell across our domain.~~ For dryland regions the wettest season will either be MAM or OND, and for the more humid Ethiopian Highlands it is more likely to be JJAS (Fig.1 & Annex D~~C~~ – Fig. ~~1~~D1~~C~~)

To capture the ~~better represent the~~ high-intensity, low-duration nature of rainfall in drylands, our analysis was conducted at hourly rather than three-hourly resolution as has been done elsewhere (Bethou et al., 2019; Kendon et al., 2019; Finney et al., 2019, 2020), as resampling to a lower ~~coarser~~ temporal resolution~~timescale~~ dampens the intensity of rainfall and impacts water partitioning (Batalha et al., 2021; Kipkemoi et al., 2021). To ensure consistency, all datasets were re-gridded using first order conservative re-gridding to the P25 grid (26 x 39 km).

### 2.4 Hydrological Modelling

#### 2.4.1 Hydrus 1-D

We used Hydrus 1-D v4.17 (Šimůnek et al., 2012) to simulate dynamic changes in infiltration, surface runoff, evaporation, transpiration, soil moisture, and bottom drainage when forced with each climate model rainfall and PET.

Hydrus 1-D uses timeseries of rainfall, PET, and Leaf Area Index (LAI) to numerically solve a version of the Richards equation (Richards, 1931; Šimůnek et al., 2012). It can simulate ~~by deep rooted plants. Hydrus 1-D can simulates~~ vertical water redistribution in the soil subsurface under a wide range of different climatic, soil, and vegetation conditions, and has been widely used to understand soil moisture, evapotranspiration, and groundwater recharge in both arid and humid landscapes (Leterme et al., 2012; McKenna and Sala, 2017; Batalha et al., 2018; Rodriguez et al., 2020; Boas and Mallants, 2022; Corona and Ge, 2022). However, ~~despite its use in dryland settings (McKenna and Sala, 2017, Rodriguez et al., 2020, Boas and Mallants, 2022),~~ it ~~doesn't~~ does not consider lateral flows, and larger scale moisture redistribution processes~~. that occur in larger catchments. and critically (in a dryland context) it cannot represent 'focused' recharge below streambeds.~~

Hydrus 1-D ~~was forced with timeseries of rainfall, PET, and Leaf Area Index (LAI) and to analyse how rainfall is partitioned between surface runoff, infiltration, actual evapotranspiration, and drainage below the soil profile (Fig. 2). To simulate the one-dimensional flow of water through saturated, partly saturated, or unsaturated media, the model numerically solves a version of the Richards equation (Richards, 1931; Šimůnek et al., 2012). Thus, it~~ requires parameterisation of soil hydraulic properties, which are typically obtained from in-situ measurements or derived using soil textures filtered through a pedotransfer function (van Genuchten, 1980). It also includes a sink term to account for root water uptake (also referred to as transpiration), which is estimated using the water stress response function detailed by Feddes (1978). For further details on Hydrus 1-D please refer to (Šimůnek et al., 2012).

#### 2.4.2 Hydrological Study Sites

~~Given the sensitivity of dryland hydrology to rainfall characteristics, we wanted to establish whether relative differences in hydrological outcomes between Hydrus simulations (when forced with CP4A and P25 rainfall/PET) varied with aridity. Hence, we~~We ran four 1-D vadose-zone hydrological simulations along an aridity gradient across the HOA, ranging from the humid Ethiopian Highlands to hyper-arid Northern Somalia (Fig. 1). We classify aridity based on aridity index (AI = P/PET) values taken from the CGIAR-CSI (Consortium of International Agricultural Research Centres' Consortium for Spatial Information) (Zomer et al., 2007) using the classification of Mirzabaev et al (2019).

The Aridity Index (AI) is a numerical indicator of climatic aridity based on long-term precipitation deficits relative to atmospheric water demand (Eq. (4)):

$$AI(AridityIndex) = MAP/MAE \tag{4}$$

Where MAP is mean annual precipitation and MAE is mean annual potential evaporation, CGIAR-CSI calculate both MAP and MAE using data obtained from WorldClim Global Climate Data (Hijmans et al, 2005). CGIAR-CSI outputs AI values at 1 km resolution, which can be used to define the climate type based on the climate classification of Mirzabaev et al, 2019, as shown in Table 1.

| Climate Type | Aridity Index |
|---|---|
| Hyper-Arid | AI < 0.05 |

| | |
|---|---|
| Arid | 0.05 <= AI < 0.2 |
| Semi-Arid | 0.2 <= AI < 0.5 |
| Dry Sub-Humid | 0.5 <= AI < 0.65 |
| Humid | AI >= 0.65 |

~~Aridity values are taken from the CGIAR-CSI (Consortium of International Agricultural Research Centres' Consortium for Spatial Information) (Zomer et al., 2007) using the classification of Mirzabaev et al (2019).~~

**Table 1 – Climate classifications based on aridity index thresholds taken from (Mirzabaev et al, 2019).**

Fig.~~ure~~ 1 shows the climatic zones of the HOA along with the locations of our four sites, with one site in ~~each of the four~~ each ~~a~~ major aridity ~~classifications~~zone: humid (9.7% of land mass), semi-arid (31.8%), arid (43.6%), and hyper-arid (7.7%). For this study we define drylands as any grid cell with an AI <= 0.5 rather than 0.65, so our 'dryland' region refers to any grid cell identified as Hyper-Arid, Arid, or Semi-Arid (not Dry Sub-Humid).

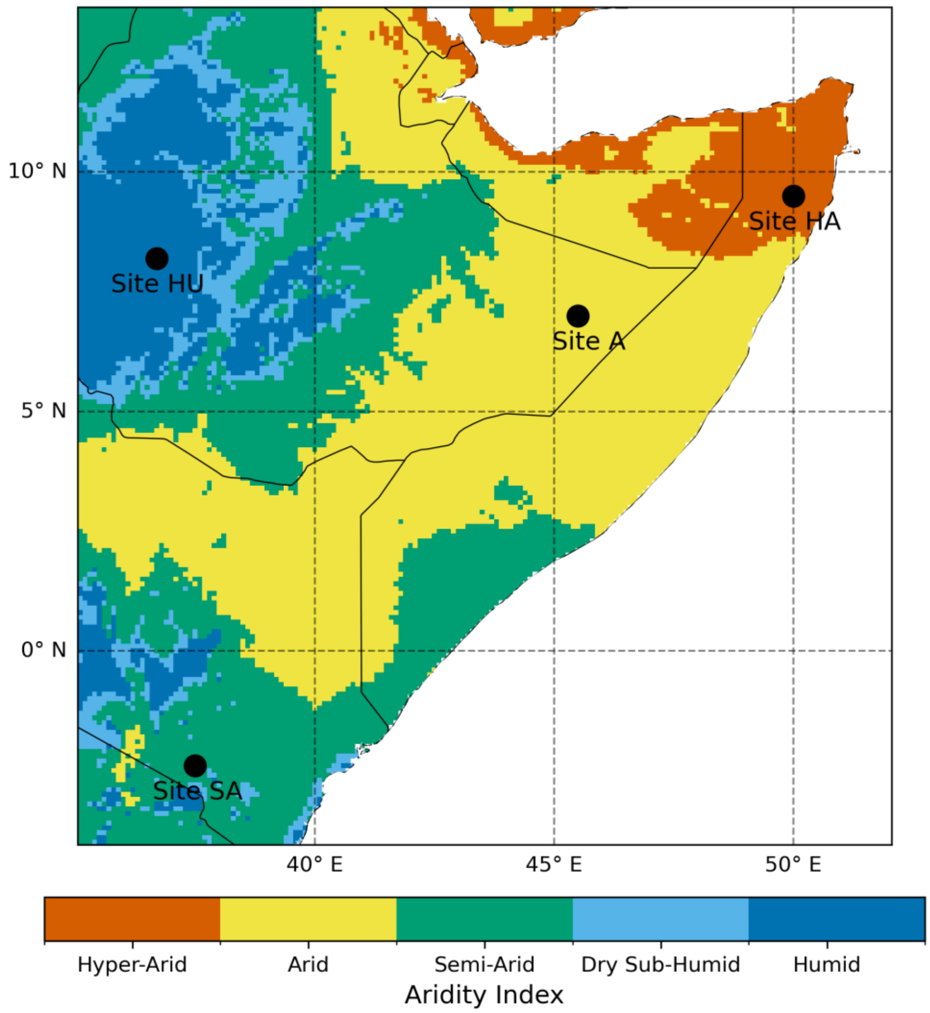


**Figure 1. Horn of Africa Aridity Index and Study Site Locations. Locations of the four Hydrus locations plotted against aridity index values taken from CGIAR-CSI. Sites are found in the humid Ethiopian Highlands (Site HU), semi-arid southern Kenya (Site SA), arid eastern Ethiopia (Site A), and hyper-arid northern Somalia (Site HA).**

For each hydrological site, ~~It is worth noting that typically dry sub-humid regions are also classed as dryland, but in this study when we refer to 'drylands', we are conservatively only referring to grid cells with an AI < 0.5. This is due to the limited spatial extent of dry sub-humid areas across the HOA (7.2%).~~ w~~To ensure our one-dimensional hydrological simulations isolate the impact of rainfall characteristics on water partitioning, w~~e tried to ~~aimed to choose~~choose locations within each aridity classification where mean annual rainfall and PET was ~~broadly~~ comparable, but in lieu of perfect matches, ~~between CP4A and P25. However,~~~~ButI~~we ~~settled on~~selected locations where P25 simulated higher mean annual rainfall (Table 2). At each site (represented by a single climate model grid cell) P25 simulated 15% (humid), 12% (semi-arid), 23% (arid), and 33% (hyper-arid) higher total annual rainfall. Choosing locations where P25 simulates higher total rainfall ensures that if fluxes such as soil moisture or bottom drainage are higher when forcing Hydrus with CP4A rainfall, it is reflective of differences in rainfall characteristics rather than simply higher annual rainfall totals. ~~It also worth noting that~~ P25 also simulated 3%, 14%, 15% higher total annual PET at our dryland sites (SA, A, and HA respectively), while PET is 9% higher using CP4A at our humid site (HU). However, this still means that at all sites the ratio of P/PET is higher using P25. ~~at all sites, it is P25 that simulates higher mean annual rainfall (12 – 29% higher) (Table 1) compared to CP4A, this ensures that if fluxes such as soil moisture or bottom drainage are higher when forcing Hydrus with CP4A rainfall, it is reflective of differences in rainfall characteristics rather than simply higher annual totals.~~

| Site | Rainfall **(CP4A)** | PET **(CP4A)** | Vegetation |
|---|---|---|---|
| Site HU (humid) – Ethiopian Highlands | 2000 mm (**1730 mm**) | 1290 mm (**1400 mm**) | Maize |
| Site SA (semi-arid) – Southern Kenya | 670 mm (**600 mm**) | 1620 mm (**1580 mm**) | Shrubs |
| Site A (arid) – Eastern Ethiopia | 430 mm (**350 mm**) | 2180 mm (**1920 mm**) | Shrubs |
| Site HA (hyper-arid) – Northern Somalia | 240 mm (**180 mm**) | 1970 mm (**1720 mm**) | Bare Soil |

**Table 2~~1~~. Mean annual rainfall, PET, and vegetation type at our four study sites. Rainfall and PET simulated by CP4A are in bold, and P25~~CP4A~~ in ~~are in bold~~non-bold. Vegetation type is taken from the iSDAsoil dataset (iSDA, 2024).**

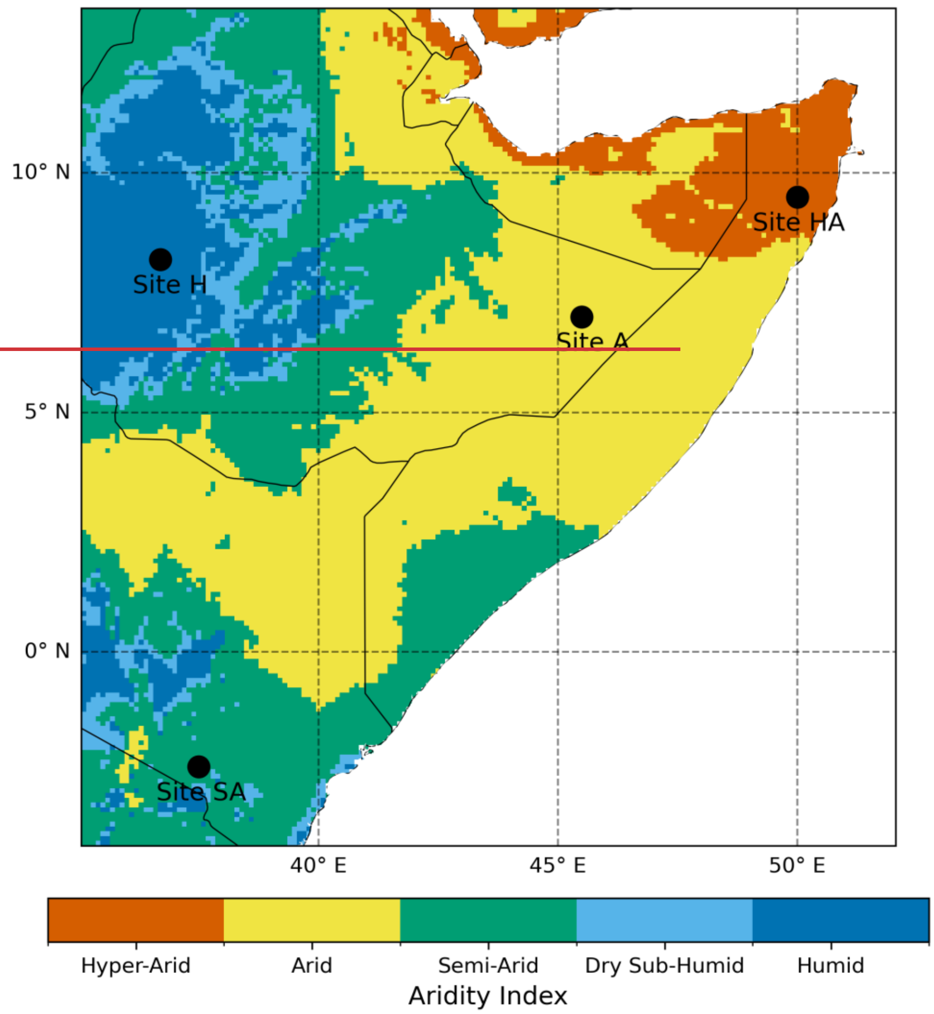


~~**Figure 1. Horn of Africa Aridity Index and Study Site Locations. Location of the four Hydrus locations plotted against aridity index values taken from CGIAR CSI. Sites are found in the humid Ethiopian Highlands (Site HU), semi-arid southern Kenya (Site SA), arid eastern Ethiopia (Site A), and hyper-arid northern Somalia (Site HA).**~~

**2.4.3 Hydrological Model Set Up, Data, and Sensitivity**

This aim of this study is to use a series of ~~Our~~ experimental, one-dimensional Hydrus simulations to examine the impact of convective representation on rainfall characteristics and subsequent partitioning when rainfall ~~how climate model representation of convection~~ rainfall ~~can control~~ affects ~~how moisture~~is propagated~~ds~~ vertically through the vadose zone at a 1D scale. ~~of a particular point-based a hydrological system~~~~and determines the 1D water balance. , it is not to ,~~ ~~rather than aiming to reproduce 'realistic' hydrological simulations.~~ ~~We acknowledge that~~ Although one-dimensional point-based hydrological modelling is a clear simplification of the hydrological system ~~in the HOA and~~ and does not ~~capture~~ represent watershed-scale surface and sub-surface ~~hydrological pathways and hydrogeological processes~~lateral flows, ~~. However,~~ the focus on the 1D water balance and processes was a deliberate decision to ensure we could most effectively isolate the impact of rainfall characteristics – specifically the representation of convection on rainfall intensity-duration – on vertical vadose zone hydrological partitioning, without the complexity that would be introduced by lateral and non-local processes if modelling was carried out at a basin or regional scale. We are not dismissing the importance of ~~Our focus on the point-scale is not based on the assumption that While~~ overland flow generation and runoff ~~and hysteresis~~ as significant hydrological processes in dryland catchments, ~~negligible in our context (Boas and Mallants, 2022), rather~~ we exclude their consideration ~~of runoff generation and subsurface lateral flows as they tend to add more water to downslope locations which may then infiltrate or evaporate. We wanted to strip away these added water sources~~ to simply understand the balance between evapotranspiration, soil moisture and deeper drainage in response to differing rainfall characteristics. And while our simulations are experimental, they ~~However, although o~~O~~ur model simulations are experimental, we did~~ use plausible soil hydraulic and vegetation parameters where available.

All Hydrus simulations utilised a three-meter soil profile (preliminary simulations suggested minimal water fluxes below this depth at some locations) with a free draining bottom boundary (no interactions between water t~~T~~able and soil profile above). ~~This is clearly~~Although a simplification, this setup is not unreasonable ~~as interactions between the water table and unsaturated zone can be significant, particularly in semi-arid to humid regions, although there is evidence that~~ as~~because~~ the water table is commonly deep across the Horn of Africa (Bonsor and MacDonald, 2011; Fan et al, 2013) and in drylands generally~~in general~~. However this does mean that the simulated bottom drainage is not necessarily indicative of groundwater recharge, as it is unlikely the water table would be so shallow (Bonsor and MacDonald., 2011; Fan et al., 2013), and there is robust evidence that dryland acacia shrubs (dominant shrub species in the HOA) are particularly deep rooted and are capable of extracting water directly from the water table (Stone and Kalisz, 1991; Maeght et al., 2013; Shadwell and February 2017).

For the top boundary layer, we used atmospheric boundary conditions with surface runoff, meaning where model rainfall exceeds the infiltration capacity of the topsoil~~, the~~ water is re-routed as runoff and cannot enter the soil profile (Fig. 2). For all simulations the soil profile was discretized in 2 cm intervals, with a minimum and maximum time step interval of 5 seconds to 20 days (high max time step needed as long periods with no rainfall in drylands). This ensured the model converged (using default Hydrus water content and pressure head tolerances) within 10 timesteps (Hydrus default) and relative mass balance errors remained below 1%. All model runs at each site were initially forced using the mean hourly IMERG and hPET climatology (over 2000-2007) until steady state conditions were reached and relative mass balance errors were below 0.1% (6 – 15 years depending on study site).

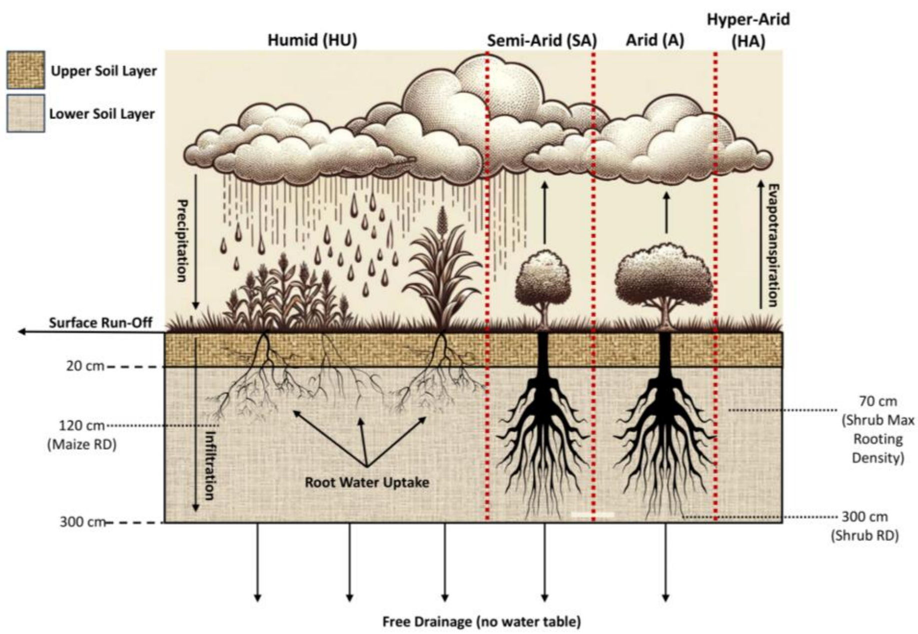


**Figure 2. Hydrus Simulations Schematic. Conceptual schematic of how water is partitioned within Hydrus 1D at any given timestep within the simulation. Please note that in the figure shrubs, maize, and bare soil are represented, whereas only one vegetation type can be modelled in any one simulation. Here the schematic is divided to represent the model set up for each site-specific simulation. For all sites the soil profile is divided into two layers (boundary is marked at 20 cm) and is discretised at a resolution of 2 cm. At Site HU, maize roots to a depth of 120 cm, while at Sites SA and A shrubs utilise moisture through the entire 300 cm profile. At Site HA we assume grass cover is extremely sparse, so here we only consider bare soil evaporation and no transpiration.**

Soil hydraulic properties were calculated using Genuchten-Mualem (Van Genuchten, 1980) equations based on soil texture values taken from the iSDAsoil database (iSDA, 2024), which applies a multiscale ensemble machine learning approach to a range of fine -and coarse-scale satellite observations to predict soil properties at 30 m resolution at two depth intervals (0 – 20 cm and 20 – 50 cm) (Hengl et al., 2021). While robust estimates of water movement would require soil textures for the entire profile, here we divided our three-meter profile into two layers following the iSDAsoil data depth intervals (which uses 0 – 20 and 20 – 50 cm). This mean we divide our profile into ~~:~~ an upper (0 – 20 cm) and lower layer (20 – 300 cm), ~~. This approach is~~ a significant simplification as it assumes that soil properties from 50 – 300 cm follows those at shallower depths (20 – 50 cm)~~are homogenous at depths below 0.2 m below ground level (mbgl)~~. ~~All simulations were run using the Van-Genuchten-Mualem single porosity model.~~ ~~his paper.~~.

To calculate transpiration Hydrus needs land cover (Table 2~~1~~) and leaf area index (LAI) data, which were taken from iSDA (as of 2019) and the National Centers for Environmental Information AVHRR LAI dataset (Vemote, 2019) respectively. Hydrus uses the Feddes' (1978) approach to estimate ~~root water uptake~~transpiration (referred to as root water uptake within Hydrus) under various pressure heads (water stress) and root densities. For Site HU (humid) we utilised Feddes' parameters for maize (from the internal Hydrus database – Wesseling (1991)) and set the maximum rooting depth to 1.2 mbgl (Zinyengere et al., 2011). Shrubs are not included in the internal Hydrus vegetation database, and there is limited information on Feddes' parameters for dryland (acacia) shrubs, so we combined data from available literature to estimate a reasonable parameter set (Appendix B~~A~~ - Table B2) (Xia and Shao, 2008; Sela et al., 2015; Watson, 2015). As dryland shrubs tend to be deep-rooted (Stone and Kalisz, 1991; Maeght et al., 2013; Shadwell and February 2017), we assumed they can utilise moisture from the entire soil profile and specified maximum root density at ~0.7 mbgl, which tends to be the depth at which shrub root water uptake is greatest (Geißler et al., 2019).

Given the uncertainty with Feddes' acacia shrub parameters, at Sites SA (southern Kenya) and A (eastern Ethiopia) (site HA is bare soil), we ran additional Hydrus simulations using a range of shrub Feddes' parameters (Appendix B - Table B2) as given by Sela et al (2015). Within the range given by Sela et al (2015) we used the upper parameter set as our 'default' run, as the wilting point corresponded better with other published data (Xia and Shao, 2008, Watson, 2015).

At all sites, we also ran Hydrus simulations using low (lowK) and high (highK) hydraulic conductivity soil parameters (Appendix B - Table B1), and to assess dryland hydrological sensitivity to PET, we also forced Hydrus with climate model rainfall but replaced climate model-derived PET with gridded hPET values (see Section 2.2). However, unless stated otherwise, all results refer to simulations forced using climate model rainfall/PET and the default soil hydraulic and Feddes' parameters given in Appendix B - Table B1 & B2. ~~At Sites SA (southern Kenya) and A (eastern Ethiopia), we ran additional Hydrus simulations using a range of shrub Feddes' parameters (Appendix A - Table B1) as given by Sela et al (2015). Within the range given by Sela et al (2015) we used the upper parameter set as our 'default' run, as the wilting point corresponded better with other published data (Xia and Shao, 2008, Watson, 2015). At all sites, we also ran Hydrus simulations using low (lowK) and high (highK) hydraulic conductivity soil parameters (Appendix A - Table 1A). Finally, due to dryland hydrological sensitivity y can also be sensitive to PET derived as well as rainfall, so we also to assess whether the impact of climate model representation of convection on PET can impact water partitioning, we also forced Hydrus with climate model rainfall but replaced climate model PET with gridded~~

~~hPET values. Unless stated otherwise, all results refer to simulations forced using climate model rainfall/PET and the default soil hydraulic and Feddes' parameters given in Appendix A Tables 1-2A.~~

~~**Figure 2. Hydrus Simulations Schematic. Conceptual schematic of how water is partitioned within Hydrus 1D at any given timestep within the simulation.**~~ Please ~~**It is important to note that in the above figure both shrubs, maize, and bare soil represented, whereas only one vegetation type can be modelled. Here the schematic is divided to represent the model set up for each site-specific simulation. For all sites the soil profile is divided into two layers (boundary is marked at 20 cm) and is discretised at a resolution of 2 cm. At Site HU, maize roots to a depth of 120 cm, while at Sites SA and A shrubs utilise moisture through the entire 300 cm profile. At Site HA we assume grass cover is extremely sparse, here we only consider bare soil evaporation and no root water uptake (transpiration).**~~

## 3. Results

### 3.1 Rainfall

Fig.~~ures~~ 3~~(~~a~~), and (~~b~~)~~ shows rainfall intensity distributions for ~~the distribution of rainfall intensities for all rainfall hours (based on a threshold of 0.1 mm/h) for~~ humid (AI >= 0.65) and dryland regions (AI < 0.50) ~~across the~~in the HOA, based on all rainfall hours >= 0.1 mm/hr.~~.~~ The plots highlight the 'drizzle' effect associated with parameterised climate models (shown by the large frequency peaks in rain~~hours~~fall intensities between $10^{-1}$ and $10^{1}$ mm/hr – dashed black circles), with P25 overestimating the frequency of rainfall events <= 1 mm/hr in both regions, but particularly drylands (Fig. 3b). CP4A does not simulate the same 'drizzle effect' in drylands, although (in both humid and dryland regions) CP4A simulates fewer rainfall events with an intensity of > 10 mm/hr compared to IMERG.

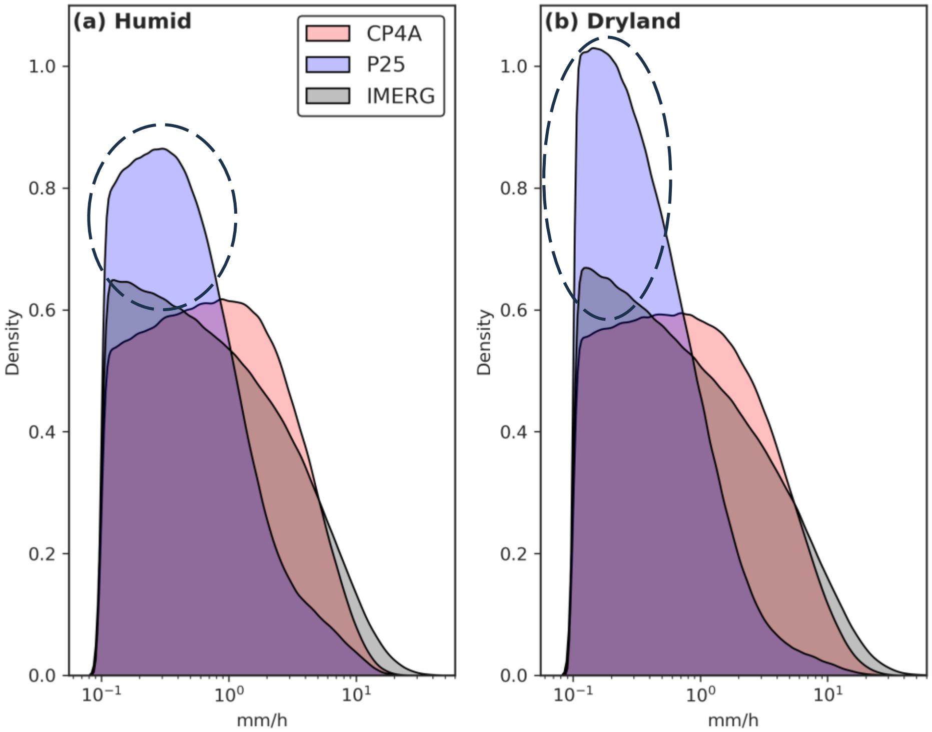


**Figure 3. Rainfall KDE Plots. Kernel density estimate (KDE) plots of CP4A, P25, and IMERG hourly rainfall in humid (a) (AI >= 0.65) and dryland (b) (AI < 0.5) regions of the Horn of Africa. Plots exclude dry hours by dropping any hours that receive < 0.1 mm/hr. Black dashed circles indicate the 'drizzle' effect seen in P25 simulations.**

~~CP4A does not simulate the same 'drizzle effect' in drylands and offers a clear improvement in the frequency of dryland rainfall, in both humid and dryland regions CP4A still simulates fewer rainfall events > 10 mm/hr compared to IMERG.~~ We used the Kolmogorov–Smirnov (KS) test with a null hypothesis that the modelled distribution of hourly rainfall intensities (based on all hours with rainfall >= 0.1 mm/h) is drawn from the same distribution as IMERG. Both P25 and CP4A show statistically significant differences from IMERG ($p < 0.05$), but the KS statistic is markedly lower for CP4A (0.03) than for P25 (0.24), indicating CP4A better matches the observed distribution (IMERG). Also ~~Using the Kolmogorov-Smirnov (KS) test shows that while there is still a statistically significant difference in the distribution on rainfall relative to IMERG, the KS statistic is lower (0.03) using CP4A compared to P25 rainfall (0.24).~~ ~~It is also worth noting that ww~~While Fig. 3 aggregates data across the entire study period, the 'drizzle' effect seen in P25 simulations remains consistent between years and across each of the four seasons in the region (Appendix C – Fig. C1).

~~**Figure 3. Rainfall KDE Plots. Kernel density estimate (kde) plots of CP4A, P25, and IMERG hourly rainfall in humid (a) (AI >= 0.65) and dryland (b) (AI < 0.5) regions of the Horn of Africa. Plots exclude dry hours by dropping any hours that receive < 0.1 mm/hr.**~~

The tendency for P25 to overestimate the frequency of light rainfall events means most annual rainfall is delivered via events with a magnitude of <= 1 mm/hr (Fig. 4a-c) across the HOA. In humid regions, on average P25 simulates 39.0% of annual rainfall falling as 'drizzle' versus 17.1% and 13.6% in CP4A and IMERG respectively. This bias is even more pronounced in dryland areas, where the median proportion of annual rainfall falling as drizzle is 51.5% in P25 versus 14.1% and 13.0% for CP4A and IMERG. Apart from a few isolated locations, no areas in the drylands receive more than 20% of rainfall via 'drizzle' in CP4A and IMERG (Table 3).~~.~~

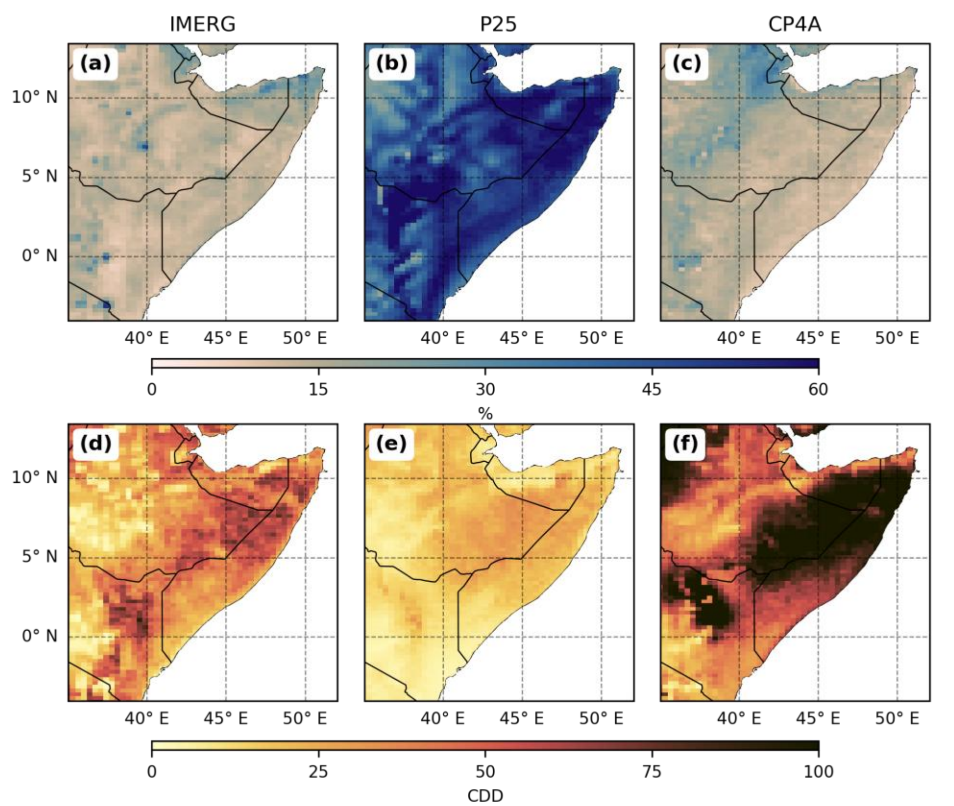


**Figure 4. Percentage of Annual Rainfall delivered as drizzle and maximum number of consecutive dry days. Percentage of mean annual rainfall that falls as 'drizzle', where 'drizzle' is any rain hour with an intensity <= 1 mm/hr (top panel) for**

**IMERG (a), P25 (b), and CP4A (c). Bottom Panel - Mean annual maximum dry spell length, where a dry hour is any hour that receives less than 0.1 mm of rain IMERG (d), P25 (e), and CP4A (f).**

~~This frequent~~The ~~-~~'drizzle' bias also means ~~in~~ P25 ~~also results in an~~ underestimates~~ion~~ ~~of~~ maximum dry spell length (CDD – consecutive dry days) compared to IMERG and CP4A (Fig. 4d - f). Both climate models replicate the spatial pattern of CDD observed in IMERG, where CDD is higher in drylands (compared to the humid Ethiopian Highlands), but P25 underestimates CDD length compared to IMERG and CP4A overestimates CDD length (Table 3). In IMERG, median CDD in drylands is ~38 days, in P25 it is ~18 days and only increases to ~20 days in arid regions (AI < 0.2). Whereas in CP4A there are dry spells of over 100 days across large parts of eastern Ethiopia, northern Somalia, and northern Kenya (Fig. 4f). In humid regions CP4A also overestimates CDD length relative to P25 and IMERG. ~~While both climate models replicate the spatial pattern of CDD observed in IMERG (CDD is higher in drylands), the relative biases of P25/CP4A compared to IMERG are opposing.~~

~~**Figure 4. Percentage of Annual Rainfall delivered as drizzle and maximum number of consecutive dry days. Percentage of mean annual rainfall that falls as 'drizzle', where 'drizzle' is any rain hour with an intensity <= 1 mm/hr (top panel) for IMERG (a), P25 (b), and CP4A (c). Bottom Panel - Mean annual maximum dry spell length, where a dry hour is any hour that receives less than 0.1 mm of rain IMERG (a), P25 (b), and CP4A (c).**~~

~~In drylands, the median longest dry spell in P25 is ~18 days, with an inter-quartile range (IQR) of 11 – 24 days. Even in arid (AI < 0.2) regions median CDD only increased to ~20 days (IQR 13 – 26 days). Whereas in CP4A there are dry spells of over 100 days across large parts of eastern Ethiopia, northern Somalia, and northern Kenya, and the CDD IQR for drylands is 48 – 95 days and 61 – 102 in arid regions. In other words, relative to IMERG, P25 underestimates CDD and CP4A overestimates CDD. In IMERG, median dry spell length in drylands is ~38 days with an IQR 27 – 51 days, which increases to 35 – 55 days in arid regions. The tendency for CP4A to overestimate CDD remains in humid regions, where the median max CDD is ~38 days (IQR 24 – 73 days) versus ~10days (7 – 14 days) and ~13 days (IQR 7 – 19 days) for P25 and IMERG respectively.~~

Fig.~~ures~~ 5a–c compares the ‘extreme’ rainfall ($99^{th}$ percentile of wet hours in the wettest rainy season) and shows both climate models underestimate the magnitude of wet extremes relative to IMERG~~ in humid and dryland regions~~. However, the bias is reduced in CP4A, which is in line with other studies using three-hourly data (Bethou et al., 2019; Kendon et al., 2019; Finney et al., 2019, 2020). The improvement IN~~when using~~ CP4A is more pronounced in drylands (Table 3), whereas ~~, where the median (IQR) hourly 99th percentile values are 15.0 mm (12.4 – 16.3 mm) (IMERG), 12.5 mm (CP4A) (10.9 – 14.4 mm), and 5.8 mm (4.6 – 7.1 mm) (P25). d~~Differences between CP4A and P25 are more muted in humid regions, where the median $99^{th}$ percentile value is ~~just~~ 36% higher in CP4A vs P25 (compared to ~~(~~over~~vs >~~ 110% in drylands)~~),~~ and IQR ranges overlap (Table 3~~CP4A: 8.4 – 11.1 mm and P25: 5.4 – 9.2 mm~~). Also, unlike CP4A, P25 simulates higher $99^{th}$ percentiles in humid (7.1 mm/hr) rather than dryland (5.8 mm/hr) regions, a ~~(7.1 mm vs 5.8 mm), a~~lthough ~~this may be related to the use of wet rather than all hours when computing percentiles~~the 99th percentile may appear lower in drylands (in P25) ~~lower~~because the large number of light rain events (most pronounced in drylands) dilutes the distribution of wet-hour rainfall (not necessarily because absolute rainfall extremes are lower). ~~, as P25 dramatically overestimates the frequency of rainfall (most notably in drylands).~~

Commented [GB9]: Update units to mm/hr.

| **Humid** | Drizzle (% of annual rainfall) | Heavy Rainfall (% of annual rainfall) | $99^{th}$ Percentiles (mm/hr) | Max CDD |
|---|---|---|---|---|
| IMERG | 12.0 – 16.2 | N/A | 14.2 – 19.3 | 7 – 19 days |
| P25 | 30.6 – 46.8 | 5.1 – 13.4 | 5.4 – 9.2 mm/hr | 7 – 14 days |
| CP4A | 14.7 – 20.0 | 8.8 – 13.3 | 8.4 – 11.1 mm/hr | 24 – 73 days |
| **Drylands** | | | | |
| IMERG | 11.6 – 14.8 | N/A | 12.4 – 16.3 mm/hr | 27 – 51 days |
| P25 | 45.2 – 56.6 | 3.8 – 11.0 | 4.6 – 7.1 mm/hr | 11 – 24 days |
| CP4A | 12.5 – 16.6 | 13.5 – 25.4 | 10.9 – 14.4 mm/hr | 48 – 95 days |

**Table 3. Interquartile ranges of the percentage of rainfall delivered as ‘drizzle’ and ‘heavy’ rain, extreme rainfall ($99^{th}$ wet season percentiles), and the maximum number of consecutive dry days (CDD) in humid (AI >= 0.65) and dryland (AI < 0.5) regions of the HOA (see Fig. 1). Where 'drizzle' is any rain hour with an intensity <= 1 mm/hr, and the ‘heavy’ rain threshold is spatially variable and is based on the $95^{th}$ percentile of hourly wet season IMERG rainfall (see Fig. 5d).**

~~Explicitly resolving convection also means A~~a greater proportion of annual rainfall is also delivered via ‘heavy’ rainfall events in CP4A relative to P25 (Fig. 5e ~~d~~– f), most notably in drylands. T~~Figures 5d – f shows t~~he percentage of annual rainfall that falls as ‘heavy’ rainfall is based on the $95^{th}$ percentile of hourly IMERG rainfall ~~, however,~~ rather than using a consistent mm/hr intensity across the entire domain. ~~, we use the $95^{th}$ percentile of IMERG rainfall as our threshold for ‘heavy’ rainfall (Appendix B – Figure 1B).~~ This means our threshold varies (Fig. 5d) grid cell by grid cell (2.3 mm/hr – 10.9 mm/hr in humid regions and 2.9 mm/hr – 16.2 mm/hr in dryland regions) and ensures we reflect the tendency for a greater percentage of rainfall to fall as ‘heavy’ events in drylands. ~~(Fig. 5d). Given we have~~

~~used the IMERG 95th percentile as our threshold, we are more focused on comparing CP4A and P25 to each other rather than IMERG.~~

In western humid regions both ~~CP4A and P25~~models simulate comparable contributions from 'heavy' rainfall, with overlapping IQRs (Table 3), ~~of 8.8% - 18.3% (CP4A) and 5.1% - 13.4% (P25). W~~whereas in drylands ~~to the east,~~ the IQR of the percentage of annual rainfall falling during 'heavy' events is 13.5% - 25.4% in CP4A versus 3.8% - 11.0% in P25 (Table 3). In arid regions (eastern Ethiopia and Somalia) the difference is more pronounced, with the median contributions of heavy rainfall being 21.5% and 7.8% in CP4A and P25 respectively. ~~This difference becomes more pronounced in the arid regions of eastern Ethiopia and Somalia where the median values are 21.5% and 7.8%~~

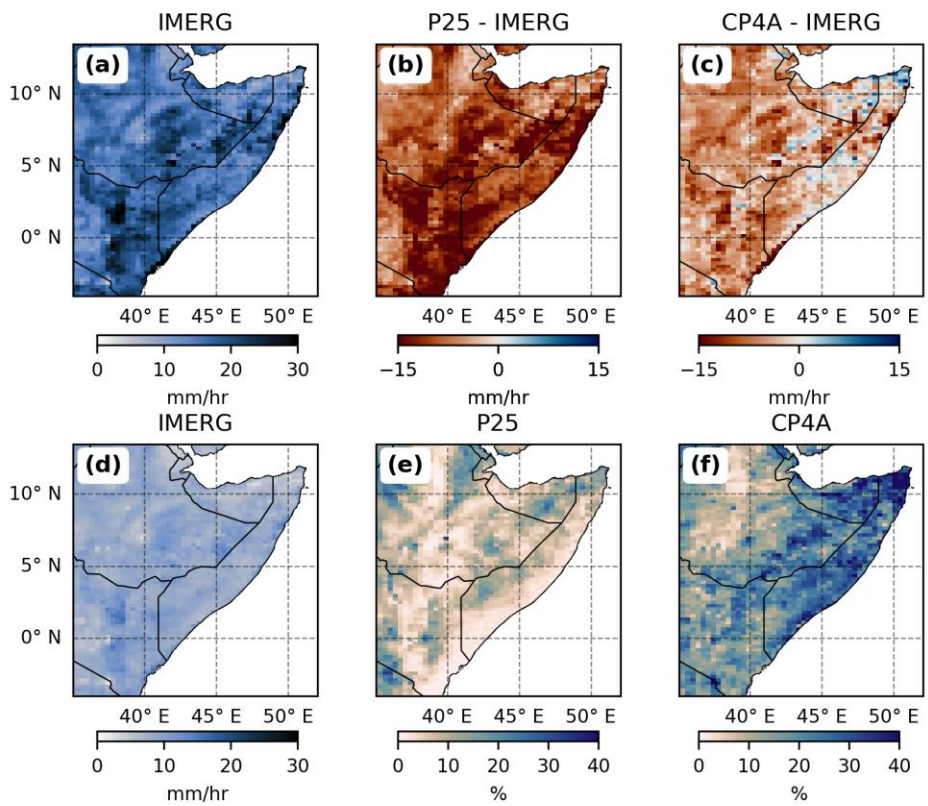


~~respectively.~~ CP4A also better replicates the spatial pattern one would expect, ~~observed in IMERG,~~ where dryland regions in the east tend to receive more rainfall via 'heavy' events relative to humid regions in the west (median values of 19.2% vs 13.8%), whereas the opposite is true ~~true~~ in P25 (median values of 6.8% vs 8.4%).

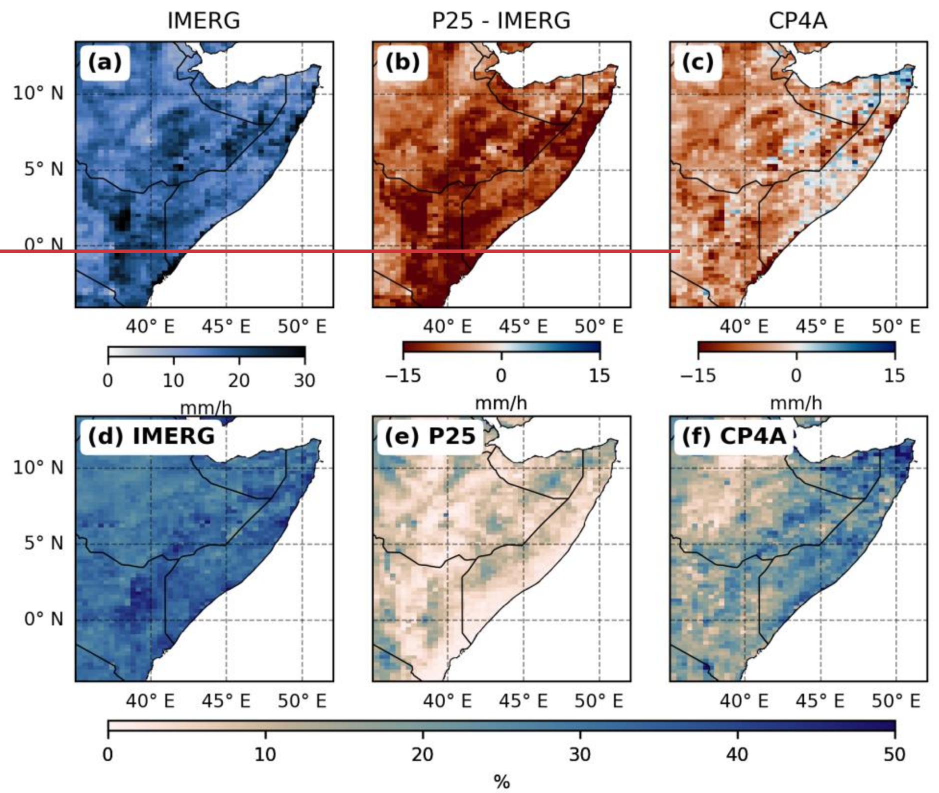


**Figure 5. 99th Percentiles and percentage of rainfall delivered via 'heavy' events. Wet season 'extreme' precipitation (top panel) for IMERG observations (a), and ~~differences~~ anomalies with respect to IMERG for P25 (b) and CP4A (c). Extreme precipitation is defined as the 99th percentile of all wet hours, where wet hours are any hours that receive >= 0.1 mm of rain. Bottom Panel ~~–~~ 95th percentile of all wet hours in IMERG observations (d), this is used as the 'heavy' rain threshold for panels (e) and (f), which show the p~~P~~ercentage of ~~mean~~ annual rainfall that falls as~~during~~ 'heavy' rainfall in ~~events~~P25 (e) and CP4A (f)~~, in this context we are defining a 'heavy' rainfall event as the 95th percentile of IMERG rainfall (wet hours)~~ respectively.~~.~~**

## 3.2 Potential Evapotranspiration (PET)

PET derived from climate model atmospheric variables captures the seasonal (Fig. 6e-g) and diurnal cycle (Fig. 6d-f) seen in hPET, although both models simulate earlier peaks in diurnal PET (12:00 vs 13:00). Both models also correctly simulate higher evaporative demand in eastern drylands compared to the more humid Ethiopian Highlands (Fig. 6a–c) and produce comparable annual magnitudes (hPET – 1715 mm, CP4A – 1787 mm, P25 – 1883 mm). CP4A

### ~~3.2 Potential Evapotranspiration (PET)~~

~~Calculating PET with climate model atmospheric variables replicates the spatial pattern of PET given by hPET, with higher evaporative demand across the drylands in the east compared to the more humid Ethiopian Highlands (Fig. 6a–c), and generally provide reasonable annual PET magnitudes across the region (hPET – 1715 mm, CP4A – 1787 mm, P25 – 1883 mm). CP4A~~ simulates marginally higher mean annual PET ~~(relative to P25)~~ in humid regions (1416 mm vs 1387 mm)~~,~~ but lower ~~while the opposite is true~~ in arid regions (1901 mm vs 2027 mm). The most pronounced differences are in ~~in PET simulations between CP4A and P25 is the~~ arid ~~regions of~~ Somalia and Eastern Ethiopia (Fig. 6g), where ~~. Across any grid cells classified as arid,~~ CP4A ~~simulates PET that~~ exceeds 2000 mm ~~a~~yr$^{-1}$ in ~~just~~ 18% of cells~~,~~ versus 53% and 43% in P25 and hPET, respectively.

During dry seasons (JF, JJAS) in arid regions, P25 PET (median = 1098 mm yr$^{-1}$) exceeds CP4A (1000 mm yr$^{-1}$) and hPET (1035 mm yr$^{-1}$). In rainy seasons (MAM, OND), P25 PET remains higher (905 mm yr$^{-1}$) relative to CP4A (860 mm), but lower compared to hPET (912 mm). Multi-linear regression (MLR) attributes CP4A-P25 PET differences mainly to temperature and dew point temperature (in both humid and dryland regions), with meridional wind speed also important in drylands (Appendix C - Table C1), with higher P25 wind speeds during JJAS partly driving the higher P25 PET during JJAS (Appendix C – Fig. C2).

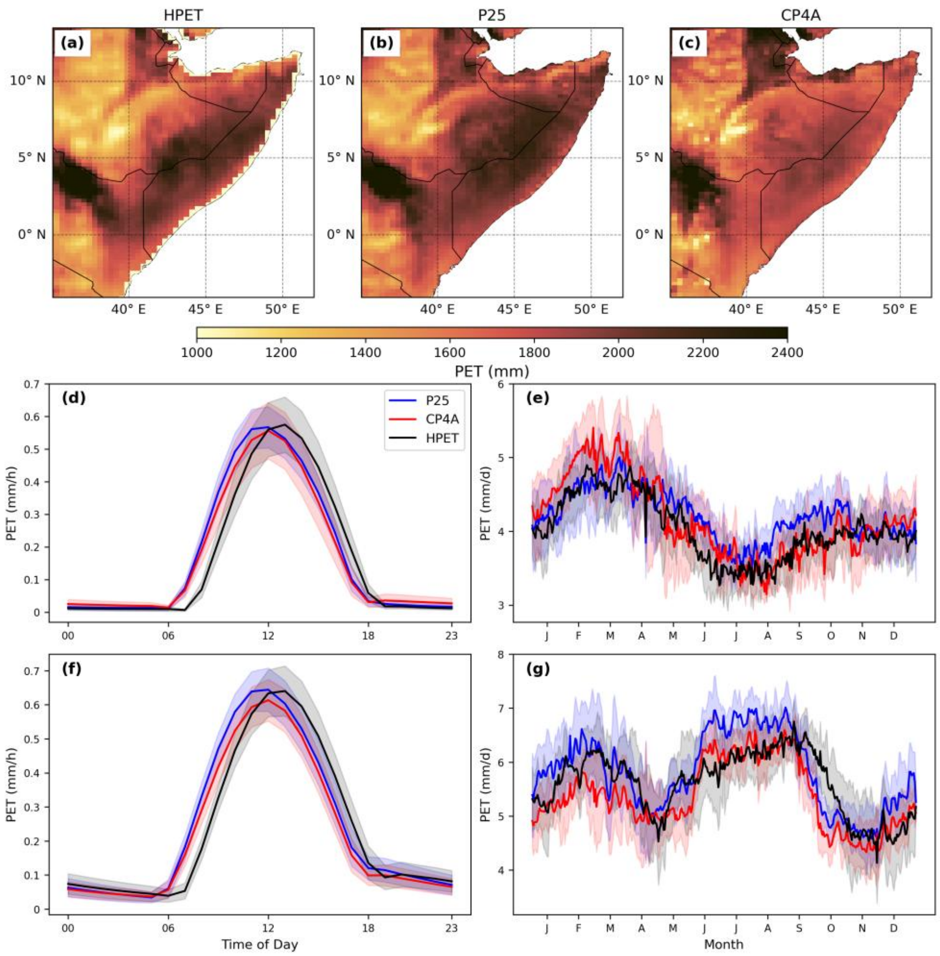


**Figure 6. Mean annual PET, diurnal PET cycle, and daily climatology of PET. Spatial plots of mean annual PET (top panel) for HPET observations (a), P25 (b), and CP4A (c). Mean diurnal cycle and daily climatology of PET in humid (AI >= 0.65) (middle panel) and arid to hyper-arid (AI <= 0.2) (bottom panel) regions of the Horn of Africa for HPET, P25, and CP4A.**

During dry seasons (JF, JJAS) ~~Both climate models also simulate a clear diurnal cycle (Fig. 6d-f) and replicate the hPET seasonal cycle (Fig. 6e-g) in both humid and arid regions, although, both models simulate earlier peaks in diurnal PET compared to hPET (12:00 vs 13:00). i~~In arid regions, P25 PET (median = 1098 mm $yr^{-1}$) exceeds CP4A (1000 mm $yr^{-1}$) and hPET (1035 mm $yr^{-1}$). In rainy seasons (MAM, OND), P25 PET remains ~~tends to simulate higher PET during the dry seasons of Jan-Feb and Jun-Sep relative to both CP4A and hPET (Fig. 6g), the IQR ranges (medians)~~

~~for each dataset in arid regions during dry seasons (JF & JJAS) are as follows: hPET: 919 mm – 1135 mm (1035 mm), CP4A: 908 mm – 1086 mm (1000 mm), P25 is 978 mm – 1185 mm (1098 mm). During the rainy seasons (MAM & OND) P25 also simulates~~ higher~~ PET~~ (905 mm ~~)~~yr$^{-1}$~~) in arid regions~~ relative to CP4A (860 mm), but lower ~~PET~~ compared to hPET (912 mm).

Multi-linear regression (MLR) attributes CP4A-P25 PET~~shows~~ differences mainly to ~~in~~ temperature and dew point temperature ~~(explain most PET variability~~ in both humid and dryland regions), ~~in both climate models (Appendix B - Table B1)~~with ~~. Although in dryland regions~~ meridional wind speed also important in drylands ~~exerts a significant effect on PET~~ (Appendix C~~B~~ - Table C~~B~~1), with higher P25 wind speeds ~~in P25~~ during JJAS ~~appearing to be~~ partly driving the higher P25 PET during JJAS (Appendix C~~B~~ – Fig.~~ure~~ ~~2~~C2~~B~~).

### 3.3 Water Partitioning

At ~~each hydrological study~~ all study sites, CP4A and P25 ~~correctly simulate the~~ reproduce the seasonal cycle of rainfall and~~ tend to~~ produced broadly comparable seasonal totals (Appendix D~~C~~ – Fig.~~ure~~ ~~1~~D1~~C~~), though ~~although on average~~ P25 delivers~~s~~ higher annual rainfall (Table 4~~2~~). Both models also produced comparable ~~seasonal~~ PET totals and simulated the same seasonal cycle, although P25 simulates substantially higher PET during JJAS at Site HA (Appendix D~~C~~ – Fig.~~ure~~ D~~2~~2~~C~~)~~.~~, Critically, ~~following the results discussed in section 3.2. d~~~~Critically, the d~~differences in rainfall characteristics follow the results discussed above in section 3.1~~, meaning at each site CP4A tends to deliver more rainfall via infrequent and intense events, while P25 delivers rainfall via near-continuous drizzle. A full breakdown of the metrics discussed above (CDD, 99th percentiles, % of rainfall delivered via 'drizzle' vs 'heavy' events) for each site is given below in (~~(Table 4)~~2~~.

| | Site HU | Site SA | Site A | Site HA |
|---|---|---|---|---|
| P25 Total Rainfall (mm) | 2000 | 670 | 430 | 240 |
| CP4A Total Rainfall (mm) | 1730 | 600 | 350 | 180 |
| P25 Total 'Drizzle' (mm) **(% of Annual Total)** | 650 **(33%)** | 358 **(53%)** | 234 **(54%)** | 133 **(55%)** |
| CP4A Total 'Drizzle' (mm) **(% of Annual Total)** | 329 **(19%)** | 80 **(13%)** | 40 **(11%)** | 22 **(12%)** |
| P25 Total 'Heavy' Rain (mm) **(% of Annual Total)** | 449 **(22%)** | 75 **(11%)** | 53 **(12%)** | 71 **(30%)** |
| CP4A Total 'Heavy' Rain (mm) **(% of Annual Total)** | 378 **(22%)** | 149 **(25%)** | 170 **(49%)** | 148 **(82%)** |
| P25 99th Percentile (mm/hr) | 8.5 | 5.8 | 5.5 | 4.3 |
| CP4A 99th Percentile (mm/hr) | 9.1 | 15.6 | 11.2 | 17.9 |
| P25 Max CDD (days) | 13 | 12 | 8 | 20 |
| CP4A Max CDD (days) | 41 | 43 | 105 | 107 |

**Table 4~~2~~. Mean annual rainfall, 'drizzle', 'heavy" rain, 99th wet season percentiles, and maximum number of consecutive dry days (CDD) at each of our four sites. The percentage of annual rainfall that falls as 'drizzle' or 'heavy' rain (based on the 95th percentile of hourly wet season IMERG rainfall) is given in brackets.**

~~From our Hydrus 1-D simulations we analysed soil moisture, surface runoff, evaporation, transpiration, and bottom drainage.~~ Fig. 7a-d shows histograms of depth-integrated soil moisture (% soil saturation in entire 300 cm of the soil profile)~~θs~~, where soil moisture is expressed as a saturation percentage (given the symbol θs). Soil saturation reflects the proportion of pore spaces filled with water relative to if all pore space is saturated (e.g. 100% means all pore space is filled with water, 0% means all pores are filled with air) ~~(% soil saturation in entire 300 cm of the soil profile) at each site,~~ . ~~where~~D ~~d~~espite simulating lower total rainfall, forcing Hydrus with CP4A rainfall results in higher θs at all dryland locations (Table 5), although the IQR of θs still overlap at all sites other than Site HA. Focusing on the depth-integrated θs masks differences relative to θs at specific depths. For example, the relative difference in θs between driving Hydrus with CP4A (vs P25) at Site SA increases from + 7.5% at a depth of 90 cm, to 16.1% at 2.1 mbgl, while at Site HA the difference ranges from 17.0% (0.2 mbgl) to 23.1% (1.2 mbgl). There are statistically significant differences (p-values are statistically significant to 95% confidence) in medians (Mann-Whitney) and distributions (Kolmogorov-Smirnov) at all depths (see Appendix D - Table D1 for depth intervals) and all sites (including Site HU), with the KS Test Statistic increasing with depth (Appendix D - Table D1). Calculating the KS Test Statistic using the entire depth-integrated θs values shows differences in distributions are more pronounced in drylands (KS Test Statistics: HU– 0.08, SA – 0.29, A – 0.37, HA – 0.92). ~~. While there is statistically significant difference in medians (Mann-Whitney) and distributions (Kolmogorov-Smirnov) at all sites, the differences are more pronounced in drylands (KS statistics: HU 0.08, SA – 0.29, A – 0.37, HA – 0.92). Within the three-meter profile, the IQR of θs using CP4A (P25) is 42.7% - 59.0% (35.4% - 45.1%), 29.74% - 33.7% (27.0% - 30.8%), 47.8% - 49.5% (40.5% - 41.1%), 60.6% - 77.7% (59.6% - 79.4%) at sites SA, A, HA, and HU, respectively (differences at site A are more pronounced if we consider depth-integrated θs at 1.2 mbgl, as below this depth there are minimal fluxes) (Appendix C – Table C1).~~

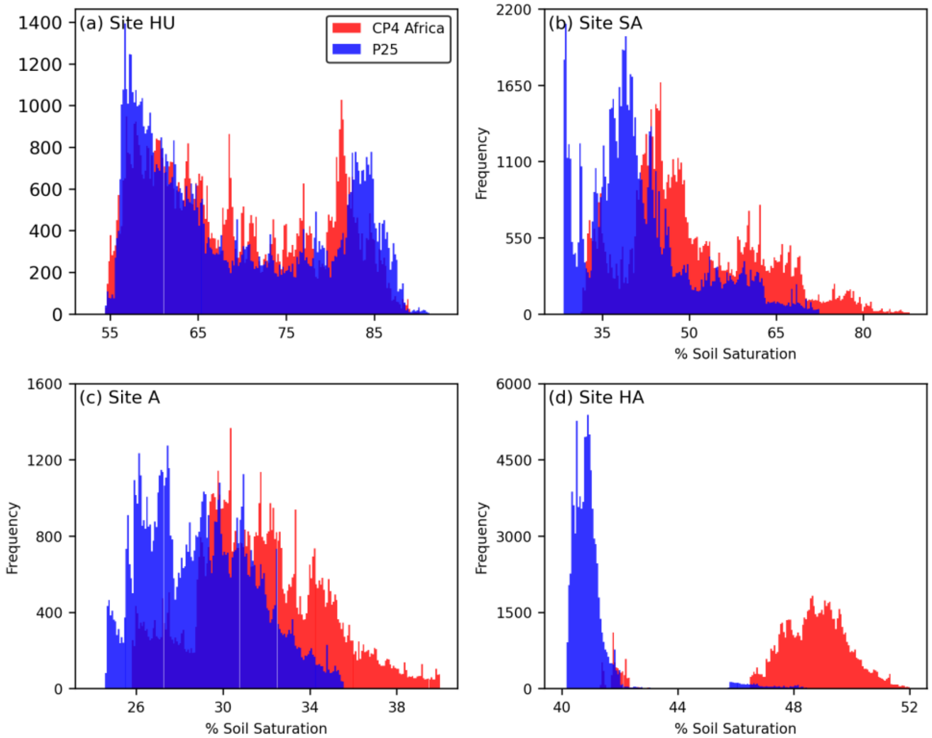
(a) Site HU
CP4 Africa
P25
(b) Site SA
(c) Site A
(d) Site HA
Frequency
% Soil Saturation
1400
1200
1000
800
600
400
200
0
55
65
75
85
2200
1650
1100
550
35
50
65
80
1600
26
30
34
38
6000
4500
3000
1500
40
44
48
52

~~At all depths (20 - 40 cm intervals) and at every location there are statistically significant differences in θs between CP4A and P25 for both medians and distributions, with differences in the KS statistic generally increasing with depth (Appendix C - Table C3). Depth-integrated θs masks differences in median θs relative to taking median θs at specific depths. For example, the relative difference in θs between driving Hydrus with CP4A (vs P25) at Site SA increases from + 7.5% at a depth of 90 cm, to 16.1% at 2.1 mbgl, while at Site HA the difference ranges from 17.0% (0.2 mbgl) to 23.1% (1.2 mbgl).~~

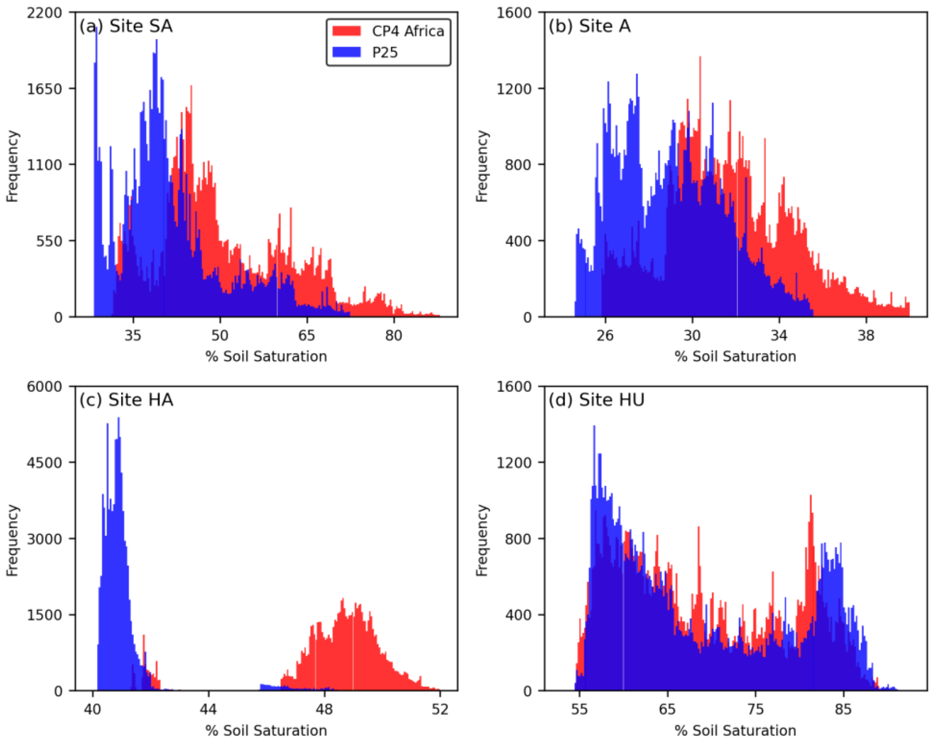


**Figure 7. Depth Integrated Soil Moisture Distributions. Modelled distribution of depth integrated soil moisture in the three-meter soil profile when driving Hydrus using P25 (blue) and CP4A (red) rainfall and PET at our humid ~~semi-arid~~ (a), semi-arid (b), ~~hyper-~~arid (c), and hyper-arid ~~humid~~ sites~~locations~~ (d).**

| 1.2 Meters Below Ground Level | Site SA | Site A | Site HA | Site HU |
|---|---|---|---|---|
| CP4A | 49.7 - 63.6 | 37.7 - 46.5 | 47.2 - 51.3 | 53.0 - 78.9 |
| P25 | 43.4 - 58.2 | 31.4 - 41.0 | 39.7 - 41.1 | 51.6 - 81.3 |
| **3.0 Meters Below Ground Level** | | | | |
| CP4A | 42.7 - 59.0 | 29.7 - 33.7 | 47.8 - 49.5 | 60.6 - 77.7 |
| P25 | 35.4 - 45.1 | 27.0 - 30.8 | 40.5 - 41.1 | 59.6 - 79.4 |

**Table 5 – Interquartile ranges of depth integrated soil moisture in the upper 1.2 meters of the soil profile (top), and the entire three-meter profile (bottom) in our CP4A and P25 default (soil and Feddes' parameters) runs. All values refer to the % saturation.**

~~The finding that driving Hydrus with CP4A rainfall and PET yields higher soil moisture remains consistent regardless of the soil hydraulic parameters used (Appendix C – Table C2), or for Sites SA and A where shrubs are the dominant vegetations, regardless of the Feddes' parameters used (Appendix C – Table C4).~~

Fig.~~ures~~ 8a-h visualises the deeper wetting fronts in drylands when forcing Hydrus with CP4A, most notably at Sites SA and HA. ~~These differences in~~Shallower wetting fronts in P25 ~~depth~~ could have ecological implications, ~~when using CP4A or P25 to model crop or vegetation health modelling.~~ f~~F~~or example, ~~while differences in median depth integrated θs at Site A is less than three percentage points, shallower wetting fronts~~at Site A ~~means~~ θs is above the wilting point (WP) (for shrubs) at a depth of 1.2 mbgl for ~~0-~~44% of the Hydrus simulation ~~when forced using P25 (depending on whether you use the upper or lower WP threshold – see Appendix A Table A2),~~compared to 83% using CP4A (Fig. 9b). However, it is important to note that this is using the 'upper' default Feddes' shrub parameters (Appendix B - Table B2), if one uses the 'lower' Feddes' parameters soil moisture never exceeds the wilting point in P25 ('upper' WP = ~25%, 'mid' WP = ~ 55%). ~~but the range is 1-83% using CP4A (Fig. 8b).~~ It is a similar story at

Site SA, where $\theta$s is above WP for 27~~-100~~% of the time using P25 ~~,~~ versus 50~~-100~~% using CP4A based on the 'upper' Feddes' parameter set (Fig. 9~~8~~a).

The large WP range depending on choice of Feddes' parameters highlights the importance of ~~se results also highlight the need to acc~~accurately quantifying the Feddes' parameters used for any given vegetation~~, as varying the threshold used to define the WP based on the shrub Feddes' parameters given by Sela et al (2015)~~ (Fig.~~Appendix~~ 9~~A – Table A2~~). ~~can reduce the time at which $\theta$s is above the WP at Site SA from 83% to 1% for CP4A and 44% to 0% for P25 respectively.~~ But the key finding is that ~~regardless of the Feddes' parameters used,~~ $\theta$s is either above the wilting point

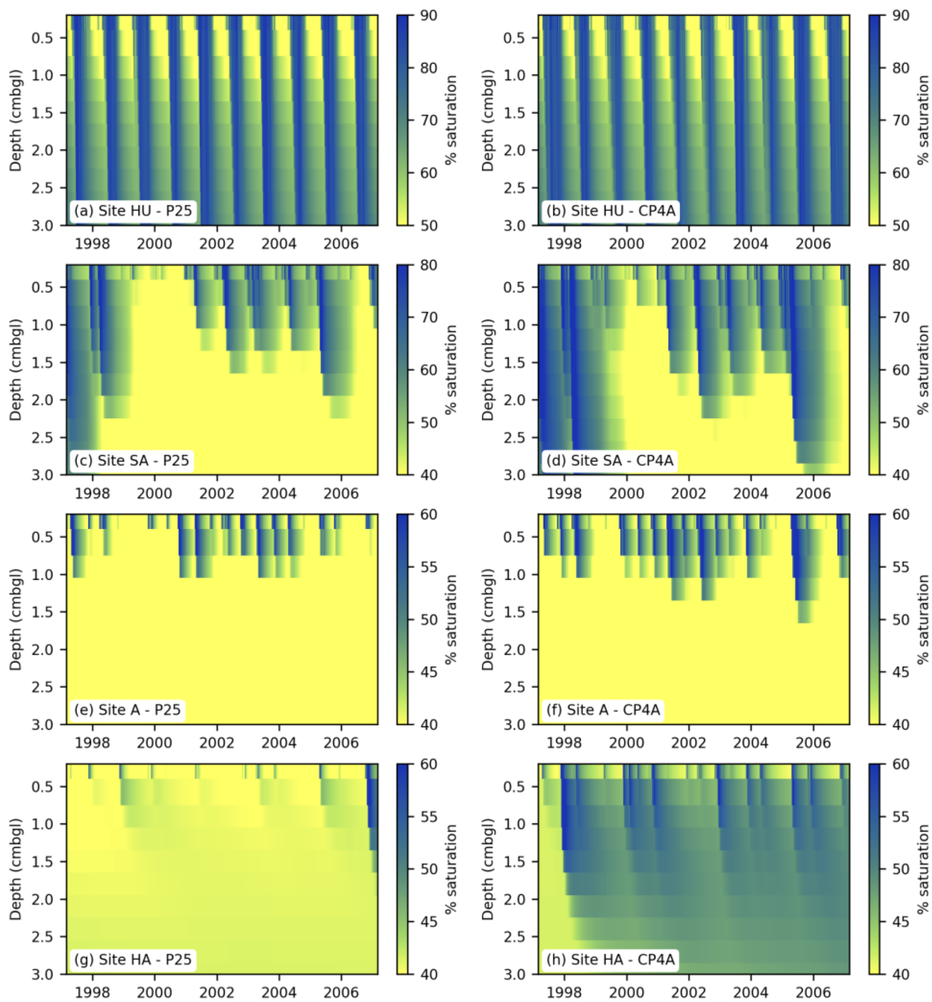

for longer when forcing Hydrus with CP4A, or where both models simulate θs as always above the WP, using CP4A means θs is high enough for vegetation to transpire at the maximum rate for longer (Site SA – 78% vs 57%, Site A – 13% vs 0%). The same is true when varying the soil hydraulic parameters, the finding that driving Hydrus with CP4A rainfall and PET yields higher soil moisture remains consistent (Appendix D - Table D2).

**Figure 8. Modelled soil moisture profiles using P25 (left) and CP4A (right) rainfall and PET to drive Hydrus at our humid (a-b), semi-arid (c-d), arid (e-f), and hyper-arid (g-h) sites across the HOA.**

~~To establish whether higher soil moisture in Hydrus CP4A sims were a function of differences in rainfall characteristics or simply lower PET in CP4A at each site, we~~We also forced Hydrus with climate model rainfall and hPET (rather than model PET), where once again~~. Once again,~~ at all depths and at every site, there are statistically significant differences in θs between Hydrus simulations~~ when forced with CP4A/P25 rainfall and hPET~~, although KS test statistics are marginally lower (Appendix D~~C~~ – Table ~~5~~D4~~C~~). However, PET alone can exert an influence; the percentage of time θs is above the WP at Site SA is lower when forcing Hydrus with CP4A rainfall and hPET (41% vs 50%), although θs is still above ~~these thresholds~~the WP for longer using CP4A compared to P25 (41% vs 24%). The reduction is especially pronounced when considering the WP at Site A, where the percentage of time θs is above the WP (using the ~~lower~~ 'upper' Feddes parameter set~~WP threshold~~) drops from 83/44% to 44/21% for CP4A and P25 respectively. ~~when running Hydrus with hPET.~~That there is a reduction ~~is a reduction~~ in soil ~~mositure~~ moisture when using hPET despite PET being ~~rainfall~~lower than P25 PET~~the PET from~~ highlights how offsets offsets between rainfall and PET can influence the antecedent conditions that govern hydrological responses to rainfall.

Commented [KM10]: I don't understand what this means

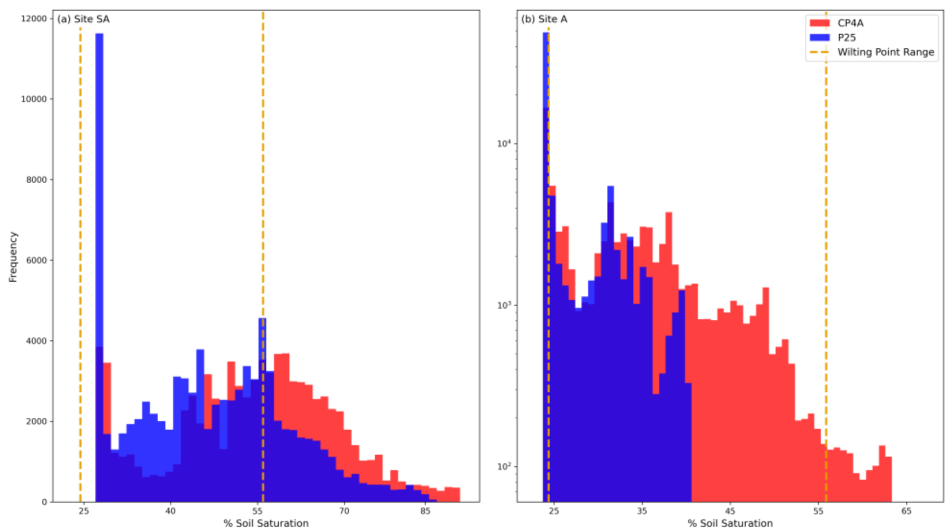
(a) Site SA
(b) Site A
CP4A
P25
Wilting Point Range
Frequency
% Soil Saturation
% Soil Saturation

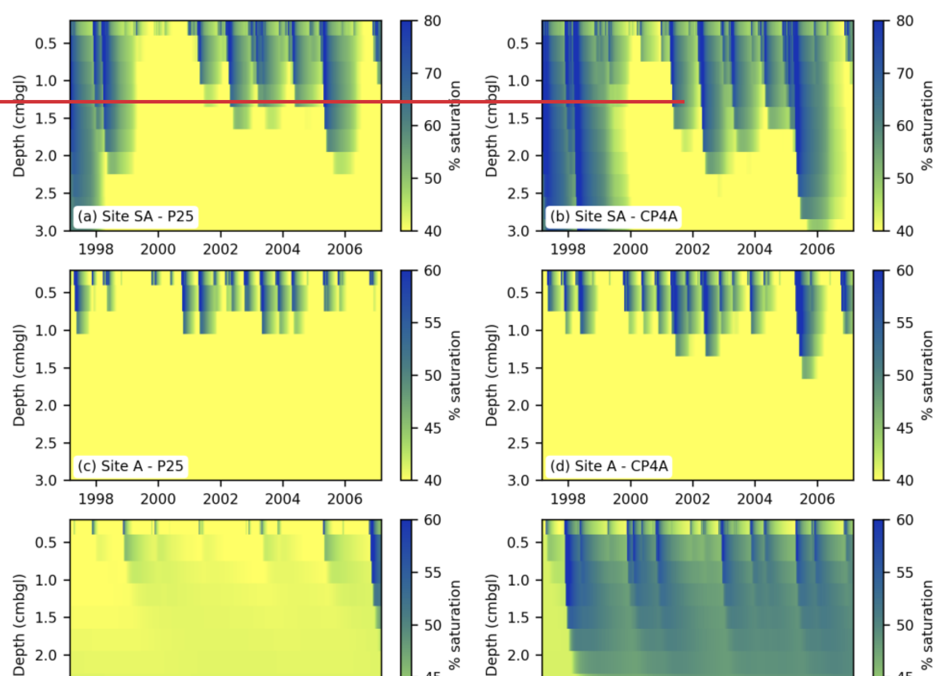
(a) Site SA - P25
(b) Site SA - CP4A
(c) Site A - P25
(d) Site A - CP4A
Depth (cmbgl)
% saturation

~~**Figure 8. Modelled soil moisture profiles using P25 (left) and CP4A (right) rainfall and PET to drive Hydrus at our semi-arid (a-b), arid (c-d), hyper-arid (e-f), and humid (g-h) locations across the HOA.**~~

**Figure 9. Soil Moisture Distributions with Wilting Points at Sites SA & A. Modelled distribution of soil moisture at 1.2 mbgl at Site SA (a) and A (b) using P25 (blue) and CP4A (red) rainfall and PET. The dashed orange lines represent the wilting point range for Acacia shrubs, based on taking the upper and lower Feddes' parameters given in Appendix 2 - Table B2 (wilting point = *P2H*) (Sela et al, 2015).**

Fig~~ure~~ 10 details how water is partitioned between surface runoff, evaporation, transpiration, and bottom drainage at our dryland sites when CP4A/P25 rainfall and PET is propagated through Hydrus (for clarity infiltration and Site HU data is not included in Fig. 10, but can be seen in ~~also see Appendix C~~ Table ~~6~~6~~C~~). Given that $\theta$s tends to be above the WP for longer in the CP4A runs, and shrubs can transpire at the maximum rate for longer, it is unsurprising that Fig~~s~~. 10a - f shows substantially higher transpiration at our semi-arid and arid sites ~~Sites SA (2392 mm vs 1724 mm) & A (893 mm vs 694)~~ when using CP4A (Table 6) ~~rainfall~~ despite total infiltration being lower. ~~. The difference in the relative percentage of infiltration lost to transpiration is even more pronounced, as P25 simulates higher total rainfall and lower surface runoff (Fig. 10a). Higher transpiration totals in drylands are~~ The ~~due to the s~~shallower wetting fronts when using ~~-~~P25 ~~rainfall~~ means ~~resulting in higher~~ evaporative losses are higher (Table 6), with ~~, at SA & A~~ 79%-83% of infiltration ~~is~~ returned to the atmosphere ~~when Hydrus is forced with P25~~at sites SA & A respectively, versus 67% – 72% using CP4A rainfall. Whereas at ~~At Site HA the respective values are 92% vs 98%, while at~~ Site HU evaporative losses are near identical (23.3% vs 23.6%)~~,~~ and transpiration is higher in the P25 Hydrus simulations (~~Appendix C~~ Table 6~~C~~).

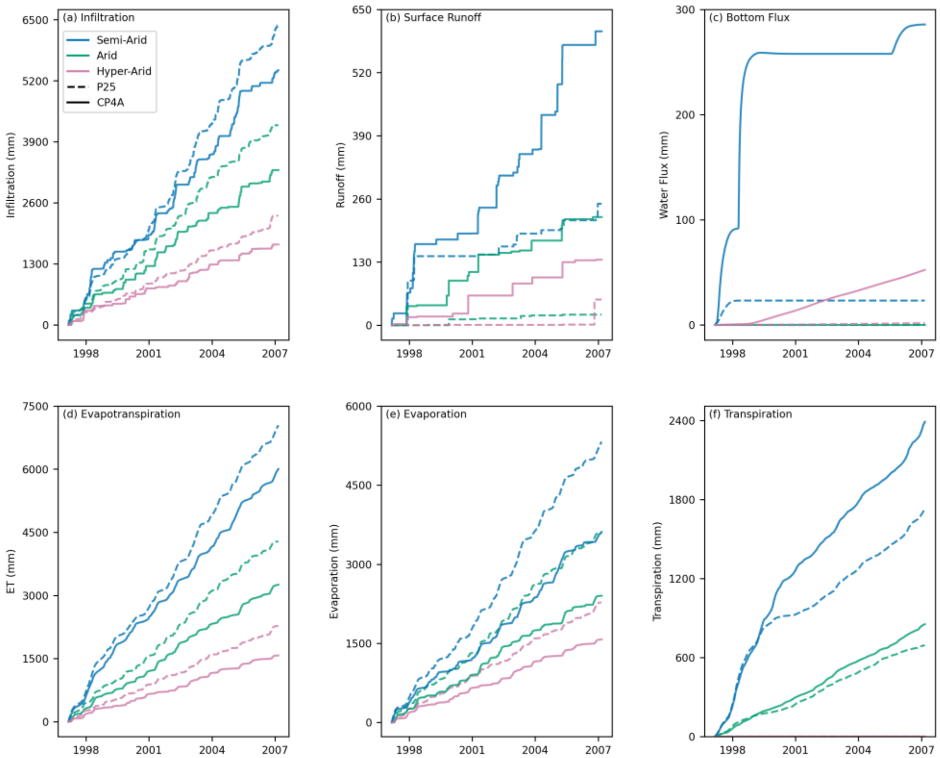

(a) Infiltration
Semi-Arid
Arid
Hyper-Arid
P25
CP4A
Infiltration (mm)
(b) Surface Runoff
Runoff (mm)
(c) Bottom Flux
Water Flux (mm)
(d) Evapotranspiration
ET (mm)
(e) Evaporation
Evaporation (mm)
(f) Transpiration
Transpiration (mm)
1998
2001
2004
2007


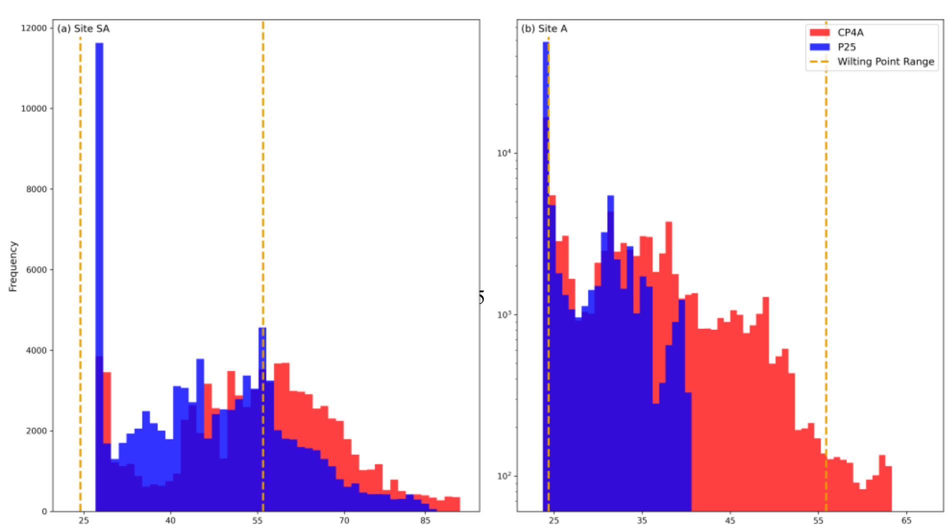

(a) Site SA
Frequency
% Soil Saturation
(b) Site A
CP4A
P25
Wilting Point Range
% Soil Saturation

~~**Figure 9. Soil Moisture Distributions with Wilting Points. Modelled distribution of soil moisture at 1.2 mbgl at Site SA (a) and A (b) using P25 (blue) and CP4A (red) rainfall and PET. Green dashed line (a) marks the 0s threshold at which shrub roots can no longer extract water at the maximum rate, red dashed line (b) marks the wilting point.**~~

**Figure 10. Cumulative Infiltration Runoff, Surface Runoff, Bottom Drainage, Evapotranspiration, Evaporation, and Transpiration. Modelled components of the water balance using CP4A (solid lines) and P25 (dashed lines) rainfall/PET as input for Hydrus 1-D at each of our dryland sites – Site SA (blue), Site A (green), and Site HA (pink). Plots show cumulative infiltration (a), surface run-off (b), bottom drainage (c), evapotranspiration (d), evaporation (e), and transpiration (f). So, for example, the solid blue line shows the CP4A semi-arid simulations, and the pink dashed line is the P25 hyper-arid simulation. To avoid using multiple axis, Site HU is not included, but the raw values are given in Table 6.**

~~Higher evaporative losses when forcing Hydrus with P25 rainfall are not solely related to higher climate model PET using P25, it remains consistent~~ E~~e~~ven when forcing Hydrus with hPET (rather than model PET) (Appendix D~~C~~ – Table ~~7~~D5~~C~~) evaporative losses are higher when using P25, the percentage of rainfall lost to evaporation in P25 (CP4A) simulations are 24% (23%), 81% (66%), 88% (75%), and 96% (90%) at Sites HU, SA, A, and HA respectively. In ~~. Counterintuitively, in~~ the CP4A runs, using hPET ~~increases evaporative losses by 4%-9% across the four sites despite mean annual lower PET being lower (temporal offsets in rainfall and evaporative demand can impact hydrological fluxes). However, while enhanced evaporative losses in CP4A Hydrus runs forced with hPET~~ reduces transpiration totals, but they remain significantly higher than P25 runs in drylands (30%-36% higher in absolute terms) (Appendix D~~C~~ – Table ~~7~~D5~~C~~). Transpiration totals are also obviously sensitive to the Feddes' parameters used, but it doesn't impact the relative bias in totals between the ~~CP4A~~CP4A and P25 Hydrus runs (Appendix D~~C~~ – Table ~~8~~D7~~C~~).

Surface runoff is also greater when using CP4A rainfall despite lower annual totals (Table 6), in dryland locations, between 6% and 10% of rainfall is lost to runoff in the CP4 Hydrus runs versus 0.3 - 2% with P25 rainfall. There are also large differences in bottom drainage from the soil profile, 286 vs 23 mm at Site SA and 52 vs 2 mm at Site HA (there was no drainage at Site A). Bottom drainage is lower in the hPET runs for both climate models, but the relative bias remains (Appendix D – Table D6). Drainage is also sensitive to the soil and Feddes' parameters used, but again in all cases CP4A runs simulate higher bottom drainage at our dryland sites (Appendix D – Table D6 & D7). Whereas at our humid location (Site HU) P25 simulated 21% higher bottom drainage, closely following the difference in the volume of cumulative rainfall delivered (15%) (Table 6).

| Default Hydrus Run | Rainfall (mm) | PET (mm) | Runoff (mm) | Infiltration (mm) | ET (mm) | Evaporation (mm) | Transpiration (mm) | Drainage (mm) |
|---|---|---|---|---|---|---|---|---|
| Site HU | 17333 (20003) | 13982 (12894) | 0 (30) | 17300 (19863) | 10474 (11418) | 4030 (4693) | 6445 (6725) | 7154 (8638) |
| Site SA | 5952 (6669) | 15750 (16230) | 605 (250) | 5423 (6398) | 6003 (7044) | 3611 (5320) | 2392 (1724) | 286 (23) |
| Site A | 3521 (4289) | 19233 (21817) | 223 (22) | 3297 (4254) | 3255 (4283) | 2402 (3598) | 853 (694) | 0 (0) |

| | | | | | | | | |
|---|---|---|---|---|---|---|---|---|
| Site HA | 1849 (2394) | 17181 (19714) | 135 (53) | 1713 (2328) | N/A | 1574 (2277) | N/A | 52 (2) |
| ~~Site HU~~ | ~~17333 (20003)~~ | ~~13982 (12894)~~ | ~~0 (30)~~ | ~~17300 (19863)~~ | ~~10474 (11418)~~ | ~~4030 (4693)~~ | ~~6445 (6725)~~ | ~~7154 (8638)~~ |

Table 6 – Cumulative rainfall, potential evapotranspiration (PET), runoff, infiltration, evapotranspiration (ET), evaporation, transpiration, and drainage from the bottom of the soil profile. All values are given in mm and are the totals over the entire ten-year Hydrus simulations. All results are taken from the default (soil and Feddes' parameters) Hydrus runs forced with CP4A/P25 rainfall/PET. Those values given in brackets are the P25 Hydrus runs, non-brackets are CP4A.

~~**Figure 10. Cumulative Rainfall, PET, Runoff, Evaporation, Transpiration, and Deep Infiltration. Modelled components of the water balance using CP4A (solid lines) and P25 (dashed lines) rainfall/PET as input for Hydrus 1-D. Plots show the infiltration (a), surface run-off (b), bottom drainage (c), evapotranspiration (d), evaporation (e), and transpiration (f) at our semi-arid, arid, and hyper-arid locations.**~~

~~Despite lower total rainfall at our dryland sites, surface runoff is greater when using CP4A rainfall, over twice as high as P25 at Sites SA and HA (605 mm vs 250 mm & 135 vs 53 mm), and up to ten times higher at Site A (223 mm vs 22 mm). In dryland locations, between 6% and 10% of rainfall is lost to runoff when Hydrus is forced with CP4A rainfall versus 0.3 - 2% with P25 rainfall. There are also large differences in bottom drainage from the soil profile, htheowever it is important to note thatthe this metric is not indicative of groundwater recharge, as in reality it is unlikely the water table would be so shallow,~~

~~and moisture could still be lost to transpiration through deep rooted shrubs (Stone and Kalisz, 1991; Maeght et al., 2013; Shadwell and February 2017). Driving Hydrus with CP4A rainfall produces higher bottom drainage at dryland sites despite receiving less rainfall overall; 283 vs 23 mm at Site SA and 52 vs 2 mm at Site HA (there was no drainage at Site A. At our humid location (Site HU) P25 simulated 21% higher bottom drainage, closely following the difference in the volume of cumulative rainfall delivered (15%).~~

**4. Discussion**

In this paper we evaluated how climate model representation of convection influences ~~its representation of~~ rainfall characteristics and PET dynamics~~characteristics~~ across the Horn of Africa (HOA), and what impact this has on the 1D water balance at four sites along an aridity gradient in the HOA. In line with other studies, we find that climate models that explicitly resolve convection (CPMs) capture key dryland rainfall characteristics more effectively than those that parameterise ~~convection-permitting climate models (CPMs) perform better than parameterised climate models (those that parameterise~~ the average effects of convection~~)~~ (when compared against satellite-derived rainfall observations). ~~(in terms of capturing key dryland rainfall metrics). So~~B~~ while b~~oth CP4A and P25 simulate comparable annual/seasonal totals, but they deliver rainfall ~~they deliver their their rainfall characteristics are~~is ~~in~~ fundamentally ~~opposing manners~~ different ways (light/frequent vs heavy/infrequent), resulting in ~~differing~~distinct hydrological outcomes at a point-based scale when their output is propagated through a vadose-zone hydrological model. This study also verifies that while dryland vadose-zone hydrology is more sensitive to PET than in humid regions, water partitioning is far more sensitive to ~~(light/frequent vs heavy/infrequent), resulting in differing~~

~~hydrological outcomes when their output is propagated through a hydrological model. This study also verifies that while dryland hydrology is more sensitive to PET than humid regions, differing hydrological outcomes are primarily driven by~~ rainfall characteristics (not rainfall totals or PET), and ~~climate model representation of~~convective representation ~~convection~~ exerts a greater control on rainfall dynamics compared to ~~over~~ PET.

Our modelling supports other work demonstrating that water partitioning in drylands is sensitive to the magnitude-duration spectrum of rainfall (R Taylor et al., 2013; Arpuv et al., 2017; Singer and Michaelides, 2017; Cuthbert et al., 2019; Kipkemoi et al., 2021; Adloff et al., 2022, Quichimbo et al., 2023), whereas in humid regions hydrological fluxes are more closely tied to seasonal rainfall totals. Our direct comparison between CPM and a traditional parameterised model (P25) provides another stark example of the importance of rainfall characteristics, where despite both models using the same global model configuration (Walters et al., 2017), simulating comparable annual totals, and seasonal cycles (Wainwright et al., 2021), hydrological outcomes differ significantly in the dryland vadose-zone when climate model rainfall is propagated through a simple 1-D model. This highlights that while any hydrological study must carefully select the driving datasets, the importance of this choice increases in drylands as one must explicitly consider both rainfall totals and characteristics.

~~The ability of CPMs~~ The ability of CPMs to~~to~~ better represent rainfall frequency, intensity, and the magnitude of extremes (with the improvement most marked in dryland regions of the HOA) ~~is well documented~~ (Prein et al., 2015, Kouadio et al., 2018; Berthou et al., 2019; Kendon et al., 2019; Finney et al., 2019; 2020; Luu et al., 2022), ~~, including in the context of the HOA (Bethou et al., 2019; Kendon et al., 2019; Finney et al., 2019; 2020)~~means they offer one promising option for any hydrological studies conducted in regions where water partitioning is sensitive to rainfall characteristics.~~.~~ ~~This study demonstrates this improvement is most marked in dryland regions of the HOA (AI <= 0.5) compared to more humid (AI > 0.65) regions (Ethiopian Highlands).~~Currently ~~This is problematic, as despite their~~conventional climate models remain widely used f~~reduced skill in drylands, conventional climate models (those that parameterise the average effects of convection) are widely used to mak~~or ~~e~~ future projections of dryland rainfall (Huang et al., 2017) and ~~used~~ as driving datasets in~~for~~ dryland hydrological modelling (Crosbie et al., 2010; Mckenna and Sala, 2017; Razack et al., 2019; Cook et al., 2022). However, our results suggesting dryland hydrological studies using inappropriate rainfall datasets may incorrectly characterise water partitioning, and while this study has only highlighted the impact rainfall characteristics on vadose zone partitioning at a point-based scale, the nature of our results also has important implications for the dryland water balance at basin scales (e.g. Quichimbo et al., 2023) and beyond.

Commented [KM11]: Ewaso paper

~~Our modelling demonstrates water partitioning in drylands is sensitive to the magnitude-duration spectrum of rainfall delivery (R Taylor et al., 2013; Arpuv et al., 2017; Singer and Michaelides, 2017; Cuthbert et al., 2019; Kipkemoi et al., 2021; Adloff et al., 2022, Quichimbo et al., 2023). That two climate model products based on the same global model configuration (Walters et al., 2017), with comparable annual totals, and seasonal cycles (Wainwright et al., 2021) produce such differing hydrological outcomes when propagated through a simple 1-D model highlights the~~

~~importance of carefully selecting driving datasets in the nature of important the drylands water balance at basin scales (e.g. Quichimbo et al ***) and beyondA key limitation with any one-dimensional modelling study is that lateral and non-local processes are explicitly excluded, however were such processes to be considered, it is unlikely to contradict our findings that using parameterised climate model output in dryland hydrological studies will lead to higher evaporative losses, lower soil moisture, transpiration, and potential groundwater recharge (bottom drainage) relative to CPMs. In fact, one could make the argument that differences would only become more pronounced were such analysis conducted at a basin/regional scale.~~

Commented [KM12]: Ewaso paper

The low infiltration rates and high rainfall intensities typical of drylands partition~~s~~ rainfall into some combination of surface runoff and infiltration (Zhu et al., 2018; Aryal et al., 2020), where runoff is predominately generated via the infiltration-excess overland flow mechanism (Hortonian overland flow) (Horton, 1933). Whether runoff is generated is a function of storm characteristics and land surface properties, with only the most intense rainfall events able to generate enough surface runoff to form the ephemeral channels/pools that lead to large recharge events (R Taylor et al., 2013; Schreiner-McGraw et al., 2019). If one was to use a basin/regional scale process-based dryland hydrological model that accounts for these processes (Quichimbo et al., 2021), it is reasonable to assume that the more intense rainfall (Prein et al., 2015, Kouadio et al., 2018; Berthou et al., 2019; Kendon et al., 2019; Finney et al., 2019; 2020; Luu et al., 2022) and higher surface runoff (Folwell et al., 2022) when using CPMs as a driving dataset (relative to conventional parameterised models) would yield more realistic surface runoff patterns and greater non-local recharge. Furthermore, within such a basin/regional simulation, local infiltration in response to light rainfall is still more likely to be lost to evaporation (as this study has demonstrated), so were one to drive a regional dryland model with parameterised climate model output (compared to a CPM), there would be less surface runoff available for non-local recharge, and less localised recharge.

~~hydrological studies. The importance of this choice increases with aridity, as while in humid regions forcing Hydrus with CP4A or P25 has minimal impact on the 1D water balance, in drylands using CP4A increases average soil moisture, and results in markedly higher surface runoff, transpiration, and bottom drainage. Although even in humid regions, studies have found differences in hydrological outcomes between CPMs and parameterised climate models, such as increased surface runoff (Folwell et al., 2022) and higher flood risk when forcing hydrological models with CPM rainfall (Ascott et al., 2023; Archer et al., 2024). And while no flood risk assessments using CP4A have been conducted across the HOA at time of writing, it is reasonable to assume that greater sub-daily rainfall extremes (Bethou et al., 2019; Kendon et al., 2019; Finney et al., 2019, 2020) and surface runoff will result in greater flood hazard potential in the HOA when forcing hydrological models with CPM rainfall.~~

Hence, regardless of the spatial scale (point-based or regional-scale), it is critical that any dryland hydrological study uses rainfall data that correctly captures rainfall totals and characteristics, discounting either risk misrepresenting societally relevant aspects of the hydrological cycle. For example, it is quite evident that any dataset that underestimates the tails of the rainfall distribution will result in lower estimates of flood risk ~~This highlights a key risk with the continuing~~ The ~~use of parameterised climate model~~ rainfall~~s in dryland hydrological~~ impact ~~studies~~ also has implications for ~~, as they could yield unrepresentative hydrological fluxes that could have implications for societies~~

~~and livelihoods. . In the HOA, g~~(Ascott et al., 2023; Archer et al., 2024), but biases in rainfall characteristics could also have implications for crop health and groundwater recharge projections. Our ~~that assessment and projections projectionsare affected by the climate model characteristics~~ ~~For example, while most hydrological studies tend not to distinguish between soil evaporation and transpiration and only report evapotranspiration,~~ ~~our~~ results showing that ~~ing moisture lost to evaporation is far higher when forcing Hydrus with P25, while~~ using CP4A increases the volume of water penetrating deeper into the soil profile and ~~leads to available for transpiration within the root zone, meaning~~ higher transpiration ~~is higher~~ rates ~~and continues~~ which continue longer into the dry season (Folwell et al., 2022)~~, compared to using rainfall from P25~~ suggests ~~which remains in the shallower levels of the soil. This difference in soil moisture dynamics~~. ~~This discrepancy is likely related to both rainfall magnitude and how rainfall frequency influences antecedent moisture conditions near the surface. Either way, our work shows that even where ET is comparable, f~~forcing crop ~~yield/suitability~~ models using parameterised climate model rainfall could ~~risk~~ result in an~~underestimating underestimating~~ underestimation of crop yields and ~~overestimating~~ an overestimation of~~in~~ ~~i~~the risk of failure. Although equally, taking P25 as an example, lower rainfall intensities (reduced crop flooding) and shorter dry periods (lower water stress) could lead to overly optimistic projections of crop health relative to CP4A. Either way, it is clear that for d~~, or incorrectly suggesting regions may become unsuitable for staple crops (particularly for deeper-rooted crops). In d~~ryland regions of sub-Saharan Africa, where livelihoods are heavily dependent on subsistence agriculture and pasture (Davenport et al., 2017, 2018; Hoffman et al., 2022), ~~incorporating CPM~~ensuring ~~representing the key dryland rainfall characteristics into~~ agricultural impact assessments use data that represents dryland rainfall characteristics is critical for ~~could~~ providing~~e~~ more realistic projections of future change.

Driving hydrological models with datasets that correctly represent dryland rainfall characteristics could also be used to produce more realistic projections of future groundwater resources, the only source of perennial freshwater in drylands (MacDonald et., 2012). Because as discussed above, groundwater recharge is highly sensitive to rainfall characteristics (R Taylor et al., 2013; Batalha et al., 2018; Boas and Mallants, 2022) and ~~Furthermore, our results showing enhanced drainage from the bottom of the soil profile when forcing Hydrus with CP4A (despite lower seasonal rainfall) supports other research showing the magnitude of groundwater recharge in drylands~~ does not linearly trend with higher seasonal rainfall totals. F~~. Groundwater recharge is sensitive to rainfall characteristics, particularly rainfall intensity, where if rainfall is of sufficient intensity it can generate overland flow, channelized streamflow, and transmission losses in ephemeral rivers (R Taylor et al., 2013; Batalha et al., 2018; Boas and Mallants, 2022). F~~or example, in the context of the HOA, despite a decline in seasonal rainfall totals, groundwater storage is increasing driven by a positive trend~~increases~~ in ~~rainfall~~ extreme rainfall intensity (Adloff et al., 2022). ~~The~~ ~~. However, this decline in seasonal rainfall has been driven by a later onset and earlier cessation of the MAM ('long') rains season rather than any reduction in rainfall intensity (Wainwright et al., 2019), with positive trends in extreme rainfall appearing to sustain groundwater storage across the region (Adloff et al., 2022).~~ In the HOA and drylands more broadly, future water resources will not simply follow changes in mean seasonal rainfall (even at point-scale where we exclude critical non-local processes, our results show enhanced drainage from the bottom of the soil profile when forcing Hydrus with CP4A despite lower seasonal rainfall), so it is critical any future assessments of groundwater

**Commented [KM13]:** This section could probably be deleted. Doesn't add much and is very speculative - doesn't link to the paper results

**Commented [KM14]:** This paragraph doesn't link to the previous paragraph...

**Commented [GB15]:** Need to update to reflect the following comment/response:

**L.32-33:** when you say "…forcing hydrological model projections with convectional climate models that parameterise the average effects of convection risks underestimating future crop health…" But viewed from another perspective, a convection-permitting model would simulate longer dry periods (increasing water stress) and more intense rainfall events (risk of crop damage or flooding), which could imply worse (but more realistic) crop health compared to the output of the conventional model. If so, wouldn't conventional climate models be mistakenly "more optimistic" and thus overestimate future crop health?
Thank you, this is a really good point that we hadn't fully considered. Here we have made this assertion based on lower soil moisture and longer periods where acacia shrubs are below the wilting point. But we would agree that crop health is dependent on other factors such as heat stress and potential flooding. To make such a statement we need to conduct specific crop modelling, so we will rewrite the above sentence to: "…forcing hydrological model projections with convectional climate models that parameterise the average effects of convection risks underestimating the soil moisture critical for crops …". In the discussion where we also consider crop health, we will incorporate your comments provided above.

**Commented [KM16]:** You don't want to make the whole premise about CPMs… More about the general point of correctly representing dryland rainfall characteristics resources utilise driving datasets that capture dryland rainfall characteristics. ~~These observed relationships and our hydrological simulations undermine the relevance of making detailed future projections of water resources using conventional climate models that cannot explicitly resolve convective processes and struggle to capture observed rainfall characteristics.~~

Although while ~~However, while improved representation of rainfall characteristics and atmospheric dynamics in~~ CPMs may provide valuable insights into ~~increases our confidence in future~~ projected~~ions of~~ changes in future rainfall characteristics (Bethou et al., 2019; Kendon et al., 2019; Finney et al., 2019, 2020)~~,~~ they ~~CPMs~~ are not currently a panacea for the wider uncertainty that limits our understanding of future climate change impacts on water resources in the HOA~~in the HOA~~. As while explicitly resolving convection can influence regional circulation patterns (Finney et al., 2020), CPMs still inherit the underlying uncertainties in the driving GCM, meaning it is unlikely they ~~it is unlikely CPMs~~ will resolve the failure of climate models to reproduce the observed drying trend in MAM ~~(long rains)~~ rainfall over the last 30 years (~~dubbed~~named as the 'East Africa Climate Paradox') (Lyon and Vigaud, 2017; Wainwright et al., 2019; Schwarzwald and Seager, 2024) and their inability to capture important modes of variability and wider large-scale processes (Schwarzwald et al., 2023). ~~As while data is limited, future projections show CP4A follows CMIP models in continuing to project higher rainfall across the HOA (including during the long rains) (Kendon et al., 2019; Wainwright et al., 2021).~~

Commented [KM17]: Please could you rewrite this sentence? I find it hard grammatically to follow and too long

So while robustly ~~Given th~~capturing rainfall characteristics is critical, the ~~is~~ uncertainty and the computational costs associated with CPM simulations means ~~,~~ utilising stochastic rainfall generators (Singer et al., 2018; Rios Gaona et al., 2024) and process-based scaling approaches consistent with CPM behaviour ~~model~~ may a better approach for ~~behaviour can be used to~~ producing~~e~~ a range of plausible time-evolving futures ~~projections to explore a range of plausible futures~~ in the HOA (Klein et al., 2021). Taking such a 'storyline' approach (Shepherd et al., 2018~~add reference~~) ~~built around stochastic scenarios~~ could provide more valuable insights than~~t~~ simply forcing hydrological simulations using RCMs or GCMs that struggle to capture the mean climate state as well ~~as~~ the ~~nature of dryland rainfall~~dryland rainfall characteristics, as doing so~~this~~ risks producing misrepresentative projections of metrics such as soil moisture, transpiration, and groundwater recharge, which could contribute to sub-optimal decision making around long-term land use or water supply policy.

## 5. Conclusions

In this study, we find that explicitly resolving convection improves the ability of climate models to capture dryland rainfall characteristics ~~the nature of dryland rainfall~~ compared with models that~~relative to those that~~ parameterise the average effects of convection, ~~. Using~~ CP4A dramatically reduces the systemic 'drizzle' bias seen in P25, and ~~n P25 and~~ better ~~captures~~ represents dry spell length, the magnitude of extremes, and the contribution of heavy rainfall events to seasonal totals. D~~This means that, d~~espite using similar model physics and simulating comparable seasonal totals, the impact of ~~climate model representation of~~ convective representation~~on~~ on rainfall characteristics results in ~~can translate into~~ different hydrological outcomes when rainfall is propagated through a simple one-dimensional vadose-zone hydrological model. In dryland locations, using CP4A to drive ~~although simulating lower total rainfall and infiltration, driving~~ Hydrus 1-D ~~with CP4A rainfall produces~~produces higher soil moisture, transpiration, and bottom drainage, despite simulating lower total rainfall and infiltration compared to P25. ~~. As although total infiltration is higher when using P25, the 'drizzle'~~The 'drizzle' bias in P25 confines~~means this~~ infiltration ~~is restricted~~ to the upper layers of the soil profile, where it is ~~and is~~ quickly returned to the atmosphere via~~as~~ evaporation. Our results also show that while PET can influence vadose-zone hydrological outcomes, dryland hydrology is~~is~~ more sensitive to the impact of ~~climate model representation of~~ convective ~~on~~ representation on rainfall characteristics. ~~While her~~~~Although our study is on the point scale, results that the dryland water balance is very sensitive to rainfall characteristics and model simulations produce distinct hydrological responses with significant differences in stores and fluxes. Thes~~These ~~e results~~findings suggest that any ~~that a~~~~Any~~ impact assessments of dryland hydrological resources must carefully consider the spatio~~al and~~ temporal resolution and characteristics of rainfall datasets (or climate model rainfall), or they risk misrepresenting societally relevant aspects of the water cycle. ~~used both in present-day simulations and future projections.~~ ~~driving datasets utilised, particularly in future projections, where the use of parameterised climate model as a driving dataset could result in misrepresentative projections of societally relevant outcomes of the hydrologic cycle relative to more physically robust CPM simulations.~~

## 6. Appendices

### 6.1 Appendix A

Appendix A provides additional detail around the calculation PET as discussed in section 2.2.

As discussed, is section 2.2 dew point temperature is not directly outputted from either climate model, it was calculated using near-surface air temperature and relative humidity using the Clausius–Clapeyron approximation (Eq. (7)) (Alduchov and Eskridge, 1996). Relative humidity is also not directly outputted from the models, so to calculate relative humidity ($RH$) we used the following equation (Eq. (5)):

$$RH = \frac{\omega}{\epsilon + \omega}\frac{\epsilon + \omega_s}{\omega_s} \tag{5}$$

Where $\omega$ is the mixing ratio, $\omega_s$ is the saturation mixing ratio, and $\epsilon$ is the molecular weight ratio of vapor to dry air.

For the above equation $\omega$ is calculated using Eq. (6), where $q$ is specific humidity:

$$\omega = \frac{q}{(1-q)} \tag{6}$$

To calculate dew point temperature (we $Td$) use the following equation (Eq. (7)):

$$Td = \frac{b \cdot \gamma(T, RH)}{a - \gamma(T, RH)} \tag{7}$$

Where $T$ is air temperature (in °C), $RH$ is the relative humidity computed in Eq. (5), $a$ refers to the empirical constant controlling the slope of the temperature–vapour pressure relationship ($a$ =17.625), and $b$ is temperature intercept in the saturation vapour pressure curve ($b$ = 243.04 °C). In the above equation $\gamma(T, RH)$ is computed using Eq. (8).

$$\gamma(T, RH) = \frac{a \cdot T}{b + T} + ln\left(\frac{RH}{100}\right) \tag{8}$$

Eq. (6) – Eq. (10) provides details the equation used to calculate the saturation vapour pressure ($e_s$), actual vapour pressure ($e_a$), slope of saturation vapour pressure ($\Delta$), net radiation ($R_n$), and the soil heat flux ($G$) used to compute PET in Eq 1 in the main body of text.

For use in Eq 1, $e_s$ and $e_a$ were calculated using the Tetens equation (Tetens, 1930) using hourly air temperature ($T_a$) and dew point temperature ($T_{dew}$) as detailed below (calculations are in in °C after converting from K):

$$e_s = 0.6108\mathrm{ex\,p}\left(\frac{17.27 * T_a}{T_a + 237.3}\right) \tag{9}$$

$$e_a = 0.6108\mathrm{ex\,p}\left(\frac{17.27 * T_{dew}}{T_{dew} + 237.3}\right) \tag{10}$$

The Slope of saturation vapour pressure ($\Delta$) and the psychrometric constant ($\gamma$) were calculated as follows:

$$\Delta = \frac{4098 e_s}{(T_a + 237.3)^2} \tag{11}$$

$$\gamma = \frac{C_p * P}{\varepsilon * \lambda} \tag{12}$$

Where $P$ is atmospheric pressure, $C_p$ is the air's specific heat at constant pressure based on the ideal gas law with a value of $1.013 \times 10^{-3}$ MJ kg$^{-1}$ per °C, ε is the ratio of the molecular weight of water vapor to that of dry air (0.622), and $\lambda$ is the latent heat of vaporization, (2.45 MJ kg$^{-1}$).

Net radiation ($R_n$) is estimated using net solar ($R_s$) and thermal radiation ($R_t$) as (all values in MJ m$^{-2}$):

$$R_n = R_s - R_t \tag{13}$$

Finally soil heat flux ($G$) is estimated as:

$$G = \begin{cases} G_{day} = 0.1 * R_n \\ G_{night} = 0.5 * R_n \end{cases} \tag{14}$$

Where the soil heat flux ($G$) is estimated to be 10% of net radiation ($R_n$) during the day and 50% during the night (as the night-time heat flux is negative). At each pixel we use net solar radiation to define day and nighttime periods. Following the method used to calculate hPET (Singer et al., 2021), nighttime PET values have not been automatically set to zero.

It is important to note that while other studies have used CP4A and other convection-permitting models to explore evapotranspiration (Folwell et al., 2022; Halladay et al., 2023, Lee and Hohenegger., 2024), they used internal model evapotranspiration (ET), rather than externally calculating PET from model-derived atmospheric variables. While studying internal ET is useful for exploring land-atmosphere interactions — particularly feedbacks between soil moisture and precipitation — it reflects the model's internal assumptions about land surface properties, such as soil type and vegetation. In the case of CP4A, for example, ET is calculated using a uniform sandy soil across the entire domain, which limits its applicability in spatially heterogeneous hydrological studies. By contrast, externally calculating PET from model-derived atmospheric variables provides a consistent measure of atmospheric evaporative demand, independent of land surface parameterizations. For hydrological purposes where more detailed or locally calibrated soil and vegetation data is available, it is preferable to use the potential atmospheric evaporative demand (PET) computed using atmospheric climate model outputs.

## 6.2 Appendix B

Appendix B details the parameters that were altered between the different Hydrus simulations used at each site. At each site we used three different soil hydraulic parameters (Table B1): lowK, def, and highK. Where def (**given in bold**) refers to the default soil parameters that are used for all simulations discussed in the main text, lowK refers to low hydraulic conductivity simulations, and highK is high hydraulic conductivity simulations. For example, at Site A hydraulic conductivity ($K_s$) ranges from 3.5 mm/hr (lowK) to 21.8 mm/hr (highK).

These soil parameters were estimated using Genuchten-Mualem (Van Genuchten, 1980) equations based on soil texture values taken from the Innovate Solutions for Decision Agriculture (iSDA) soil database (Hengl et al., 2021). Where *Qr* refers to residual soil water content, *Qs* is the saturated water content, *Alpha* is Parameter *a* in the soil water retention function [$L^{-1}$], *n* is parameter *n* in the soil water retention function, $K_s$ is the saturated hydraulic conductivity [$LT^{-1}$], and *I* is the tortuosity parameter in the conductivity function [-]. iSDA provides a lower and upper bound of sand, silt, and clay percentages (Hengl et al., 2021), our default ('def') parameter set was estimated using the mid-point of these lower and upper bounds for each soil texture.

While to create our low ('lowK') and high hydraulic conductivity ('highK') soil parameters, we used the lower and upper bound of the sand percentage respectively, and then proportionally adjusted the silt and clay percentage to ensure values equalled 100. So, for example, our 'highK' scenarios have higher saturated hydraulic conductivity ($K_s$) as the relative percentage of sand is higher than in our 'def' and 'lowK' scenarios. We used the same labelling for each site as they follow the same methodology and are designed to be comparable across sites, although soil parameters will differ between sites based on the relative proportion of sand, silt, and clay at each site.

| **Site HU (Humid)** | | | | | | | |
|---|---|---|---|---|---|---|---|
| Scenario | Depth | *Qr* | *Qs* | *Alpha* | *n* | *Ks (mm/hr)* | *I* |
| LowK | 0 - 20 cm | 0.103 | 0.545 | 0.002 | 1.339 | 18.342 | 0.500 |
| LowK | 20 - 500 cm | 0.105 | 0.543 | 0.002 | 1.315 | 15.650 | 0.500 |
| **Def** | **0 - 20 cm** | **0.096** | **0.525** | **0.002** | **1.384** | **19.117** | **0.500** |
| **Def** | **20 - 500 cm** | **0.100** | **0.529** | **0.002** | **1.349** | **17.833** | **0.500** |
| HighK | 0 - 20 cm | 0.084 | 0.510 | 0.002 | 1.405 | 22.588 | 0.500 |
| HighK | 20 - 500 cm | 0.090 | 0.512 | 0.002 | 1.384 | 19.996 | 0.500 |
| **Site SA (Semi-Arid)** | | | | | | | |
| Scenario | Depth | *Qr* | *Qs* | *Alpha* | *n* | *Ks (mm/hr)* | *I* |
| LowK | 0 - 20 cm | 0.076 | 0.416 | 0.001 | 1.405 | 3.221 | 0.500 |
| LowK | 20 - 500 cm | 0.081 | 0.423 | 0.002 | 1.351 | 3.204 | 0.500 |
| **Def** | **0 - 20 cm** | **0.068** | **0.409** | **0.002** | **1.400** | **5.658** | **0.500** |
| **Def** | **20 - 500 cm** | **0.076** | **0.418** | **0.002** | **1.354** | **4.175** | **0.500** |
| HighK | 0 - 20 cm | 0.066 | 0.408 | 0.002 | 1.401 | 6.663 | 0.500 |
| HighK | 20 - 500 cm | 0.072 | 0.417 | 0.002 | 1.367 | 6.100 | 0.500 |
| **Site A (Arid)** | | | | | | | |
| Scenario | Depth | *Qr* | *Qs* | *Alpha* | *n* | *Ks (mm/hr)* | *I* |
| LowK | 0 - 20 cm | 0.081 | 0.431 | 0.001 | 1.426 | 3.542 | 0.500 |
| LowK | 20 - 500 cm | 0.085 | 0.436 | 0.001 | 1.404 | 3.338 | 0.500 |
| **Def** | **0 - 20 cm** | **0.067** | **0.418** | **0.002** | **1.415** | **7.558** | **0.500** |
| **Def** | **20 - 500 cm** | **0.069** | **0.419** | **0.002** | **1.404** | **6.363** | **0.500** |
| HighK | 0 - 20 cm | 0.055 | 0.414 | 0.003 | 1.475 | 21.817 | 0.500 |
| HighK | 20 - 500 cm | 0.058 | 0.413 | 0.002 | 1.439 | 16.004 | 0.500 |
| **Site HA (Hyper-Arid)** | | | | | | | |

| Scenario | Depth | *Qr* | *Qs* | *Alpha* | *n* | *Ks (mm/hr)* | *l* |
|---|---|---|---|---|---|---|---|
| LowK | 0 - 20 cm | 0.070 | 0.417 | 0.002 | 1.400 | 5.779 | 0.500 |
| LowK | 20 - 500 cm | 0.069 | 0.417 | 0.002 | 1.394 | 6.783 | 0.500 |
| **Def** | **0 - 20 cm** | **0.067** | **0.417** | **0.002** | **1.406** | **7.633** | **0.500** |
| **Def** | **20 - 500 cm** | **0.069** | **0.417** | **0.002** | **1.394** | **6.783** | **0.500** |
| HighK | 0 - 20 cm | 0.056 | 0.413 | 0.003 | 1.480 | 21.646 | 0.500 |
| HighK | 20 - 500 cm | 0.056 | 0.411 | 0.003 | 1.466 | 19.329 | 0.500 |

**Table B1 - Soil Hydraulic parameters used in all Hydrus simulation at our humid (HU), semi-arid (SA), arid (A), and hyper-arid (HA) sites across the HOA.**

Table B2 shows the Feddes' parameters used to compute transpiration (root water uptake) within Hydrus (Feddes, 1978). Where *P0* is pressure value at which roots start to extract water from the soil, *POpt* is the pressure head at which roots extract water at the maximum possible rate, *P2H* is the pressure head at which roots can no longer extract water at the maximum possible rate (assumes a potential transpiration rate of *r2H*), *P2L* is the same above but instead assumes a maximum possible transpiration rate of *r2L*, and *P3* is the value of the pressure head at which roots can no uptake any water from the soil (wilting point). Vegetation type was taken from iSDA based on 2019 data (iSDA, 2024).

Hydrus has an internal database of Feddes' parameters for various crop types; the maize parameters were taken from this database and are based on Wesseling (1991). However, shrubs are not in this database and there is very little published information on Feddes' parameters for shrubs. We were able to locate some thresholds for dryland shrubs: *Acacia Mearsii*, *Caragana korshinkii*, and *Sarcopoterium spinosum* (Xia and Shao, 2008, Sela et al., 2015, Watson, 2015). Sela et al (2015) provided a range of Feddes' parameters used in their calibration process to correctly quantify transpiration rates of *Caragana korshinkii* in Hydrus 1-D, settling on an optimal parameter set (Table B2). However, we decided to use the upper range (here referred to as def) of the parameters given by Sela et al (2015) as they better matched estimates given by Xia and Shoa (2008) and Watson (2015), particularly the wilting point. However, to ensure results any biases seen between CP4A and P25 Hydrus runs were consistent regardless of the Feddes' parameters chosen, we also used the optimal and lower values provided by Sela et al (2015) at sites SA and A (where shrubs are the dominant land cover). However, unless stated otherwise all results reported in the main body of text were computed using the upper (def) Feddes' values – **given in bold below.**

| Feddes' Parameter | *P0 (mm)* | *POpt (mm)* | *P2H (mm)* | *P2L (mm)* | *P3 (mm)* | *r2H (mm/hr)* | *r2L (mm/hr)* |
|---|---|---|---|---|---|---|---|
| **Shrubs Upper (def)** | **-150** | **-300** | **-5000** | **-15000** | **-240000** | **0.208** | **0.042** |
| Shrubs Mid | -58 | -224 | -326 | -6700 | -15570 | 0.208 | 0.042 |
| Shrubs Lower | 0 | -150 | -300 | -5000 | -15000 | 0.208 | 0.042 |
| Maize | -150 | -300 | -3250 | -6000 | -80000 | 0.208 | 0.042 |

**Table B2 – Feddes parameters controlling root water uptake (transpiration) for shrubs and maize used in Hydrus 1-D simulations. Values were for shrubs were taken from Sela et al (2015) and maize from Wesseling (1991).**

## 6.2 Appendix C

Appendix C provides additional figures and materials on the analyses of CP4A/P25 rainfall and PET simulations (sections 3.1 and 3.2). Fig. C1 is a replication of Fig. 3 in the main body of text, plotting the distribution of rainfall intensities for all rainfall hours (based on a threshold of 0.1 mm/hr) for humid (AI >= 0.65) and dryland regions (AI < 0.50) in each season across the HOA. The plots highlight the 'drizzle' effect simulated by P25 (shown by the large frequency peaks in rain hours between $10^{-1}$ and $10^{1}$ mm/hr) is consistent across seasons, with P25 overestimating the number of wet hours in both wet (MAM & OND) and dry (JF & JJAS) seasons.

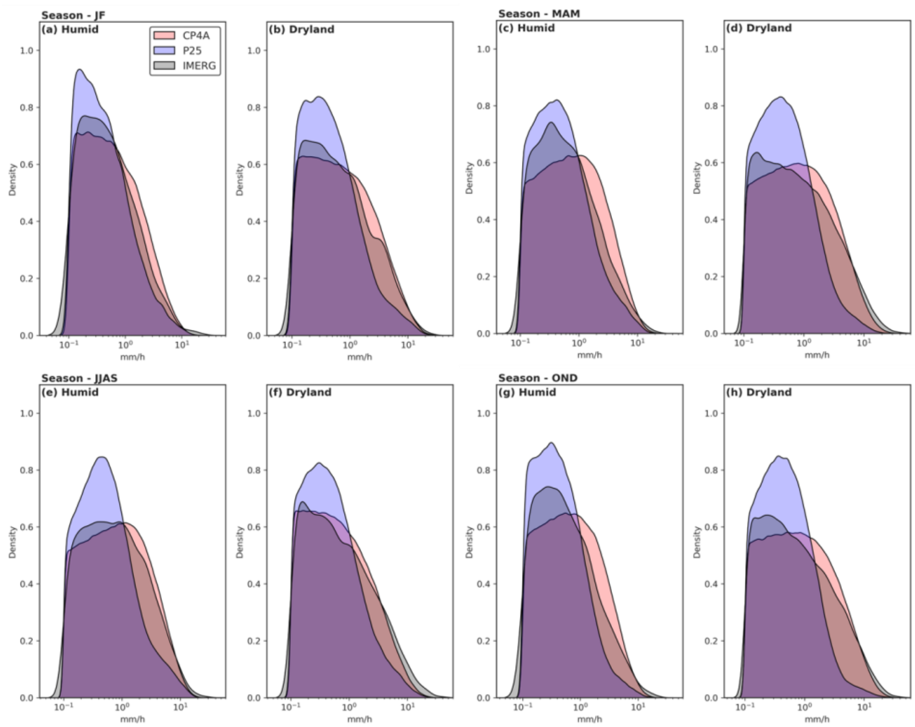


**Figure C1. Rainfall KDE Plots. Kernel density estimate (kde) plots of CP4A, P25, and IMERG hourly rainfall in humid (AI >= 0.65) and dryland (AI < 0.5) regions of the Horn of Africa for JF (a-b), MAM (c-d), JJAS (e-f), and OND (g-h). Plots exclude dry hours by dropping any hours that receive < 0.1 mm/hr of rainfall.**

To understand the drivers of PET differences between CP4A and P25 we conducted a multiple-linear regression between PET and the seven atmospheric variables described in section 2.2. Table C1 shows the results of this multi-linear regression between the daily PET climatology and the daily climatology of the seven atmospheric variables used to compute PET in humid and arid regions of the Horn of Africa (discussed in section 3.2).

| Humid Regions | | | | | |
|---|---|---|---|---|---|
| Variable | Coefficient | Std Error | P>\|t\| | 0.025 CI | 0.975 CI |
| Temp | 0.127 (**0.438**) | 0.028 (**0.046**) | 0 (**0.000**) | 0.072 (**0.349**) | 0.182 (**0.529**) |
| Dew Point | 0.152 (**-0.129**) | 0.021 (**0.031**) | 0 (**0.000**) | 0.112 (**-0.191**) | 0.193 (**-0.068**) |
| Surface Pressure | 0.0001 (**-0.002**) | 0.000 (**0.000**) | 0.58 (**0.000**) | 0.000 (**-0.002**) | 0.000 (**-0.001**) |
| Short Wave Radiation | 7.2e-7 (**7.9e-07**) | 1.6e-7 (**2.2e-7**) | 0.000 (**0.001**) | 4.1e-7 (**3.4e-7**) | 1.0e-6 (**1.2e-6**) |
| Long Wave Radiation | -7.9e-6 (**2.6e-6**) | 1.4e-6 (**1.8e-6**) | 0.000 (**0.149**) | -1.1E-5 (**-9.5e-7**) | -5.1E-6 (**6.2e-6**) |

| | | | | | |
|---|---|---|---|---|---|
| Meridional Wind | 0.041 (**-0.108**) | 0.024 (**0.034**) | 0.081 (**0.002**) | -0.005 (**-0.174**) | 0.088 (**-0.041**) |
| Zonal Wind | -0.181 (**-0.178**) | 0.027 (**0.039**) | 0 (**0.000**) | -0.235 (**-0.255**) | -0.127 (**-0.100**) |
| Arid Regions | | | | | |
| Variable | Coefficient | Std Error | P>\|t\| | 0.025 CI | 0.975 CI |
| Temp | 0.285 (**0.232**) | 0.033 (**0.027**) | 0.000 (**0.000**) | 0.220 (**0.179**) | 0.349 (**0.285**) |
| Dew Point | -0.364 (**-0.391**) | 0.026 (**0.018**) | 0.000 (**0.000**) | -0.401 (**-0.426**) | -0.327 (**-0.356**) |
| Surface Pressure | 0.0009 (**-0.001**) | 0.000 (**0.000**) | 0.58 (**0.000**) | -0.001 (**-0.001**) | -0.001 (**-0.000**) |
| Short Wave Radiation | 2.0e-06 (**7.0e-6**) | 2.1e-07 (**4.5e-7**) | 0.000 (**0.001**) | 1.6e-06 (**6.1e-06**) | 2.4e-06 (**7.8e-06**) |
| Long Wave Radiation | 9.6e-06 (**1.2e-5**) | 1.4e-06 (**1.2e-6**) | 0.000 (**0.149**) | 6.8e-06 (**1.0e-5**) | 1.2e-05 (**1.5e-5**) |
| Meridional Wind | 0.178 (**0.103**) | 0.025 (**0.019**) | 0.000 (**0.002**) | 0.130 (**0.066**) | 0.226 (**0.139**) |
| Zonal Wind | -0.095 (**0.016**) | 0.026 (**0.019**) | 0.000 (**0.000**) | -0.146 (**-0.022**) | -0.044 (**0.053**) |

**Table C1 - Results of the multi-linear regression analysis on the drivers of PET in CP4A and P25 in humid (top panel) (AI >= 0.65) and arid (AI < 0.2) regions of the HOA. Bold values refer to CP4A, while non-bold values refer to P25.**

Table C1 suggests meridional wind speed is relatively important in arid regions, Fig. C2 shows the daily meridional wind speed climatology in arid regions of the Horn of Africa. It appears that the positive significant relationship between meridional wind speed and PET (Table C1) is the driving factor behind higher PET in P25 during the months of June to September (see Fig. 3g), as Fig. C2 closely matches Fig. 3g.

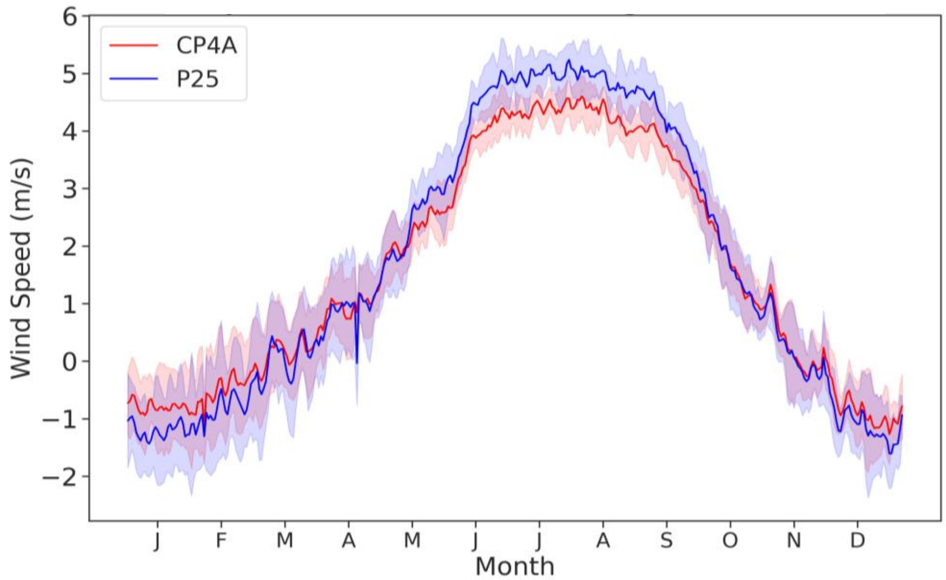


**Figure C2 - Daily climatology of meridional wind speed in arid (AI < 0.2) regions of the HOA.**

## 6.3 Appendix D

Appendix D provides additional figures and tables relevant to the analysis of Hydrus simulations (section 3.3). Fig. D1 shows the mean monthly CP4A and P25 rainfall at each of our four sites. Both models broadly capture the observed seasonality in the region (Wainwright et al., 2019), simulating the bimodal rainfall regime at our dryland sites (Sites SA, A, and HA) and the unimodal regime in the humid Ethiopian Highlands (Site HU). However, it is worth noting that P25 tends to simulate rainfall in every month (including July and August) at our dryland sites (CP4A simulates negligible rainfall) and simulates substantially higher rainfall totals during June and July at Site HU.

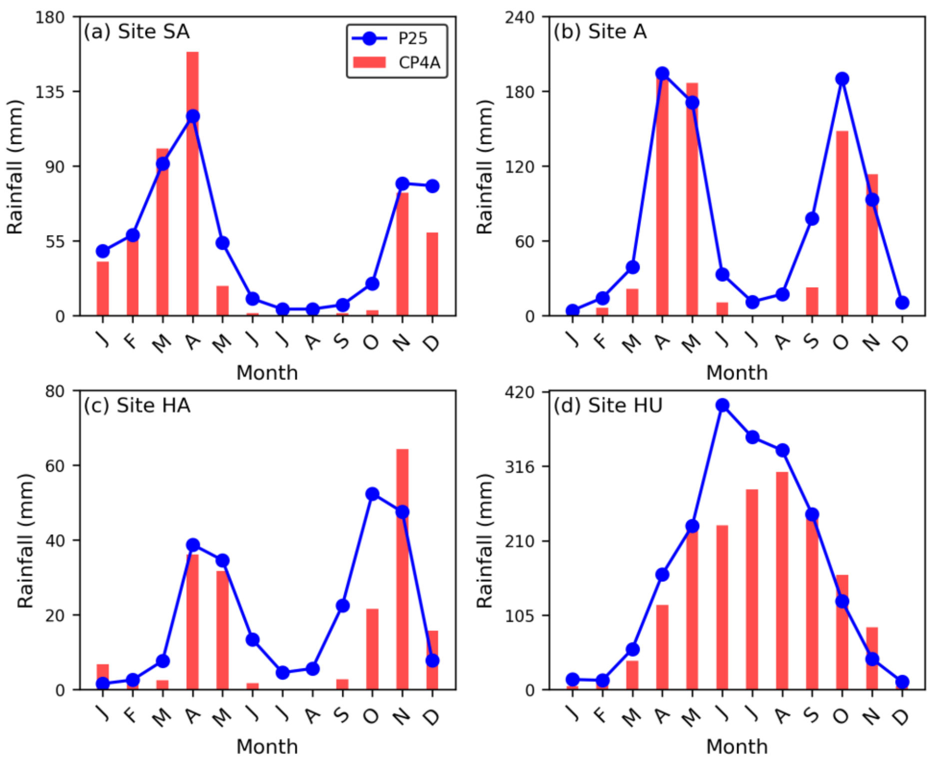


**Figure D1 – Mean monthly rainfall at each of our four hydrological study sites.**

Fig. D2 shows mean monthly CP4A and P25 PET at each of our four study sites. At all sites both models simulate comparable seasonal cycles and totals, although P25 consistently simulates higher PET at Sites A and HA. It is also worth noting that P25 simulates substantially higher PET during the months June – August, matching the higher JJAS PET simulated by P25 across the entire arid region of the HOA.

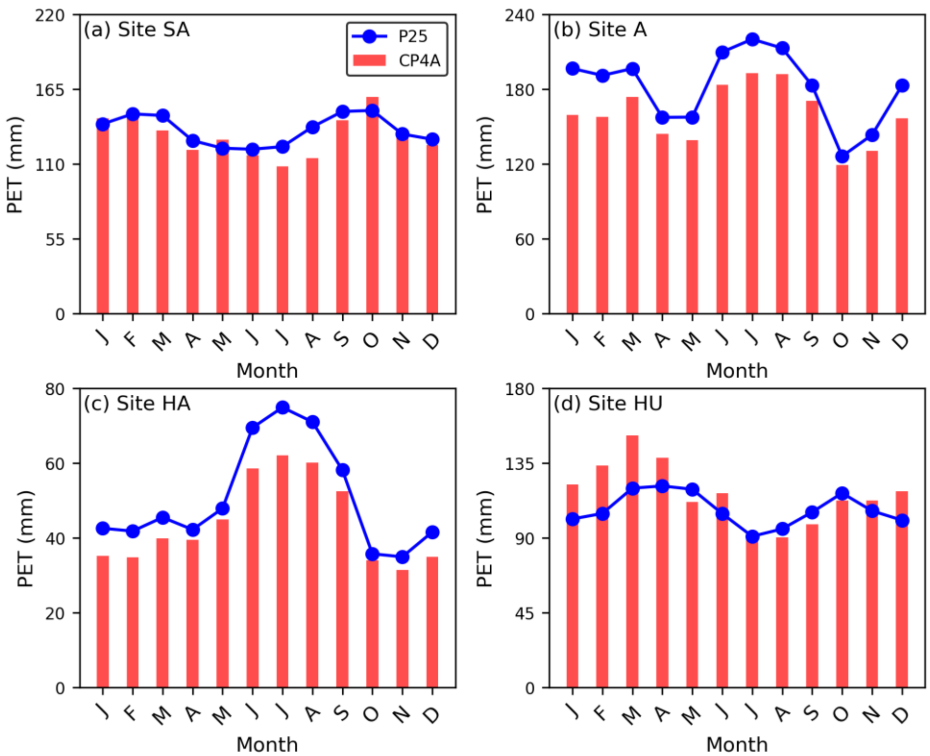

**Figure D2 – Mean monthly PET at each of our four hydrological study sites.**

Fig. D3 shows the raw time series of rainfall at each study site, it provides a clear demonstration of the tendency for CP4A to simulate heavier extreme rainfall events, as well as more frequent intense rainfall events at our dryland study sites (Sites SA, A, and HA). Whereas at our humid site in the Ethiopian Highlands, the differences are far more muted and at times it is P25 that is simulating heavier rainfall events.

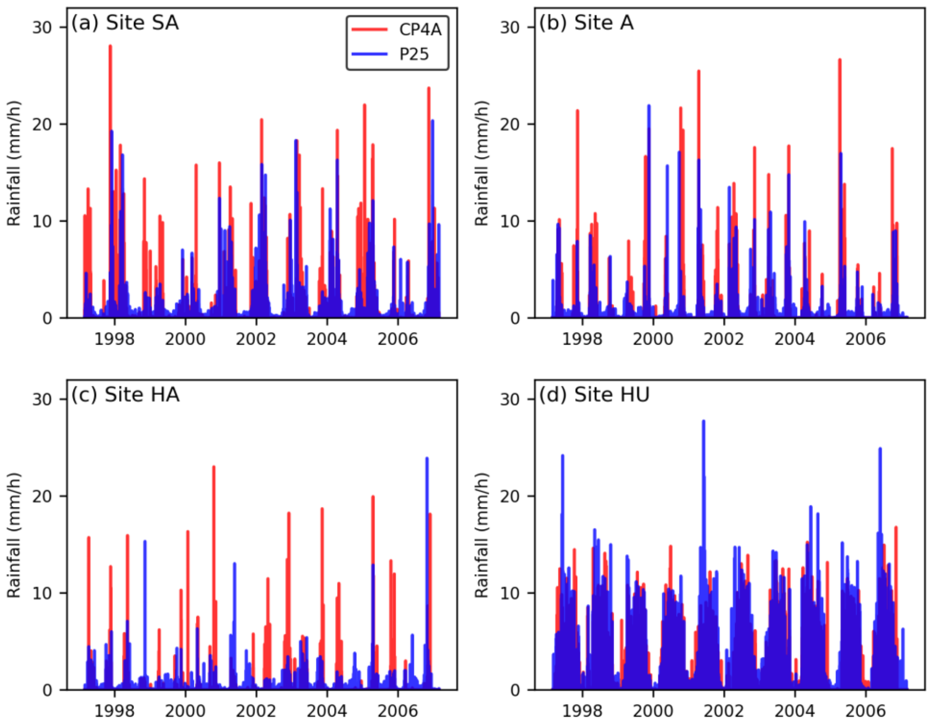


**Figure D3 – Raw time series of rainfall at each of our four hydrological study sites.**

The following tables will provide additional detail on the soil moisture results for each site, building and complimenting what was discussed in the main body of text.

Table D1 shows that differences in soil moisture distributions are more pronounced (based on the Kolmogorov-Smirnov Test statistic) at the dryland sites versus Site HU. In all cases there are statistically significant differences between the CP4A and P25 runs ($p < 0.05$).

| Depth (meters below ground level) | Site SA | Site A | Site HA | Site HU |
|---|---|---|---|---|
| 0.2 mbgl | 0.16 | 0.14 | 0.74 | 0.07 |
| 0.6 mbgl | 0.22 | 0.27 | 0.89 | 0.07 |
| 0.9 mbgl | 0.22 | 0.44 | 0.93 | 0.08 |
| 1.2 mbgl | 0.23 | 0.40 | 0.94 | 0.08 |
| 1.5 mbgl | 0.35 | 0.49 | 0.98 | 0.08 |
| 1.8 mbgl | 0.46 | 0.15 | 0.99 | 0.09 |
| 2.1 mbgl | 0.41 | 0.00 | 1.00 | 0.09 |

| | | | | |
|---|---|---|---|---|
| 2.4 mbgl | 0.49 | 0.00 | 1.00 | 0.09 |
| 2.7 mbgl | 0.38 | 0.00 | 1.00 | 0.09 |
| 3.0 mbgl | 0.38 | 0.00 | 0.85 | 0.08 |

**Table D1 - Kolmogorov–Smirnov (KS) test statistics comparing soil moisture distributions at our hydrological four sites across different depths. Higher KS values indicate greater differences between distributions. All results are statistically significant ($p < 0.05$). Site HA consistently shows the largest differences, while Site HU exhibits the smallest KS values, suggesting the least divergence. All results refer to Hydrus simulations driven by CP4A rainfall and PET using default soil and Feddes' parameters.**

Table D2 shows that forcing Hydrus with CP4A rainfall yields higher soil moisture values regardless of the soil hydraulic parameters used (Table B1).

| **Hydrus Run (depth - meters below ground level)** | **Site SA** | **Site A** | **Site HA** | **Site HU** |
|---|---|---|---|---|
| Low Hydraulic Conductivity (1.2 mbgl) | 10.6 | 10.5 | 17.0 | 5.2 |
| Low Hydraulic Conductivity (3.0 mbgl) | 14.4 | 5.1 | 14.7 | 2.5 |
| **Default (1.2 mbgl)** | **10.3** | **15.5** | **21.4** | **2.5** |
| **Default (3.0 mbgl)** | **20.7** | **9.1** | **19.4** | **5.2** |
| High Hydraulic Conductivity (1.2 mbgl) | 10.4 | 32.0 | 22.3 | 5.7 |
| High Hydraulic Conductivity (3.0 mbgl) | 22.6 | 21.9 | 25.5 | 2.6 |

**Table D2 – Relative percentage difference in median depth integrated soil moisture between CP4A and P25 Hydrus runs. Default (given in bold) refers to the default soil parameters that are used for all simulations discussed in the main body of text, lowK refers to low hydraulic conductivity simulations, and highK is high hydraulic conductivity simulations. See Appendix 6.2 (Table B2) for more details on each simulation. For all values reported, it is a positive percentage difference between CP4A and P25 soil moisture. Eg CP4A simulates higher soil moisture in all cases.**

Table D3 shows that forcing Hydrus with CP4A rainfall also yields higher soil moisture values regardless of the Feddes' parameters (Table B2) used to estimate the root water uptake (transpiration) of dryland shrubs (Table D3).

| **Hydrus Run (depth meters below ground level)** | **Site SA (Semi-Arid)** | **Site A (Arid)** |
|---|---|---|
| Low (least water resilient) Feddes' Parameters (1.2 mbgl) | 6.2 | 3.6 |
| Low (least water resilient) Feddes' Parameters (3.0 mbgl) | 10.7 | 2.4 |
| Mid Feddes' Parameters (1.2 mbgl) | 6.4 | 8.5 |
| Mid Feddes' Parameters (3.0 mbgl) | 10.9 | 4.7 |
| **Default/Upper (most water resilient) Feddes' Parameters (1.2 mbgl)** | **10.3** | **15.5** |
| **Default/Upper (most water resilient) Feddes' Parameters (3.0 mbgl)** | **20.7** | **9.1** |

**Table D3 - Relative percentage difference in median depth integrated soil moisture between CP4A and P25 Hydrus runs. Default/Upper (given in bold) refers to the default Feddes' parameters that are used for all simulations discussed in the main text, low refers to simulations using the low (least water resilient) Feddes' parameters, and mid refers to simulations**

**using the mid-range Feddes' parameter set. The low, mid, and upper Feddes' parameters are taken from Sela et al (2015). See Appendix 6.2 for more details on each simulation. For all values reported, it is a positive percentage difference between CP4A and P25 soil moisture. Eg CP4A simulates higher soil moisture in all cases.**

**Commented [GB18]:** Not mentioned in main body of text

Running Hydrus with CP4A rainfall and hPET PET data (rather than CP4A PET) also demonstrates that differences in soil moisture between the CP4A and P25 Hydrus runs are primarily driven by rainfall. As while the KS test statistic is lower (suggesting smaller differences in soil moisture distributions) compared to Hydrus simulations driven by CP4A rainfall and PET (Table D4), there are still statistically significant differences between CP4A and P25 at all sites ($p < 0.05$) and at all depths. The tendency for the KS statistic to be higher in drylands also remains (Table D4).

| CP4A + hPET Hydrus Runs | Depth | Site SA | Site A | Site HA | Site HU |
|---|---|---|---|---|---|
| | 0.2 mbgl | 0.12 | 0.13 | 0.67 | 0.09 |
| | 0.6 mbgl | 0.16 | 0.28 | 0.84 | 0.10 |
| | 0.9 mbgl | 0.14 | 0.37 | 0.86 | 0.10 |
| | 1.2 mbgl | 0.19 | 0.29 | 0.86 | 0.10 |
| | 1.5 mbgl | 0.30 | 0.19 | 0.85 | 0.10 |
| | 1.8 mbgl | 0.33 | 0.12 | 0.84 | 0.10 |
| | 2.1 mbgl | 0.35 | 0.00 | 0.85 | 0.10 |
| | 2.4 mbgl | 0.27 | 0.00 | 0.83 | 0.10 |
| | 2.7 mbgl | 0.34 | 0.00 | 0.80 | 0.10 |
| | 3.0 mbgl | 0.20 | 0.00 | 0.79 | 0.10 |

**Table D4 - Kolmogorov–Smirnov (KS) test statistics comparing soil moisture distributions at our hydrological four sites across different depths. Higher KS values indicate greater differences between distributions. All results are statistically significant ($p < 0.05$). Compared to Hydrus simulations driven by CP4A rainfall and PET, those driven by CP4A rainfall and hPET exhibit marginally lower KS values. However, all results remain statistically significant ($p < 0.05$), the KS test statistic at Site HU still exhibit the smallest values, suggesting the least divergence.**

The following tables provide additional detail around the water balance components results discussed in section 3.3.

Table D5 shows the same results as Table 6 in the main body of text, but for the Hydrus simulations using CP4A rainfall and hPET PET (rather than CP4A PET). It shows that while the raw values differ, the pattern where P25 loses more infiltration to evaporation and CP4A simulates higher transpiration and bottom drainage remains.

| CP4A/hPET Hydrus Run | Rainfall (mm) | PET (mm) | Runoff (mm) | Infiltration (mm) | ET (mm) | Evaporation (mm) | Transpiration (mm) | Drainage (mm) |
|---|---|---|---|---|---|---|---|---|
| Site SA | 5952 (6669) | 15243 | 566 (246) | 5450 (6405) | 6052 (7007) | 3936 (5382) | 2117 (1625) | 162 (22) |
| Site A | 3521 (4289) | 20223 | 158 (10) | 3330 (4297) | 2637 (3789) | 2637 (3789) | 693 (509) | 0 (0) |
| Site HA | 1849 (2394) | 18972 | 94 (51) | 1750 (2325) | N/A | 1665 (2291) | N/A | 36 (1) |
| Site HU | 17333 (20003) | 13086 | 0 (29) | 17171 (19810) | 10926 (11237) | 4188 (4620) | 6737 (6617) | 6601 (8634) |

**Table D5 – Cumulative rainfall, potential evapotranspiration (PET), runoff, infiltration, evapotranspiration (ET), evaporation, transpiration, and drainage from the bottom of the soil profile. All values are given in mm and are the totals over the entire ten-year Hydrus simulations. All results are taken from the default (soil and Feddes' parameters) Hydrus runs forced with CP4A/P25 rainfall and hPET, rather than climate model PET. Those values given in brackets are the P25 rainfall Hydrus runs, all others are forced using CP4A rainfall.**

Table D5 shows the same cumulative water balance components at each site under our low hydraulic conductivity (LK), high hydraulic conductivity (HK) scenarios. In line with the soil moisture results, altering soil hydraulic parameters does not alter the biases seen between CP4A and P25, where P25 loses more infiltration to evaporation and CP4A simulates higher transpiration, surface runoff, and bottom drainage. The same can be said for the choice of Feddes' parameters, Table D7 shows the cumulative water balance values at sites SA and A under our different Feddes' parameters. It shows that whether we use the high or low water resilient set of parameters, the results remain consistent (P25 – higher evaporative losses, CP4A – higher transpiration, runoff, and bottom drainage).

| **LK Run Type** | **Runoff (mm)** | **Infiltration (mm)** | **ET (mm)** | **Evaporation (mm)** | **Transpiration (mm)** | **Drainage (mm)** |
|---|---|---|---|---|---|---|
| Site SA | 983 (391) | 5043 (6256) | 5660 (6928) | 3573 (5319) | 2087 (1608) | 145 (23) |
| Site A | 326 (34) | 3192 (4239) | 3159 (4273) | 2477 (3681) | 681 (592) | 0 (0) |
| Site HA | 147 (66) | 1700 (2314) | N/A | 1590 (2273) | N/A | 31 (2) |
| Site HU | 4 (43) | 17300 (19849) | 10485 (11424) | 4045 (4709) | 6440 (6715) | 7145 (8620) |
| **HK Run Type** | | | | | | |
| Site SA | 467 (197) | 5564 (6450) | 6116 (7075) | 3590 (5294) | 2525 (1781) | 376 (24) |
| Site A | 7 (0) | 3512 (4273) | 3458 (4308) | 2357 (3599) | 1100 (709) | 0 (0) |
| Site HA | 2 (4) | 1846 (2377) | N/A | 1641 (2271) | N/A | 97 (5) |
| Site HU | 0 (12) | 17299 (19880) | 10437 (11384) | 3999 (4667) | 6438 (6717) | 7189 (8685) |

**Table D6 – Cumulative rainfall, potential evapotranspiration (PET), runoff, infiltration, evapotranspiration (ET), evaporation, transpiration, and drainage from the bottom of the soil profile. All values are given in mm and are the totals over the entire ten-year Hydrus simulations. lowK refers to low hydraulic conductivity simulations, and highK is high hydraulic conductivity simulations. Those values given in brackets are the P25 Hydrus runs, all others are forced by CP4A.**

Table D7 shows the cumulative water balance values at sites SA and A under our different Feddes' parameters.

| **Lower Feddes Run** | **Runoff** | **Infiltration** | **ET** | **Evaporation** | **Transpiration** | **Drainage** |
|---|---|---|---|---|---|---|
| Site SA | 611 (254) | 5418 (6394) | 5807 (6859) | 3707 (5433) | 2099 (1426) | 394 (35) |
| Site A | 176 (23) | 3344 (4253) | 3314 (4271) | 2657 (3734) | 657 (537) | 4 (3) |
| **Mid Feddes Run** | | | | | | |
| Site SA | 610 (253) | 5418 (6394) | 5819 (6859) | 3697 (5424) | 2121 (1435) | 382 (31) |
| Site A | 226 (11) | 3292 (4261) | 3266 (4286) | 2514 (3813) | 752 (474) | 4 (3) |
| **Def Run Type** | | | | | | |
| **Site SA** | **605 (250)** | **5423 (6398)** | **6003 (7044)** | **3611 (5320)** | **2392 (1724)** | **286 (23)** |
| **Site A** | **223 (22)** | **3297 (4254)** | **3255 (4283)** | **2402 (3598)** | **853 (694)** | **0 (0)** |

**Table D7 – Cumulative rainfall, potential evapotranspiration (PET), runoff, infiltration, evapotranspiration (ET), evaporation, transpiration, and drainage from the bottom of the soil profile. All values are given in mm and are the totals over the entire ten-year Hydrus simulations. The lower Feddes' refers to simulations using the low (least water resilient) Feddes' parameters, mid refers to simulations using the mid-range Feddes' parameter set, and the Def run is our default run which uses the most water resilient parameter set (see Table B2). Def is the run reported in the main body of text. The low, mid, and upper (def) Feddes' parameters are taken from Sela et al (2015). See Appendix 6.2 for more details on each simulation. Those values given in brackets are the P25 Hydrus runs, all others are forced by CP4A.**

## ~~6. Appendices~~

### ~~6.1 Appendix A~~

~~Appendix A details the parameters that were altered between the different Hydrus simulations used at each site. Table A1 lists the soil parameters used for our three simulation categories: lowK, def, and highK. Where def (**given in bold**) refers to default soil parameters that are used for all simulations discussed in the main text, lowK refers to low hydraulic conductivity simulations, and highK is high hydraulic conductivity simulations. For example, at Site A hydraulic conductivity ($K_s$) ranges from 3.5 mm/h to 21.8 mm/h.~~

~~These soil parameters were estimated using Genuchten-Mualem (Van Genuchten, 1980) equations based on soil texture values taken from the Innovate Solutions for Decision Agriculture (iSDA) soil database (Hengl et al., 2021). Where *Qr* refers to residual soil water content, *Qs* is the saturated water content, *Alpha* is Parameter $a$ in the soil water retention function [$L^{-1}$], $n$ is parameter $n$ in the soil water retention function, $K_s$ is the saturated hydraulic conductivity [$LT^{-1}$], and $I$ is the tortuosity parameter in the conductivity function [-]. Differences in parameters between the lowK and highK simulations were based on taking the lower and upper sand percentage given in the iSDA soil database (Hengl et al., 2021).~~

| ~~**Site H (Humid)**~~ | | | | | | | |
|---|---|---|---|---|---|---|---|
| ~~Scenario~~ | ~~Depth~~ | ~~*Qr*~~ | ~~*Qs*~~ | ~~*Alpha*~~ | ~~*n*~~ | ~~*Ks (mm/h)*~~ | ~~*I*~~ |
| ~~LowK~~ | ~~0 – 20 cm~~ | ~~0.103~~ | ~~0.545~~ | ~~0.002~~ | ~~1.339~~ | ~~18.342~~ | ~~0.500~~ |
| ~~LowK~~ | ~~20 - 500 cm~~ | ~~0.105~~ | ~~0.543~~ | ~~0.002~~ | ~~1.315~~ | ~~15.650~~ | ~~0.500~~ |
| ~~**Def**~~ | ~~**0 - 20 cm**~~ | ~~**0.096**~~ | ~~**0.525**~~ | ~~**0.002**~~ | ~~**1.384**~~ | ~~**19.117**~~ | ~~**0.500**~~ |
| ~~**Def**~~ | ~~**20 - 500 cm**~~ | ~~**0.100**~~ | ~~**0.529**~~ | ~~**0.002**~~ | ~~**1.349**~~ | ~~**17.833**~~ | ~~**0.500**~~ |
| ~~HighK~~ | ~~0 – 20 cm~~ | ~~0.084~~ | ~~0.510~~ | ~~0.002~~ | ~~1.405~~ | ~~22.588~~ | ~~0.500~~ |
| ~~HighK~~ | ~~20 – 500 cm~~ | ~~0.090~~ | ~~0.512~~ | ~~0.002~~ | ~~1.384~~ | ~~19.996~~ | ~~0.500~~ |
| ~~**Site SA (Semi-Arid)**~~ | | | | | | | |
| ~~Scenario~~ | ~~Depth~~ | ~~*Qr*~~ | ~~*Qs*~~ | ~~*Alpha*~~ | ~~*n*~~ | ~~*Ks (mm/h)*~~ | ~~*I*~~ |
| ~~LowK~~ | ~~0 – 20 cm~~ | ~~0.076~~ | ~~0.416~~ | ~~0.001~~ | ~~1.405~~ | ~~3.221~~ | ~~0.500~~ |
| ~~LowK~~ | ~~20 – 500 cm~~ | ~~0.081~~ | ~~0.423~~ | ~~0.002~~ | ~~1.351~~ | ~~3.204~~ | ~~0.500~~ |
| ~~**Def**~~ | ~~**0 – 20 cm**~~ | ~~**0.068**~~ | ~~**0.409**~~ | ~~**0.002**~~ | ~~**1.400**~~ | ~~**5.658**~~ | ~~**0.500**~~ |
| ~~**Def**~~ | ~~**20 – 500 cm**~~ | ~~**0.076**~~ | ~~**0.418**~~ | ~~**0.002**~~ | ~~**1.354**~~ | ~~**4.175**~~ | ~~**0.500**~~ |
| ~~HighK~~ | ~~0 – 20 cm~~ | ~~0.066~~ | ~~0.408~~ | ~~0.002~~ | ~~1.401~~ | ~~6.663~~ | ~~0.500~~ |
| ~~HighK~~ | ~~20 – 500 cm~~ | ~~0.072~~ | ~~0.417~~ | ~~0.002~~ | ~~1.367~~ | ~~6.100~~ | ~~0.500~~ |
| ~~**Site A (Arid)**~~ | | | | | | | |
| ~~Scenario~~ | ~~Depth~~ | ~~*Qr*~~ | ~~*Qs*~~ | ~~*Alpha*~~ | ~~*n*~~ | ~~*Ks (mm/h)*~~ | ~~*I*~~ |
| ~~LowK~~ | ~~0 – 20 cm~~ | ~~0.081~~ | ~~0.431~~ | ~~0.001~~ | ~~1.426~~ | ~~3.542~~ | ~~0.500~~ |
| ~~LowK~~ | ~~20 – 500 cm~~ | ~~0.085~~ | ~~0.436~~ | ~~0.001~~ | ~~1.404~~ | ~~3.338~~ | ~~0.500~~ |
| ~~**Def**~~ | ~~**0 – 20 cm**~~ | ~~**0.067**~~ | ~~**0.418**~~ | ~~**0.002**~~ | ~~**1.415**~~ | ~~**7.558**~~ | ~~**0.500**~~ |
| ~~**Def**~~ | ~~**20 – 500 cm**~~ | ~~**0.069**~~ | ~~**0.419**~~ | ~~**0.002**~~ | ~~**1.404**~~ | ~~**6.363**~~ | ~~**0.500**~~ |
| ~~HighK~~ | ~~0 – 20 cm~~ | ~~0.055~~ | ~~0.414~~ | ~~0.003~~ | ~~1.475~~ | ~~21.817~~ | ~~0.500~~ |
| ~~HighK~~ | ~~20 – 500 cm~~ | ~~0.058~~ | ~~0.413~~ | ~~0.002~~ | ~~1.439~~ | ~~16.004~~ | ~~0.500~~ |
| ~~**Site HA (Hyper-Arid)**~~ | | | | | | | |

| ~~Scenario~~ | ~~Depth~~ | ~~*Qr*~~ | ~~*Qs*~~ | ~~*Alpha*~~ | ~~*n*~~ | ~~*Ks (mm/h)*~~ | ~~*l*~~ |
|---|---|---|---|---|---|---|---|
| ~~LowK~~ | ~~0 - 20 cm~~ | ~~0.070~~ | ~~0.417~~ | ~~0.002~~ | ~~1.400~~ | ~~5.779~~ | ~~0.500~~ |
| ~~LowK~~ | ~~20 - 500 cm~~ | ~~0.069~~ | ~~0.417~~ | ~~0.002~~ | ~~1.394~~ | ~~6.783~~ | ~~0.500~~ |
| ~~**Def**~~ | ~~**0 - 20 cm**~~ | ~~**0.067**~~ | ~~**0.417**~~ | ~~**0.002**~~ | ~~**1.406**~~ | ~~**7.633**~~ | ~~**0.500**~~ |
| ~~**Def**~~ | ~~**20 - 500 cm**~~ | ~~**0.069**~~ | ~~**0.417**~~ | ~~**0.002**~~ | ~~**1.394**~~ | ~~**6.783**~~ | ~~**0.500**~~ |
| ~~HighK~~ | ~~0 - 20 cm~~ | ~~0.056~~ | ~~0.413~~ | ~~0.003~~ | ~~1.480~~ | ~~21.646~~ | ~~0.500~~ |
| ~~HighK~~ | ~~20 - 500 cm~~ | ~~0.056~~ | ~~0.411~~ | ~~0.003~~ | ~~1.466~~ | ~~19.329~~ | ~~0.500~~ |

~~**Table A1 - Soil Hydraulic parameters used in all Hydrus simulation at our humid (HU), semi-arid (SA), arid (A), and hyper-arid (HA) sites across the HOA.**~~

~~Table A2 shows the Feddes' parameters used to compute root water uptake (transpiration) within Hydrus (Feddes, 1978). Where *P0* is pressure value at which roots start to extract water from the soil, *POpt* is the pressure head at which roots extract water at the maximum possible rate, *P2H* is the pressure head at which roots can no longer extract water at the maximum possible rate (assumes a potential transpiration rate of *r2H*), *P2L* is the same above but instead assumes a maximum possible transpiration rate of *r2L*, and *P3* is the value of the pressure head at which roots can no uptake any water from the soil (wilting point). Vegetation type was taken from iSDA based on 2019 data (iSDA, 2024).~~

~~Hydrus has an internal database of Feddes' parameters for various crop types, the maize parameters were taken from this database and are based on Wesseling (1991). However, shrubs are not in this database and there is very little published information on Feddes' parameters for shrubs. We were able to locate some thresholds for dryland shrubs: *Acacia Mearsii*, *Caragana korshinkii*, and *Sarcopoterium spinosum* (Xia and Shao, 2008, Sela et al., 2015, Watson, 2015). Sela et al (2015) provided a range of Feddes' parameters used in their calibration process to correctly quantify transpiration rates of *Caragana korshinkii* in Hydrus 1-D, settling on an optimal parameter set. However, we decided to use the upper range (here referred to as def) of the parameters given by Sela et al (2015) as they better matched estimates given by Xia and Shoa (2008) and Watson (2015), particularly the wilting point. However, to ensure results were consistent regardless of the Feddes' parameters chosen, we also using the optimal and lower values provided by Sela et al (2015). However, unless stated otherwise all results reported in the main body of text were computed using the upper (def) Feddes' values – **given in bold below.**~~

| ~~Feddes' Parameter~~ | ~~*P0*~~ | ~~*POpt*~~ | ~~*P2H*~~ | ~~*P2L*~~ | ~~*P3*~~ | ~~*r2H (mm/h)*~~ | ~~*r2L (mm/h)*~~ |
|---|---|---|---|---|---|---|---|
| ~~**Shrubs Upper (def)**~~ | ~~**-150**~~ | ~~**-300**~~ | ~~**-5000**~~ | ~~**-15000**~~ | ~~**-240000**~~ | ~~**0.208**~~ | ~~**0.042**~~ |
| ~~Shrubs Mid~~ | ~~-58~~ | ~~-224~~ | ~~-326~~ | ~~-6700~~ | ~~-15570~~ | ~~0.208~~ | ~~0.042~~ |
| ~~Shrubs Lower~~ | ~~0~~ | ~~-150~~ | ~~-300~~ | ~~-5000~~ | ~~-15000~~ | ~~0.208~~ | ~~0.042~~ |
| ~~Maize~~ | ~~-150~~ | ~~-300~~ | ~~-3250~~ | ~~-6000~~ | ~~-80000~~ | ~~0.208~~ | ~~0.042~~ |

~~**Table A2 – Feddes parameters controlling root water uptake for shrubs and maize used in Hydrus 1-D simulations. Values were for shrubs were taken from Sela et al (2015) and maize from Wesseling (1991).**~~

## ~~6.2 Appendix B~~

~~Appendix B provides additional figures and materials on the analyses of CP4A/P25 rainfall and PET simulations (sections 3.1 and 3.2). Figure 1B shows the magnitude of the 95th percentile of IMERG wet season rainfall (wet hours only). These values were used as the threshold to define want rainfall intensity can be deemed 'heavy' within Fig. 5a-c in the main body of text. In humid regions the intensity ranges from 2 to 11 mm/h (mean of 7.7 mm/h), and in arid regions it ranges from 3 to 16 mm/h (mean of 8.5 mm/h).~~

~~Table B1 shows the results of a multi-linear regression between the daily PET climatology and the daily climatology of the seven atmospheric variables used to compute PET in humid and arid regions of the Horn of Africa. These results are discussed in the main body of text under section 3.2.~~

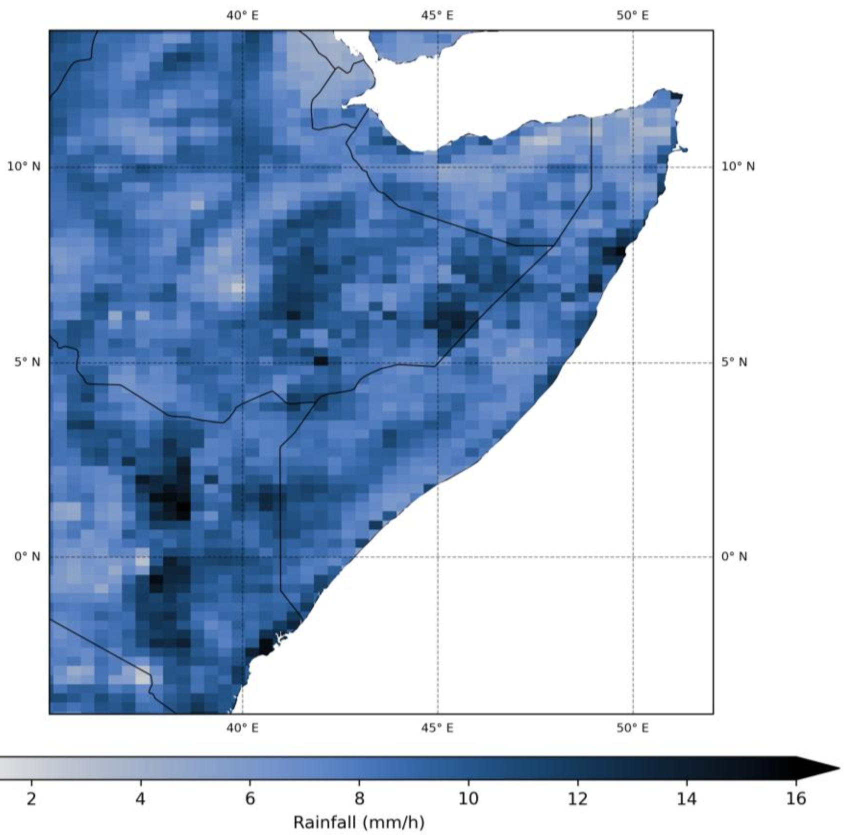


**Figure B1 - 95th percentile of IMERG wet season precipitation. Calculated using wet hours, where any wet hours are any hour that receives >= 0.1 mm of rainfall.**

| ~~Humid Regions~~ | | | | | |
|---|---|---|---|---|---|
| ~~Variable~~ | ~~Coefficient~~ | ~~Std Error~~ | ~~P>\|t\|~~ | ~~0.025 CI~~ | ~~0.975 CI~~ |
| ~~Temp~~ | ~~0.127 (**0.438**)~~ | ~~0.028 (**0.046**)~~ | ~~0 (**0.000**)~~ | ~~0.072 (**0.349**)~~ | ~~0.182 (**0.529**)~~ |

| | | | | | |
|---|---|---|---|---|---|
| Dew Point | 0.152 (**-0.129**) | 0.021 (**0.031**) | 0 (**0.000**) | 0.112 (**-0.191**) | 0.193 (**-0.068**) |
| Surface Pressure | 0.0001 (**-0.002**) | 0.000 (**0.000**) | 0.58 (**0.000**) | 0.000 (**-0.002**) | 0.000 (**-0.001**) |
| Short Wave Radiation | 7.2e-7 (**7.9e-07**) | 1.6e-7 (**2.2e-7**) | 0.000 (**0.001**) | 4.1e-7 (**3.4e-7**) | 1.0e-6 (**1.2e-6**) |
| Long Wave Radiation | -7.9e-6 (**2.6e-6**) | 1.4e-6 (**1.8e-6**) | 0.000 (**0.149**) | -1.1E-5 (**-9.5e-7**) | -5.1E-6 (**6.2e-6**) |
| Meridional Wind | 0.041 (**-0.108**) | 0.024 (**0.034**) | 0.081 (**0.002**) | -0.005 (**-0.174**) | 0.088 (**-0.041**) |
| Zonal Wind | -0.181 (**-0.178**) | 0.027 (**0.039**) | 0 (**0.000**) | -0.235 (**-0.255**) | -0.127 (**-0.100**) |
| Arid Regions | | | | | |
| Variable | Coefficient | Std Error | P>\|t\| | 0.025 CI | 0.975 CI |
| Temp | 0.285 (**0.232**) | 0.033 (**0.027**) | 0.000 (**0.000**) | 0.220 (**0.179**) | 0.349 (**0.285**) |
| Dew Point | -0.364 (**-0.391**) | 0.026 (**0.018**) | 0.000 (**0.000**) | -0.401 (**-0.426**) | -0.327 (**-0.356**) |
| Surface Pressure | 0.0009 (**-0.001**) | 0.000 (**0.000**) | 0.58 (**0.000**) | -0.001 (**-0.001**) | -0.001 (**-0.000**) |
| Short Wave Radiation | 2.0e-06 (**7.0e-6**) | 2.1e-07 (**4.5e-7**) | 0.000 (**0.001**) | 1.6e-06 (**6.1e-06**) | 2.4e-06 (**7.8e-06**) |
| Long Wave Radiation | 9.6e-06 (**1.2e-5**) | 1.4e-06 (**1.2e-6**) | 0.000 (**0.149**) | 6.8e-06 (**1.0e-5**) | 1.2e-05 (**1.5e-5**) |
| Meridional Wind | 0.178 (**0.103**) | 0.025 (**0.019**) | 0.000 (**0.002**) | 0.130 (**0.066**) | 0.226 (**0.139**) |
| Zonal Wind | -0.095 (**0.016**) | 0.026 (**0.019**) | 0.000 (**0.000**) | -0.146 (**-0.022**) | -0.044 (**0.053**) |

**Table B1 - Results of the multi-linear regression analysis on the drivers of PET in CP4A and P25 in humid (AI > 0.65) and arid (AI <= 0.2) regions of the HOA. Bold values refer to CP4A, while non-bold values refer to P25.**

~~Figure B2 shows the daily meridional wind speed climatology in arid regions of the Horn of Africa. It appears that the positive significant relationship between meridional wind speed and PET (Table B1) is the driving factor behind higher PET in P25 during the months of June to September (see Fig. 3g)~~

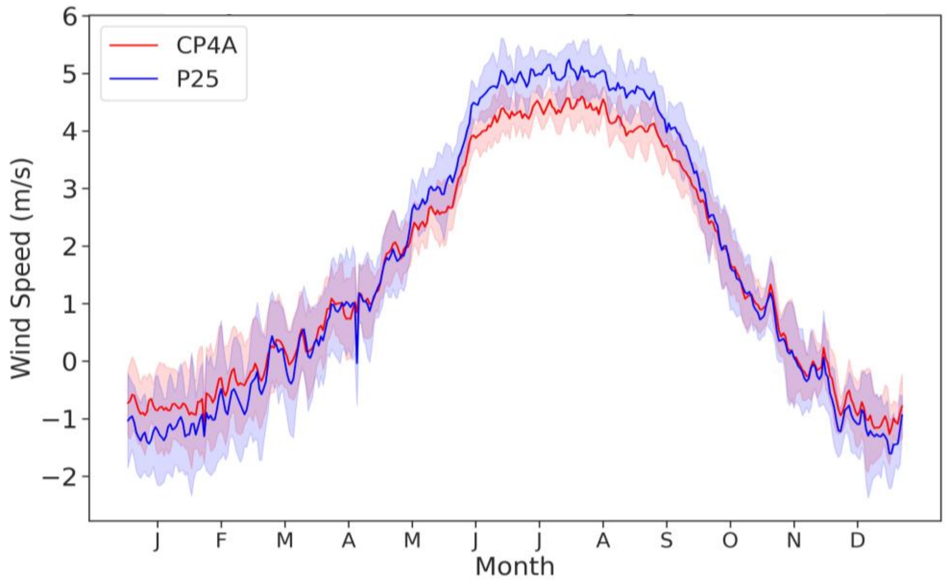


~~**Figure B2 - Daily climatology of meridional wind speed in arid (AI < 0.2) regions of the HOA.**~~

~~**6.3 Appendix C**~~

~~Appendix C provides additional figures and tables relevant to the analysis of Hydrus simulations (section 3.3). Figure C1 shows the mean monthly CP4A and P25 rainfall at each of our four sites. Both models broadly capture the observed seasonality in the region (Wainwright et al., 2019), simulating the bimodal rainfall regime at our dryland sites (Sites SA, A, and HA) and the unimodal regime in the humid Ethiopian Highlands (Site HU). However, it is worth noting that P25 tends to simulate rainfall in every month (including July and August) at our dryland sites (CP4A simulates negligible rainfall) and simulates substantially higher rainfall totals during June and July at Site HU.~~

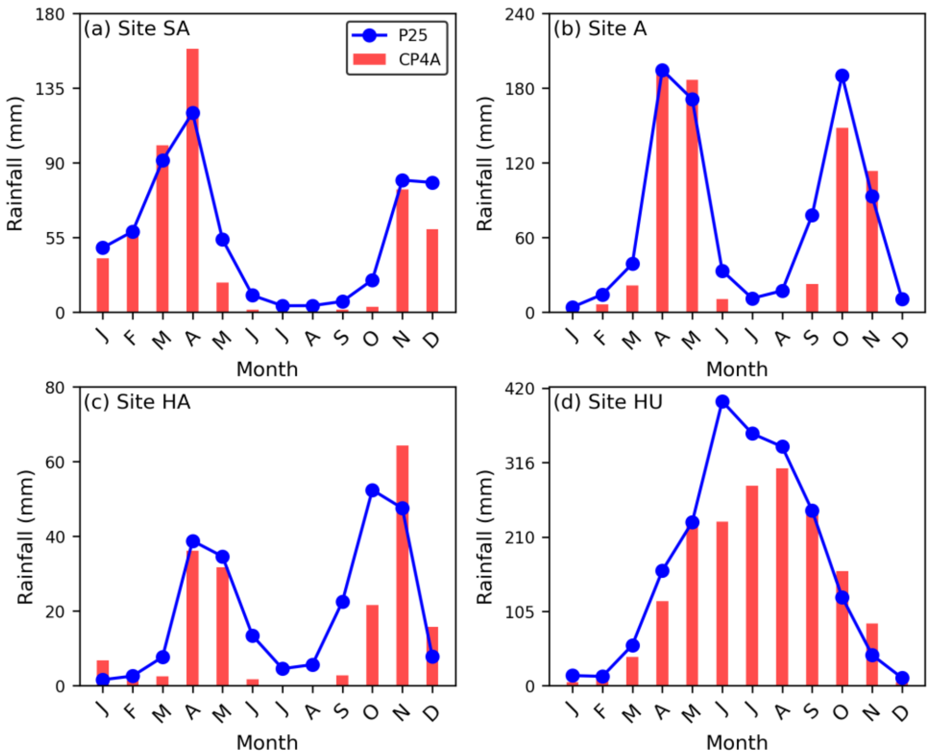


**Figure D~~C~~1 – Mean monthly rainfall at each of our four hydrological study sites.**

~~Figure C2 shows mean monthly CP4A and P25 PET at each of our four study sites. At all sites both models simulate comparable seasonal cycles and totals, although P25 consistently simulates higher PET at Sites A and HA. It is also worth noting that P25 simulates substantially higher PET during the months June – August, matching the higher JJAS PET simulated by P25 across the entire arid region of the HOA.~~

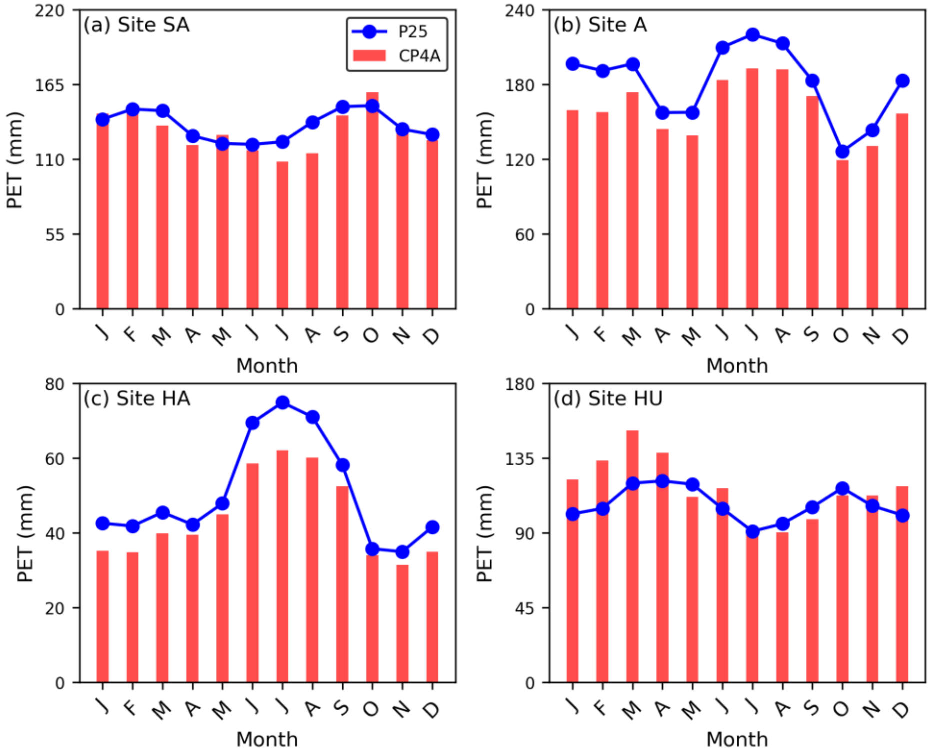


**Figure D~~C~~2 – Mean monthly PET at each of our four hydrological study sites.**

~~Figure C3 shows the raw time series of rainfall at each study site, it provides a clear demonstration of the tendency for CP4A to simulate heavier rainfall events, as well as more frequent intense rainfall events at our dryland study sites (Sites SA, A, and HA). Whereas at our humid site in the Ethiopian Highlands, the differences are far more muted and at times it is P25 that is simulating heavier rainfall events.~~

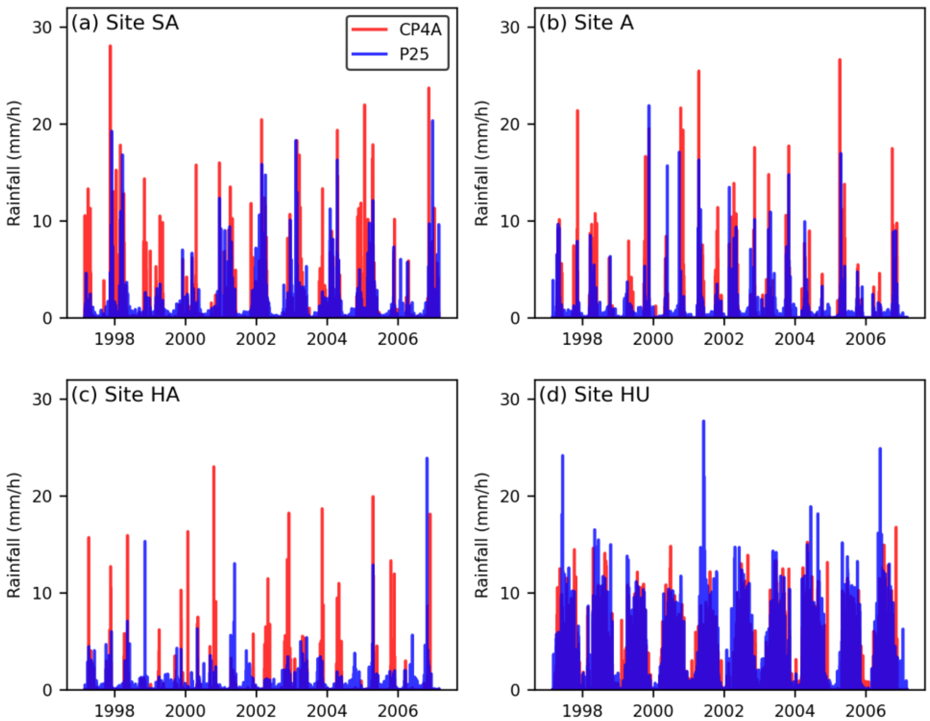


**Figure D~~C~~3 – Raw time series of rainfall at each of our four hydrological study sites.**

~~Table C1 shows the interquartile ranges (IQRs) of soil moisture in the upper 1.2 meters of the soil profile and the entire three-meter profile at each study site.~~

~~While the IQR does overlap at each site between the Hydrus simulations driven by CP4A and P25, soil moisture is always higher when Hydrus is forced by CP4A rainfall. This is supported by Table C2 which shows the relative percentage difference in median soil moisture between CP4A and P25, with CP4A simulating 710-20% higher median soil moisture at our dryland sites in the default Hydrus runs.~~

| ~~1.2 Meters Below Ground Level~~ | ~~Site SA~~ | ~~Site A~~ | ~~Site HA~~ | ~~Site HU~~ |
|---|---|---|---|---|
| ~~CP4A~~ | ~~49.7 – 63.6~~ | ~~37.7 – 46.5~~ | ~~47.2 – 51.3~~ | ~~53.0 – 78.9~~ |
| ~~P25~~ | ~~45.4 – 58.2~~ | ~~31.4 – 41.0~~ | ~~39.7 – 41.1~~ | ~~51.6 – 81.3~~ |
| ~~3.0 Meters Below Ground Level~~ | | | | |
| ~~CP4A~~ | ~~52.7 – 59.0~~ | ~~39.7 – 43.7~~ | ~~47.8 – 49.5~~ | ~~60.6 – 77.7~~ |
| ~~P25~~ | ~~35.4 – 45.1~~ | ~~27.0 – 30.8~~ | ~~40.5 – 41.1~~ | ~~59.6 – 79.4~~ |

~~**Table C1 – Interquartile ranges of depth integrated soil moisture in the upper 1.2 meters of the soil profile, and the entire three-meter profile. All values refer to the % saturation.**~~

| ~~**Depth (meters below ground level)**~~ | ~~**Site SA**~~ | ~~**Site A**~~ | ~~**Site HA**~~ | ~~**Site HU**~~ |
|---|---|---|---|---|
| ~~0.2 mbgl~~ | ~~0.16~~ | ~~0.14~~ | ~~0.74~~ | ~~0.07~~ |
| ~~0.6 mbgl~~ | ~~0.22~~ | ~~0.~~ | ~~0.89~~ | ~~0.07~~ |

| | | | | |
|---|---|---|---|---|
| | | ~~27~~ | | |
| ~~0.9 mbgl~~ | ~~0.22~~ | ~~0.44~~ | ~~0.93~~ | ~~0.08~~ |
| ~~1.2 mbgl~~ | ~~0.23~~ | ~~0.40~~ | ~~0.94~~ | ~~0.08~~ |
| ~~1.5 mbgl~~ | ~~0.35~~ | ~~0.49~~ | ~~0.98~~ | ~~0.08~~ |
| ~~1.8 mbgl~~ | ~~0.46~~ | ~~0.15~~ | ~~0.99~~ | ~~0.09~~ |
| ~~2.1 mbgl~~ | ~~0.41~~ | ~~0.00~~ | ~~1.00~~ | ~~0.09~~ |
| ~~2.4 mbgl~~ | ~~0.49~~ | ~~0.00~~ | ~~1.00~~ | ~~0.09~~ |
| ~~2.7 mbgl~~ | ~~0.38~~ | ~~0.00~~ | ~~1.00~~ | ~~0.09~~ |
| ~~3.0 mbgl~~ | ~~0.38~~ | ~~0.00~~ | ~~0.85~~ | ~~0.08~~ |

| ~~Hydrus Run (depth – meters below ground level)~~ | ~~Site SA~~ | ~~Site A~~ | ~~Site HA~~ | ~~Site HU~~ |
|---|---|---|---|---|
| ~~Low Hydraulic Conductivity (1.2 mbgl)~~ | ~~10.6~~ | ~~10.5~~ | ~~17.0~~ | ~~5.2~~ |
| ~~Low Hydraulic Conductivity (3.0 mbgl)~~ | ~~14.4~~ | ~~5.1~~ | ~~14.7~~ | ~~2.5~~ |

| | | | | |
|---|---|---|---|---|
| **~~Default (1.2 mbgl)~~** | **~~10.3~~** | **~~15.5~~** | **~~21.4~~** | **~~2.5~~** |
| **~~Default (3.0 mbgl)~~** | **~~20.7~~** | **~~9.1~~** | **~~19.4~~** | **~~5.2~~** |
| ~~High Hydraulic Conductivity (1.2 mbgl)~~ | ~~10.4~~ | ~~32.0~~ | ~~22.3~~ | ~~5.7~~ |
| ~~High Hydraulic Conductivity (3.0 mbgl)~~ | ~~22.6~~ | ~~21.9~~ | ~~25.5~~ | ~~2.6~~ |

~~This tendency for differences between CP4A and P25 Hydrus runs to be higher in drylands is also supported by Table C3, which shows that differences in soil moisture distributions are more pronounced (based on the Kolmogorov-Smirnov statistic) at the dryland sites versus Site HU.~~

**~~Table C2 – Relative percentage difference in median depth integrated soil moisture between CP4A and P25 Hydrus runs. Default (given in bold) refers to default soil parameters that are used for all simulations discussed in the main text, lowK refers to low hydraulic conductivity simulations, and highK is high hydraulic conductivity simulations. See Appendix 6.1 for more details on each simulation. For all values reported, it is a positive percentage difference between CP4A and P25 soil moisture. Eg CP4A simulates higher soil moisture in all cases.~~**

| **~~Depth (meters below ground level)~~** | **~~Site SA~~** | **~~Site A~~** | **~~Site HA~~** | **~~Site HU~~** |
|---|---|---|---|---|
| ~~0.2 mbgl~~ | ~~0.16~~ | ~~0.14~~ | ~~0.74~~ | ~~0.07~~ |
| ~~0.6 mbgl~~ | ~~0.22~~ | ~~0.27~~ | ~~0.89~~ | ~~0.07~~ |
| ~~0.9 mbgl~~ | ~~0.22~~ | ~~0.44~~ | ~~0.93~~ | ~~0.08~~ |
| ~~1.2 mbgl~~ | ~~0.23~~ | ~~0.40~~ | ~~0.94~~ | ~~0.08~~ |
| ~~1.5 mbgl~~ | ~~0.35~~ | ~~0.49~~ | ~~0.98~~ | ~~0.08~~ |
| ~~1.8 mbgl~~ | ~~0.46~~ | ~~0.15~~ | ~~0.99~~ | ~~0.09~~ |
| ~~2.1 mbgl~~ | ~~0.41~~ | ~~0.00~~ | ~~1.00~~ | ~~0.09~~ |
| ~~2.4 mbgl~~ | ~~0.49~~ | ~~0.00~~ | ~~1.00~~ | ~~0.09~~ |
| ~~2.7 mbgl~~ | ~~0.38~~ | ~~0.00~~ | ~~1.00~~ | ~~0.09~~ |
| ~~3.0 mbgl~~ | ~~0.38~~ | ~~0.00~~ | ~~0.85~~ | ~~0.08~~ |

**~~Table C3 - Kolmogorov–Smirnov (KS) test statistics comparing soil moisture distributions at our hydrological four sites across different depths. Higher KS values indicate greater differences between distributions. All results are statistically significant ($p < 0.05$). Site HA consistently shows the largest differences, while Site HU exhibits the smallest KS values, suggesting the least divergence. All results refer to Hydrus simulations driven by CP4A rainfall and PET.~~**

~~It is also worth noting that forcing Hydrus with CP4A rainfall yields higher soil moisture values regardless of the soil hydraulic parameters used (see Table 3B) or the Feddes' parameters used to estimate the root water uptake of dryland shrubs (see Table 3D).~~

| **~~Hydrus Run (depth meters below ground level)~~** | **~~Site SA (Semi-Arid)~~** | **~~Site A (Arid)~~** |
|---|---|---|
| ~~Low (least water resilient) Feddes' Parameters (1.2 mbgl)~~ | ~~6.2~~ | ~~3.6~~ |
| ~~Low (least water resilient) Feddes' Parameters (3.0 mbgl)~~ | ~~10.7~~ | ~~2.4~~ |
| ~~Mid Feddes' Parameters (1.2 mbgl)~~ | ~~6.4~~ | ~~8.5~~ |
| ~~Mid Feddes' Parameters (3.0 mbgl)~~ | ~~10.9~~ | ~~4.7~~ |

| | | |
|---|---|---|
| **~~Default/Upper (most water resilient) Feddes' Parameters (1.2 mbgl)~~** | **~~10.3~~** | **~~15.5~~** |
| **~~Default/Upper (most water resilient) Feddes' Parameters (3.0 mbgl)~~** | **~~20.7~~** | **~~9.1~~** |

~~Table C4 - Relative percentage difference in median depth integrated soil moisture between CP4A and P25 Hydrus runs. Default/Upper (given in bold) refers to default Feddes' parameters that are used for all simulations discussed in the main text, low refers to simulations using the low (least water resilient) Feddes' parameters, and mid refers to simulations using the mid-range Feddes' parameter set. The low, mid, and upper Feddes' parameters are taken from Sela et al (2015). See Appendix 6.1 for more details on each simulation. For all values reported, it is a positive percentage difference between CP4A and P25 soil moisture. Eg CP4A simulates higher soil moisture in all cases.~~

| ~~CP4A + hPET Hydrus Runs~~ | ~~Depth~~ | ~~Site SA~~ | ~~Site A~~ | ~~Site HA~~ | ~~Site HU~~ |
|---|---|---|---|---|---|
| | ~~0.2 mbgl~~ | ~~0.12~~ | ~~0.13~~ | ~~0.67~~ | ~~0.09~~ |
| | ~~0.6 mbgl~~ | ~~0.16~~ | ~~0.28~~ | ~~0.84~~ | ~~0.10~~ |
| | ~~0.9 mbgl~~ | ~~0.14~~ | ~~0.37~~ | ~~0.86~~ | ~~0.10~~ |
| | ~~1.2 mbgl~~ | ~~0.19~~ | ~~0.29~~ | ~~0.86~~ | ~~0.10~~ |
| | ~~1.5 mbgl~~ | ~~0.30~~ | ~~0.19~~ | ~~0.85~~ | ~~0.10~~ |
| | ~~1.8 mbgl~~ | ~~0.33~~ | ~~0.12~~ | ~~0.84~~ | ~~0.10~~ |
| | ~~2.1 mbgl~~ | ~~0.35~~ | ~~0.00~~ | ~~0.85~~ | ~~0.10~~ |
| | ~~2.4 mbgl~~ | ~~0.27~~ | ~~0.00~~ | ~~0.83~~ | ~~0.10~~ |
| | ~~2.7 mbgl~~ | ~~0.34~~ | ~~0.00~~ | ~~0.80~~ | ~~0.10~~ |
| | ~~3.0 mbgl~~ | ~~0.20~~ | ~~0.00~~ | ~~0.79~~ | ~~0.10~~ |

~~Table C5 - Kolmogorov–Smirnov (KS) test statistics comparing soil moisture distributions at our hydrological four sites across different depths. Higher KS values indicate greater differences between distributions. All results are statistically significant ($p < 0.05$). Compared to Hydrus simulations driven by CP4A rainfall and PET, those driven by CP4A rainfall and hPET exhibit marginally lower KS values. However, all results remain statistically significant ($p < 0.05$), KS values are Site HU also still exhibit the smallest KS values, suggesting the least divergence.~~

| ~~Default Hydrus Run~~ | ~~Rainfall~~ | ~~PET~~ | ~~Runoff~~ | ~~Infiltration~~ | ~~ET~~ | ~~Evaporation~~ | ~~Transpiration~~ | ~~Drainage~~ |
|---|---|---|---|---|---|---|---|---|
| ~~Site SA~~ | ~~5952 (6669)~~ | ~~15750 (16230)~~ | ~~605 (250)~~ | ~~5423 (6398)~~ | ~~6003 (7044)~~ | ~~3611 (5320)~~ | ~~2392 (1724)~~ | ~~286 (23)~~ |
| ~~Site A~~ | ~~3521 (4289)~~ | ~~19233 (21817)~~ | ~~223 (22)~~ | ~~3297 (4254)~~ | ~~3255 (4283)~~ | ~~2402 (3598)~~ | ~~853 (694)~~ | ~~0 (0)~~ |
| ~~Site HA~~ | ~~1849 (2394)~~ | ~~17181 (19714)~~ | ~~135 (53)~~ | ~~1713 (2328)~~ | ~~N/A~~ | ~~1574 (2277)~~ | ~~N/A~~ | ~~52 (2)~~ |
| ~~Site HU~~ | ~~17333 (20003)~~ | ~~13982 (12894)~~ | ~~0 (30)~~ | ~~17300 (19863)~~ | ~~10474 (11418)~~ | ~~4030 (4693)~~ | ~~6445 (6725)~~ | ~~7154 (8638)~~ |

~~Table C6 – Cumulative rainfall, potential evapotranspiration (PET), runoff, infiltration, evapotranspiration (ET), evaporation, transpiration, and drainage from the bottom of the soil profile. All values are given in mm and are the totals over the entire ten year Hydrus simulations. All results are taken from the default Hydrus run forced with CP4A/P25 rainfall and PET. Those values given in brackets are the P25 Hydrus runs, all others are forced by CP4A.~~

| ~~hPET – Hydrus Run~~ | ~~Rainfall~~ | ~~PET~~ | ~~Runoff~~ | ~~Infiltration~~ | ~~ET~~ | ~~Evaporation~~ | ~~Transpiration~~ | ~~Drainage~~ |
|---|---|---|---|---|---|---|---|---|
| ~~Site SA~~ | ~~5952 (6669)~~ | ~~15243~~ | ~~566 (246)~~ | ~~5450 (6405)~~ | ~~6052 (7007)~~ | ~~3936 (5382)~~ | ~~2117 (1625)~~ | ~~162 (22)~~ |

| | | | | | | | | |
|---|---|---|---|---|---|---|---|---|
| ~~Site A~~ | ~~3521 (4289)~~ | ~~20223~~ | ~~158 (10)~~ | ~~3330 (4297)~~ | ~~2637 (3789)~~ | ~~2637 (3789)~~ | ~~693 (509)~~ | ~~0 (0)~~ |
| ~~Site HA~~ | ~~1849 (2394)~~ | ~~18972~~ | ~~94 (51)~~ | ~~1750 (2325)~~ | ~~N/A~~ | ~~1665 (2291)~~ | ~~N/A~~ | ~~36 (1)~~ |
| ~~Site HU~~ | ~~17333 (20003)~~ | ~~13086~~ | ~~0 (29)~~ | ~~17171 (19810)~~ | ~~10926 (11237)~~ | ~~4188 (4620)~~ | ~~6737 (6617)~~ | ~~6601 (8634)~~ |

~~Table C7 – Cumulative rainfall, potential evapotranspiration (PET), runoff, infiltration, evapotranspiration (ET), evaporation, transpiration, and drainage from the bottom of the soil profile. All values are given in mm and are the totals over the entire ten-year Hydrus simulations. All results are taken from the default Hydrus run forced with CP4A/P25 rainfall and hPET, rather than climate model PET. Those values given in brackets are the P25 rainfall Hydrus runs, all others are forced by CP4A rainfall.~~

| **~~LK Run Type~~** | **~~Runoff~~** | **~~Infiltration~~** | **~~ET~~** | **~~Evaporation~~** | **~~Transpiration~~** | **~~Drainage~~** |
|---|---|---|---|---|---|---|
| ~~Site SA~~ | ~~983 (391)~~ | ~~5043 (6256)~~ | ~~5660 (6928)~~ | ~~3573 (5319)~~ | ~~2087 (1608)~~ | ~~145 (23)~~ |
| ~~Site A~~ | ~~326 (34)~~ | ~~3192 (4239)~~ | ~~3159 (4273)~~ | ~~2477 (3681)~~ | ~~681 (592)~~ | ~~0 (0)~~ |
| ~~Site HA~~ | ~~147 (66)~~ | ~~1700 (2314)~~ | ~~N/A~~ | ~~1590 (2273)~~ | ~~N/A~~ | ~~31 (2)~~ |
| ~~Site HU~~ | ~~4 (43)~~ | ~~17300 (19849)~~ | ~~10485 (11424)~~ | ~~4045 (4709)~~ | ~~6440 (6715)~~ | ~~7145 (8620)~~ |
| **~~HK Run Type~~** | | | | | | |
| ~~Site SA~~ | ~~467 (197)~~ | ~~5564 (6450)~~ | ~~6116 (7075)~~ | ~~3590 (5294)~~ | ~~2525 (1781)~~ | ~~376 (24)~~ |
| ~~Site A~~ | ~~7 (0)~~ | ~~3512 (4273)~~ | ~~3458 (4308)~~ | ~~2357 (3599)~~ | ~~1100 (709)~~ | ~~0 (0)~~ |
| ~~Site HA~~ | ~~2 (4)~~ | ~~1846 (2377)~~ | ~~N/A~~ | ~~1641 (2271)~~ | ~~N/A~~ | ~~97 (5)~~ |
| ~~Site HU~~ | ~~0 (12)~~ | ~~17299 (19880)~~ | ~~10437 (11384)~~ | ~~3999 (4667)~~ | ~~6438 (6717)~~ | ~~7189 (8685)~~ |
| **~~Lower Feddes Run~~** | | | | | | |
| ~~Site SA~~ | ~~611 (254)~~ | ~~5418 (6394)~~ | ~~5807 (6859)~~ | ~~3707 (5433)~~ | ~~2099 (1426)~~ | ~~394 (35)~~ |
| ~~Site A~~ | ~~176 (23)~~ | ~~3344 (4253)~~ | ~~3314 (4271)~~ | ~~2657 (3734)~~ | ~~657 (537)~~ | ~~4 (3)~~ |
| **~~Mid Feddes Run~~** | | | | | | |
| ~~Site SA~~ | ~~610 (253)~~ | ~~5418 (6394)~~ | ~~5819 (6859)~~ | ~~3697 (5424)~~ | ~~2121 (1435)~~ | ~~382 (31)~~ |
| ~~Site A~~ | ~~226 (11)~~ | ~~3292 (4261)~~ | ~~3266 (4286)~~ | ~~2514 (3813)~~ | ~~752 (474)~~ | ~~4 (3)~~ |
| **~~Def Run Type~~** | | | | | | |
| **~~Site SA~~** | **~~605 (250)~~** | **~~5423 (6398)~~** | **~~6003 (7044)~~** | **~~3611 (5320)~~** | **~~2392 (1724)~~** | **~~286 (23)~~** |
| **~~Site A~~** | **~~223 (22)~~** | **~~3297 (4254)~~** | **~~3255 (4283)~~** | **~~2402 (3598)~~** | **~~853 (694)~~** | **~~0 (0)~~** |

**~~Table C8 – Cumulative rainfall, potential evapotranspiration (PET), runoff, infiltration, evapotranspiration (ET), evaporation, transpiration, and drainage from the bottom of the soil profile. All values are given in mm and are the totals over the entire ten-year Hydrus simulations. lowK refers to low hydraulic conductivity simulations, and highK is high hydraulic conductivity simulations, while low Feddes' refers to simulations using the low (least water resilient) Feddes' parameters, and mid refers to simulations using the mid-range Feddes' parameter set. The low, mid, and upper (def) Feddes' parameters are taken from Sela et al (2015). See Appendix 6.1 for more details on each simulation. Default (given in bold) values refers to default soil parameters and the upper (default) Feddes' parameters that are used for all simulations discussed in the main text, For All results are taken from the default Hydrus run forced with CP4A/P25 rainfall and PET. Those values given in brackets are the P25 rainfall Hydrus runs, all others are forced by CP4A rainfall.~~**

## 7. Code Availability

The code used to extract precipitation and all variables needed to compute climate model PET (as well as the code to compute PET) can be found at: https://doi.org/10.6084/m9.figshare.28187072.v2. All other code used to analyse CP4A rainfall/PET data and Hydrus simulations can be provided upon request.

## 8. Data Availability

CP4A and P25 data is publicly available at the Centre for Environmental Data Analysis Archive under the IMPALA: Improving model processes for African climate. The CP4A/P25 PET datasets for the Horn of Africa can be downloaded separately from https://doi.org/10.6084/m9.figshare.28187072.v2. Or you can use the provided code to compute PET for another domain. IMERG is publicly available at the NASA Global Precipitation Measurement Mission Data Directory, and the code needed to extract hPET data for any region of interest can be found at: https://github.com/Dagmawi-TA/hPET

## 9. Author Contribution

GB, KM, EK, MC, and MBS designed this study. GB performed all analysis of climate model data, PET computation, and all Hydrus simulations. EK facilitated access to CP4A data via JASMIN. KM and EK assisted GB in analysis of results. MC assisted in Hydrus parameterisation and model set up. All authors contributed to writing and revising the manuscript.

## 10. Acknowledgements

This work was funded by the UKRI Natural Research Environment Council under reference NE/S007504/1 with assistance from those funded under the Horizon 2020 DOWN2EARTH project. I would also like to acknowledge the UK Met Office, which provided additional funding and facilitated access to CP4A via JASMIN.

Aspects of the schematic of our Hydrus simulations provided in Fig.~~ure~~ 2 were created with the use of Artificial Intelligence (DALL·E 3).

## 11. Competing Interests

The authors declare that they have no conflict of interest.

## References

Adloff, M., Singer, M. B., MacLeod, D. A., Michaelides, K., Mehrnegar, N., Hansford, E., Funk, C., and Mitchell, D.: Sustained water storage in Horn of Africa drylands dominated by seasonal rainfall extremes, Geophys. Res. Lett., 49, **https://doi.org/10.1029/2022GL099299**, 2022.

Ageet, S., Fink, A. H., Maranan, M., Diem, J. E., Hartter, J., Ssali, A. L., and Ayabagabo, P.: Validation of satellite rainfall estimates over equatorial East Africa, J. Hydrometeorol., 23, 129–151, https://doi.org/10.1175/JHM-D-21-0145.1, 2022.

Alduchov, O.A. and Eskridge, R.E.: Improved Magnus form approximation of saturation vapor pressure. *Journal of Applied Meteorology*, pp.601-609, 1996.

Allen, R. G., Pereira, L. S., Raes, D., and Smith, M.: Crop evapotranspiration-Guidelines for computing crop water requirements-FAO Irrigation and Drainage Paper 56, FAO, Rome, 300 pp, 1998.

Apurv, T., Sivapalan, M. and Cai, X.,: Understanding the role of climate characteristics in drought propagation. *Water Resources Research*, *53*(11), pp.9304-9329, **https://doi.org/10.1002/2017WR021445**, 2017.

Archer, L., Hatchard, S., Devitt, L., Neal, J.C., Coxon, G., Bates, P.D., Kendon, E.J. and Savage, J: Future Change in Urban Flooding Using New Convection-Permitting Climate Projections. *Water Resources Research*, *60*(1), **https://doi.org/10.1029/2023WR035533**, 2024.

Aryal, S.K., Silberstein, R.P., Fu, G., Hodgson, G., Charles, S.P. and McFarlane, D.: Understanding spatio-temporal rainfall-runoff changes in a semi-arid region. *Hydrological Processes*, *34*(11), pp.2510-2530, 2020.

Ascott, M.J., Christelis, V., Lapworth, D.J., Macdonald, D.M.J., Tindimugaya, C., Iragena, A., Finney, D., Fitzpatrick, R., Marsham, J.H. and Rowell, D.P.: On the application of rainfall projections from a convection-permitting climate model to lumped catchment models. *Journal of Hydrology*, *617*, p.129097, https://doi.org/10.1016/j.jhydrol.2023.129097, 2023.

Ban, N., Schmidli, J., and Schär, C.: Evaluation of the convection-resolving regional climate modeling approach in decade-long simulations, J. Geophys. Res.-Atmos., 119, 7889–7907, **https://doi.org/10.1002/2014JD021478**, 2014.

Batalha, M. S., Barbosa, M. C., Faybishenko, B., and Van Genuchten, M. T.: Effect of temporal averaging of meteorological data on predictions of groundwater recharge, J. Hydrol. Hydromech., 66, 143–152, 2018.

Berthou, S., Rowell, D. P., Kendon, E. J., Roberts, M. J., Stratton, R. A., Crook, J. A., and Wilcox, C.: Improved climatological precipitation characteristics over West Africa at convection-permitting scales, Clim. Dyn., 53, https://doi.org/10.1007/s00382-019-04759-4, 2019.

Boas, T., and Mallants, D.: Episodic extreme rainfall events drive groundwater recharge in arid zone environments of central Australia, J. Hydrol. Reg. Stud., 40, https://doi.org/10.1016/j.ejrh.2022.101005, 2022.

Bonsor, H.C. and MacDonald, A.M..: An initial estimate of depth to groundwater across Africa, 2011.

Cheechi, F and Robinson, C. H.: Mortality among populations of southern and central Somalia affected by severe food insecurity and famine during 2010-2012, FAO, Rome, 87pp., 2013

Clark, P., Roberts, N., Lean, H., Ballard, S. P., and Charlton-Perez, C.: Convection-permitting models: A step-change in rainfall forecasting, Meteorol. Appl., 23, 165–181, **https://doi.org/10.1002/met.1538**, 2016.

Cocking, K., Singer, M.B., MacLeod, D., Cuthbert, M.O., Rosolem, R., Muthusi, F., Paron, P., Kimutai, J., Omondi, P., Hassan, A.M. and Teshome, A.: Locally defined seasonal rainfall characteristics within the Horn of Africa drylands from rain gauge observations. *Journal of Hydrometeorology*, *25*(12), pp.1845-1861, 2024.

Cook, P. A., Black, E. C., Verhoef, A., Macdonald, D. M. J., and Sorensen, J. P. R.: Projected increases in potential groundwater recharge and reduced evapotranspiration under future climate conditions in West Africa, J. Hydrol. Reg. Stud., 41, 101076, https://doi.org/10.1016/j.ejrh.2022.101076, 2022.

Corona, C. R., and Ge, S.: Examining subsurface response to an extreme precipitation event using HYDRUS-1D, Vadose Zone J., 21, **https://doi.org/10.1002/vzj2.20189**, 2022.

Crosbie, R. S., McCallum, J. L., Walker, G. R., Francis, H., and Chiew, S.: Modelling climate-change impacts on groundwater recharge in the Murray-Darling Basin, Australia, Hydrogeol. J., 18, 2010.

Cuthbert, M. O., Acworth, R. I., Andersen, M. S., Larsen, J. R., McCallum, A. M., Rau, G. C., and Tellam, J. H.: Understanding and quantifying focused, indirect groundwater recharge from ephemeral streams using water table fluctuations, Water Resour. Res., 52, 827–840, **https://doi.org/10.1002/2015WR017503**, 2016.

Cuthbert, M.O., Gleeson, T., Moosdorf, N., Befus, K.M., Schneider, A., Hartmann, J. and Lehner, B.: Global patterns and dynamics of climate–groundwater interactions. *Nature Climate Change*, *9*(2), https://doi.org/10.1038/s41558-018-0386-4, 2019

Davenport, F., Grace, K., Funk, C., and Shukla, S.: Child health outcomes in sub-Saharan Africa: a comparison of changes in climate and socio-economic factors, Global Environ. Change, 46, 72–87, https://doi.org/10.1016/j.gloenvcha.2017.04.009, 2017.

Davenport, F., Funk, C., and Galu, G.: How will East African maize yields respond to climate change and can agricultural development mitigate this response?, Clim. Change, 147, 491–506, https://doi.org/10.1007/s10584-018-2149-7, 2018.

FAO-SWALIM: Devastating floods overwhelm parts of Somalia, Somalia Flood Update Series: https://www.faoswalim.org/resources/site_files/Devastating%20floods%20Overwhelm%20parts%20of%20Somalia_0.pdf, last access: 19 October 2021.

Fan, Y., Li, H. and Miguez-Macho, G.: Global patterns of groundwater table depth. *Science*, *339*(6122), pp.940-943, 2013.

Feddes, R. A.: Simulation of field water use and crop yield, in: Simulation of Plant Growth and Crop Production, pp. 194–209, 1978.

Finney, D. L., Marsham, J. H., Jackson, L. S., Kendon, E. J., Rowell, D. P., Boorman, P. M., Keane, R. J., Stratton, R. A., and Senior, C. A.: Implications of improved representation of convection for the East Africa water budget using a convection-permitting model, J. Climate, 32, 2109–2129, https://doi.org/10.1175/JCLI-D-18-0387.1, 2019.

Finney, D. L., Marsham, J. H., Rowell, D. P., Kendon, E. J., Tucker, S. O., Stratton, R. A., and Jackson, L. S.: Effects of explicit convection on future projections of mesoscale circulations, rainfall, and rainfall extremes over Eastern Africa, J. Climate, 33, 2701–2718, https://doi.org/10.1175/JCLI-D-19-0328.1, 2020.

Folwell, S.S., Taylor, C.M. and Stratton, R.A.: Contrasting contributions of surface hydrological pathways in convection permitting and parameterised climate simulations over Africa and their feedbacks on the atmosphere. *Climate Dynamics*, *59*(1), pp.633-648., https://doi.org/10.1007/s00382-022-06144-0, 2022.

Funk, C., Shukla, S., Thiaw, W. M., Rowland, J., Hoell, A., McNally, A., Husak, G., Novella, N., Budde, M., Peters-Lidard, C., and Adoum, A.: Recognizing the famine early warning systems network: Over 30 years of drought early warning science advances and partnerships promoting global food security, B. Am. Meteorol. Soc., 100, 1011–1027, https://doi.org/10.1175/BAMS-D-17-0233.1, 2019.

Geißler, K., Heblack, J., Uugulu, S., Wanke, H., and Blaum, N.: Partitioning of water between differently sized shrubs and potential groundwater recharge in a semiarid savanna in Namibia, Front. Plant Sci., 10, 1411, https://doi.org/10.3389/fpls.2019.01411, 2019.

Halladay, K., Kahana, R., Johnson, B., Still, C., Fosser, G. and Alves, L.: Convection-permitting climate simulations for South America with the met office unified model. *Climate Dynamics*, *61*(11), pp.5247-5269, 2023.

Hengl, T., Miller, M. A., Križan, J., Shepherd, K. D., Sila, A., Kilibarda, M., Antonijević, O., Glušica, L., Dobermann, A., Haefele, S. M., and McGrath, S. P.: African soil properties and nutrients mapped at 30 m spatial resolution using two-scale ensemble machine learning, Sci. Rep., 11, 6130, https://doi.org/10.1038/s41598-021-85639-y, 2021.

Hijmans, R.J., Cameron, S.E., Parra, J.L., Jones, P.G. and Jarvis, A.: Very high-resolution interpolated climate surfaces for global land areas. *International Journal of Climatology: A Journal of the Royal Meteorological Society*, *25*(15), pp.1965-1978, 2005.

Hill, P. G., Stein, T. H., and Cafaro, C.: Convective systems and rainfall in East Africa, Q. J. R. Meteorol. Soc, **https://doi.org/10.1002/qj.4540**, 2023.

Hoffmann, R., Wiederkehr, C., Dimitrova, A., and Hermans, K.: Agricultural livelihoods, adaptation, and environmental migration in sub-Saharan drylands: a meta-analytical review, Environ. Res. Lett., 17, 083003, 2022.

Horton, R.E.: The role of infiltration in the hydrologic cycle. *Eos, Transactions American Geophysical Union*, *14*(1), pp.446-460, 1993.

Hsu, H., Lo, M. H., Guillod, B. P., Miralles, D. G., and Kumar, S.: Relation between precipitation location and antecedent/subsequent soil moisture spatial patterns, J. Geophys. Res.-Atmos., 122, 6319–6328, **https://doi.org/10.1002/2016JD026042**, 2017.

Huang, J., Yu, H., Dai, A., Wei, Y. and Kang, L.: Drylands face potential threat under 2 C global warming target. *Nature Climate Change*, *7*(6), pp.417-422, https://doi.org/10.1038/nclimate3275, 2017.

Huffman, G.J., Bolvin, D.T., Braithwaite, D., Hsu, K., Joyce, R., Xie, P. and Yoo, S.H., 2015. NASA global precipitation measurement (GPM) integrated multi-satellite retrievals for GPM (IMERG). *Algorithm theoretical basis document (ATBD) version*, *4*(26), pp.2020-05.

iSDA: The first field-level soil map for Africa: https://www.isda-africa.com/isdasoil/, last access: 20 October 2024

Kendon, E. J., Ban, N., Roberts, N. M., Fowler, H. J., Roberts, M. J., Chan, S. C., Evans, J. P., Fosser, G., and Wilkinson, J. M.: Do convection-permitting regional climate models improve projections of future precipitation change?, Am. Meteorol. Soc., 98, 79–93, https://doi.org/10.1175/BAMS-D-15-0004.1, 2017.

Kendon, E. J., Stratton, R. A., Tucker, S., Marsham, J. H., Berthou, S., Rowell, D. P., and Senior, C. A.: Enhanced future changes in wet and dry extremes over Africa at convection-permitting scale, Nat. Commun., 10, 1794, https://doi.org/10.1038/s41467-019-09776-9, 2019.

Kimutai, J., Barnes, C., Zachariah, M., Philip, S., Kew, S., Pinto, I., Wolski, P., Koren, G., Vecchi, G., Yang, W. and Li, S.: Human-induced climate change increased drought severity in Horn of Africa. https://doi.org/10.1016/j.wace.2025.100745, Weather and Climate Extremes, Vol. 47, https://doi.org/10.1016/j.wace.2025.100745, 2025.

Kipkemoi, I., Michaelides, K., Rosolem, R., and Singer, M. B.: Climatic expression of rainfall on soil moisture dynamics in drylands, Hydrol. Earth Syst. Sci. Discuss., 1–24, https://doi.org/10.5194/hess-2021-48, 2021.

Klein, C., Jackson, L. S., Parker, D. J., Marsham, J. H., Taylor, C. M., Rowell, D. P., Guichard, F., Vischel, T., Famien, A. M., and Diedhiou, A.: Combining CMIP data with a regional convection-permitting model and observations to project extreme rainfall under climate change, Environ. Res. Lett., 16, 2021.

Kouadio, K., Bastin, S., Konare, A., and Ajayi, V. O.: Does convection-permitting simulate better rainfall distribution and extreme over Guinean coast and surroundings?, Clim. Dyn., 55, 153–174, https://doi.org/10.1007/s00382-018-4308-y, 2020.

Lee, J. and Hohenegger, C.: Weaker land–atmosphere coupling in global storm-resolving simulation. *Proceedings of the National Academy of Sciences*, *121*(12), 2024.

Leterme, B., Mallants, D., and Jacques, D.: Estimation of future groundwater recharge using climatic analogues and Hydrus-1D, Hydrol. Earth Syst. Sci. Discuss., 9, 2012.

Lobell, D. B., Bänziger, M., Magorokosho, C., and Vivek, B.: Nonlinear heat effects on African maize as evidenced by historical yield trials, Nat. Clim. Change, 1, 42–45, https://doi.org/10.1038/nclimate1043, 2011.

Luu, L. N., Vautard, R., Yiou, P., and Soubeyroux, J. M.: Evaluation of convection-permitting extreme precipitation simulations for the south of France, Earth Syst. Dynam., 13, 687–702, https://doi.org/10.5194/esd-13-687-2022, 2022.

Lyon, B. and Vigaud, N.: Unraveling East Africa's climate paradox. *Climate extremes: Patterns and mechanisms*, **https://doi.org/10.1002/9781119068020.ch16**, 2017.

Lyon, B.: Seasonal drought in the Greater Horn of Africa and its recent increase during the March–May long rains. *Journal of Climate*, *27*(21), https://doi.org/10.1175/JCLI-D-13-00459.1, 2014.

Maeght, J. L., Rewald, B., and Pierret, A.: How to study deep roots—and why it matters, Front. Plant Sci., 4, 299, https://doi.org/10.3389/fpls.2013.00299, 2013.

MacDonald, A.M., Bonsor, H.C., Dochartaigh, B.É.Ó. and Taylor, R.G.: Quantitative maps of groundwater resources in Africa. *Environmental Research Letters*, *7*(2), 2012.

McKenna, O. P., and Sala, O. E.: Groundwater recharge in desert playas: current rates and future effects of climate change, Environ. Res. Lett., 13, 014025, 2017.

Mirzabaev, A., et al.: Desertification, in: Climate Change and Land: an IPCC special report on climate change, desertification, land degradation, sustainable land management, food security, and greenhouse gas fluxes in terrestrial ecosystems, IPCC, 2019.

Muñoz Sabater, J.: ERA5-Land hourly data from 1950 to present, Copernicus Climate Change Service (C3S) Climate Data Store (CDS), https://doi.org/10.24381/cds.e2161bac, 2019.

Nazarieh, F., Ansari, H., Ziaei, A. N., Izady, A., Davari, K., and Brunner, P.: Spatial and temporal dynamics of deep percolation, lag time and recharge in an irrigated semi-arid region, Hydrogeol. J., 26, 2507–2520, 2018.

Nicholson, S. E.: Dryland Climatology, Cambridge University Press, Cambridge, 2011.

Osborn, H. B.: Timing and duration of high rainfall rates in the southwestern United States, Water Resour. Res., 19, 1036–1042, 1983.

Porporato, A., D'Odorico, P., Laio, F., Ridolfi, L., and Rodriguez-Iturbe, I.: Ecohydrology of water-controlled ecosystems, Adv. Water Resour., 25, 1335–1348, https://doi.org/10.1016/S0309-1708(02)00058-1, 2002.

Prein, A. F., Gobiet, A., Suklitsch, M., Truhetz, H., Awan, N. K., Keuler, K., and Georgievski, G.: Added value of convection-permitting seasonal simulations, Clim. Dyn., 41, 2655–2677, https://doi.org/10.1007/s00382-013-1744-6, 2013.

Prein, A. F., Langhans, W., Fosser, G., Ferrone, A., Ban, N., Goergen, K., Keller, M., Tölle, M., Gutjahr, O., Feser, F., and Brisson, E.: A review on regional convection-permitting climate modeling: Demonstrations, prospects, and challenges, Rev. Geophys., 53, 323–361, **https://doi.org/10.1002/2014RG000475**, 2015.

Quichimbo, E. A., Singer, M. B., and Cuthbert, M. O.: Characterising groundwater–surface water interactions in idealised ephemeral stream systems, Hydrol. Process., 34, 3792–3806, **https://doi.org/10.1002/hyp.13847**, 2021.

Quichimbo, E. A., Singer, M. B., Michaelides, K., Rosolem, R., MacLeod, D. A., Asfaw, D. T., and Cuthbert, M. O.: Assessing the sensitivity of modelled water partitioning to global precipitation datasets in a data-scarce dryland region, Hydrol. Process., 37, e15047, **https://doi.org/10.1002/hyp.15047**, 2023.

Quichimbo, E.A., Singer, M.B., Michaelides, K., Hobley, D.E., Rosolem, R. and Cuthbert, M.O.: DRYP 1.0: a parsimonious hydrological model of DRYland Partitioning of the water balance. *Geoscientific Model Development Discussions*, *2021*, pp.1-34, 2021.

Razack, M., Jalludin, M., and Houmed-Gaba, A.: Simulation of climate change impact on a coastal aquifer under arid climate. The Tadjourah Aquifer (Republic of Djibouti, Horn of Africa), **https://doi.org/10.3390/w11112347**, 2019.

Reynolds, J. F., Smith, D. M. S., Lambin, E. F., Turner, B. L., Mortimore, M., Batterbury, S. P., Downing, T. E., Dowlatabadi, H., Fernández, R. J., Herrick, J. E., and Huber-Sannwald, E.: Global desertification: building a science for dryland development, Science, 316, 847–851, 2007.

Reynolds, R. W., Smith, T. M., Liu, C., Chelton, D. B., Casey, K. S., and Schlax, M. G.: Daily high-resolution-blended analyses for sea surface temperature, J. Clim., 20, 5473–5496, https://doi.org/10.1175/2007JCLI1824.1, 2007.

Richards, L. A.: Capillary conduction of liquids through porous mediums, Phys., 1, 318–333, 1931.

Rios Gaona, M.F., Michaelides, K. and Singer, M.B.: STORM v. 2: A simple, stochastic rainfall model for exploring the impacts of climate and climate change at and near the land surface in gauged watersheds. *Geoscientific Model Development*, *17*(13), pp.5387-5412, https://doi.org/10.5194/gmd-17-5387-2024, 2024.

Rodriguez, P., Giménez, R., Nosetto, M. D., Jobbágy, E. G., and Magliano, P. N.: Changes in water fluxes partition related to the replacement of native dry forests by crops in the Dry Chaco, J. Arid Environ., 183, 104281, https://doi.org/10.1016/j.jaridenv.2020.104281, 2020.

Scanlon, B. R., Keese, K. E., Flint, A. L., Flint, L. E., Gaye, C. B., Edmunds, W. M., and Simmers, I.: Global synthesis of groundwater recharge in semiarid and arid regions, Hydrol. Process., 20, 3335–3370, **https://doi.org/10.1002/hyp.6335**, 2006.

Schimel, D. S.: Drylands in the earth system, Science, 327, 418–419, 2010.

Schoener, G., and Stone, M. C.: Impact of antecedent soil moisture on runoff from a semiarid catchment, J. Hydrol., 569, 627–636, https://doi.org/10.1016/j.jhydrol.2018.12.025, 2019.

Schoener, G.: Soil Moisture Dependent Runoff in a Dryland Region: An Investigation of the Role of Antecedent Conditions, Monitoring, and Modeling Strategies, PhD Thesis, University of New Mexico, 2021.

Schreiner-McGraw, A.P., Ajami, H. and Vivoni, E.R.: Extreme weather events and transmission losses in arid streams. *Environmental Research Letters*, *14*(8), p.084002, 2019.

Schwarzwald, K., and Seager, R.: Revisiting the 'East African Paradox': CMIP6 models also fail to simulate observed drying trends in the Horn of Africa Long Rains, Copernicus Meetings, No. EGU24-4687, 2024.

Schwarzwald, K., Goddard, L., Seager, R., Ting, M., and Marvel, K.: Understanding CMIP6 biases in the representation of the Greater Horn of Africa long and short rains, Clim. Dyn., 61, 1229–1255, https://doi.org/10.1007/s00382-022-06622-5, 2023.

Seddon, D., Kashaigili, J. J., Taylor, R. G., Cuthbert, M. O., Mwihumbo, C., and MacDonald, A. M.: Focused groundwater recharge in a tropical dryland: Empirical evidence from central, semi-arid Tanzania, J. Hydrol. Reg. Stud., 37, https://doi.org/10.1016/j.ejrh.2021.100919, 2021.

Sela, S., Svoray, T., and Assouline, S.: The effect of soil surface sealing on vegetation water uptake along a dry climatic gradient, Water Resour. Res., 51, 7452–7466, **https://doi.org/10.1002/2015WR017109**, 2015.

Seneviratne, S.I., Corti, T., Davin, E.L., Hirschi, M., Jaeger, E.B., Lehner, I., Orlowsky, B. and Teuling, A.J.: Investigating soil moisture–climate interactions in a changing climate: A review. *Earth-Science Reviews*, *99*(3-4), pp.125-161, 2010.

Shadwell, E., and February, E.: Effects of groundwater abstraction on two keystone tree species in an arid savanna national park, PeerJ, 5, 2017.

Shepherd, T.G., Boyd, E., Calel, R.A., Chapman, S.C., Dessai, S., Dima-West, I.M., Fowler, H.J., James, R., Maraun, D., Martius, O. and Senior, C.A.: Storylines: an alternative approach to representing uncertainty in physical aspects of climate change. *Climatic change*, *151*, pp.555-571, 2018.

Šimunek, J., Van Genuchten, M.T. and Šejna, M., 2012. HYDRUS: Model use, calibration, and validation. *Transactions of the ASABE*, *55*(4), pp.1263-1274.

Singer, M. B., and Michaelides, K.: Deciphering the expression of climate change within the Lower Colorado River basin by stochastic simulation of convective rainfall, Environ. Res. Lett., 12, 2017.

Singer, M. B., Michaelides, K., and Hobley, D. E. J.: STORM 1.0: A simple, flexible, and parsimonious stochastic rainfall generator for simulating climate and climate change, Geosci. Model Dev., 11, 3713–3726, https://doi.org/10.5194/gmd-11-3713-2018, 2018.

Singer, M.B., Asfaw, D.T., Rosolem, R., Cuthbert, M.O., Miralles, D.G., MacLeod, D., Quichimbo, E.A. and Michaelides, K.: Hourly potential evapotranspiration at 0.1 resolution for the global land surface from 1981-present. *Scientific Data*, *8*(1), https://doi.org/10.1038/s41597-021-01003-9, 2021.

Stephens, G. L., L'Ecuyer, T., Forbes, R., Gettelmen, A., Golaz, J. C., Bodas-Salcedo, A., Suzuki, K., Gabriel, P., and Haynes, J.: Dreary state of precipitation in global models, J. Geophys. Res.-Atmos., 115, D24211, **https://doi.org/10.1029/2010JD014532**, 2010.

Stone, E. L., and Kalisz, P. J.: On the maximum extent of tree roots, For. Ecol. Manage., 46, 59–102, 1991.

Stratton, R. A., and Stirling, A. J.: Improving the diurnal cycle of convection in GCMs, Q. J. R. Meteorol. Soc., 138, 1121–1134, **https://doi.org/10.1002/qj.991**, 2012.

Stratton, R. A., Senior, C. A., Vosper, S. B., Folwell, S. S., Boutle, I. A., Earnshaw, P. D., Kendon, E., Lock, A. P., Malcolm, A., Manners, J., and Morcrette, C. J.: A Pan-African convection-permitting regional climate simulation with the Met Office Unified Model: CP4-Africa, J. Clim., 31, 3485–3508, https://doi.org/10.1175/JCLI-D-17-0503.1,2018.

Stringer, L. C., Dyer, J. C., Reed, M. S., Dougill, A. J., Twyman, C., and Mkwambisi, D.: Adaptations to climate change, drought and desertification: local insights to enhance policy in southern Africa, Environ. Sci. Policy, 12, 748–765, https://doi.org/10.1016/j.envsci.2009.04.002, 2009.

Taylor, C. M., de Jeu, R. A., Guichard, F., Harris, P. P., and Dorigo, W. A.: Afternoon rain more likely over drier soils, Nature, 489, 423–426, https://doi.org/10.1038/nature11377, 2012.

Taylor, C. M., Gounou, A., Guichard, F., Harris, P. P., Ellis, R. J., Couvreux, F., and De Kauwe, M.: Frequency of Sahelian storm initiation enhanced over mesoscale soil-moisture patterns, Nat. Geosci., 4, 430–433, https://doi.org/10.1038/ngeo1173, 2011.

Taylor, R. G., Todd, M. C., Kongola, L., Maurice, L., Nahozya, E., Sanga, H., and MacDonald, A. M.: Evidence of the dependence of groundwater resources on extreme rainfall in East Africa, Nat. Clim. Change, 3, 374–378, https://doi.org/10.1038/nclimate1731, 2013.

Tetens, O.: Uber einige meteorologische Begriffe. *Z. geophys*, *6*, pp.297-309, 1930.

Tugwell-Wootton, T., Skrzypek, G., Dogramaci, S., McCallum, J., and Grierson, P. F.: Soil moisture evaporative losses in response to wet-dry cycles in a semiarid climate, J. Hydrol., 590, 125533, https://doi.org/10.1016/j.jhydrol.2020.125533, 2020.

Van Genuchten, M. T.: A closed-form equation for predicting the hydraulic conductivity of unsaturated soils, Soil Sci. Soc. Am. J., 44, 892–898, 1980.

Vermote, E.: NOAA Climate Data Record (CDR) of AVHRR Leaf Area Index (LAI) and Fraction of Absorbed Photosynthetically Active Radiation (FAPAR), Version 5, NOAA National Centers for Environmental Information, 2019.

Vicente-Serrano, S. M., Miralles, D. G., Domínguez-Castro, F., Azorin-Molina, C., El Kenawy, A., McVicar, T. R., Tomás-Burguera, M., Beguería, S., Maneta, M., and Peña-Gallardo, M.: Global assessment of the standardized evapotranspiration deficit index (SEDI) for drought analysis and monitoring, J. Clim., 31, 5371–5393, https://doi.org/10.1175/JCLI-D-17-0775.1, 2018.

Wainwright, C.M., Marsham, J.H., Keane, R.J., Rowell, D.P., Finney, D.L., Black, E. and Allan, R.P., 2019. 'Eastern African Paradox' rainfall decline due to shorter not less intense Long Rains. *npj Climate and Atmospheric Science*, *2*(1), https://doi.org/10.1038/s41612-019-0091-7, 2019.

Wainwright, C. M., Finney, D. L., Kilavi, M., Black, E., and Marsham, J. H.: Extreme rainfall in East Africa, October 2019–January 2020 and context under future climate change, Weather, 76, 26–31, **https://doi.org/10.1002/wea.3824**, 2021.

Walters, D., Boutle, I., Brooks, M., Melvin, T., Stratton, R., Vosper, S., Wells, H., Williams, K., Wood, N., Allen, T. and Bushell, A.: The Met Office unified model global atmosphere 6.0/6.1 and JULES global land 6.0/6.1 configurations. *Geoscientific Model Development*, *10*(4), pp.1487-1520, https://doi.org/10.5194/gmd-10-1487-2017, 2017.

Watson, A.: The use of environmental isotopes, soil water measurements and soil water modelling to understand tree water use of an Acacia mearnsii (Black Wattle) stand in KwaZulu-Natal, MSc Thesis, University of KwaZulu-Natal, 135 pp., 2015.

Wesseling, J. G., Elbers, J. A., Kabat, P., and Van den Broek, B. J.: SWATRE: instructions for input, Internal Note, Winand Staring Centre, Wageningen, the Netherlands, p. 700, 1991.

Xia, Y. Q., and Shao, M. A.: The process modeling of soil water carrying capacity for vegetation in small watershed within the wind-water crisscrossed erosion zone on the Loess Plateau, Institute of Geographical Sciences and Natural Resources Research, Chinese Academy of Sciences, 2008.

Zarate, E., Hobley, D., MacDonald, A. M., Swift, R. T., Chambers, J., Kashaigili, J. J., Mutayoba, E., Taylor, R. G., and Cuthbert, M. O.: The role of superficial geology in controlling groundwater recharge in the weathered crystalline basement of semi-arid Tanzania, J. Hydrol. Reg. Stud., 36, 100833, https://doi.org/10.1016/j.ejrh.2021.100833, 2021.

Zhang, Y. K., and Schilling, K. E.: Effects of land cover on water table, soil moisture, evapotranspiration, and groundwater recharge: a field observation and analysis, J. Hydrol., 319, 328–338, https://doi.org/10.1016/j.jhydrol.2005.06.044, 2006.

Zhou, S., Williams, A. P., Lintner, B. R., Berg, A. M., Zhang, Y., Keenan, T. F., Cook, B. I., Hagemann, S. I., Seneviratne, S. I., and Gentine, P.: Soil moisture–atmosphere feedbacks mitigate declining water availability in drylands, Nat. Clim. Change, 11, 38–44, https://doi.org/10.1038/s41558-020-00945-z, 2021.

Zhu, Z., Wright, D.B. and Yu, G.: The impact of rainfall space-time structure in flood frequency analysis. *Water Resources Research*, *54*(11), pp.8983-8998, 2018.

Zinyengere, N., Mhizha, T., Mashonjowa, E., Chipindu, B., Geerts, S., and Raes, D.: Using seasonal climate forecasts to improve maize production decision support in Zimbabwe, Agric. For. Meteorol., 151, 1792–1799, https://doi.org/10.1016/j.agrformet.2011.07.015, 2011.

Zomer, R., Trabucco, A., van Straaten, O., and Bossio, D.: Carbon, land and water: A global analysis of the hydrologic dimensions of climate change mitigation through afforestation/reforestation, IWMI, Vol. 101, 2007.